Journal of New Theory

ISSN: 2149-1402

Editor-in-Chief
Naim Çağman

CONTENTS

About

Journal of New Theory (abbreviated as J. New Theory or JNT) is a mathematical journal focusing on new mathematical theories or a mathematical theory's applications to science.

J. New Theory is an international open access journal.

Language: JNT accepts contributions in English only.

JNT was founded on 18 November 2014, and its first issue was published on 27 January 2015.

Editor-in-Chief: [Naim Çağman](#)

E-mail: journalofnewtheory@gmail.com

APC: JNT incurs no article processing charges.

Review Process: Blind Peer Review

Policy of Screening for Plagiarism: JNT accepts submissions for pre-review only if their reference-excluded similarity rate is a **maximum of 30%**.

Creative Commons License: JNT is licensed under a [Creative Commons Attribution-NonCommercial 4.0 International Licence (CC BY-NC)](#)

Publication Ethics: The governance structure of Journal New Theory and its acceptance procedures are transparent and designed to ensure the highest quality of published material. JNT adheres to the international standards developed by the Committee on Publication Ethics (COPE).

Aim & Scope

Journal of New Theory aims to share new ideas in pure or applied mathematics with the world of science.

Journal of New Theory publishes original research articles and reviews from all science branches that use mathematics theories.

Journal of New Theory is concerned with the studies in the areas of AMS2020, but not limited to:

· Fuzzy Sets

· Soft Sets

· Neutrosophic Sets

· Decision-Making

· Algebra

· Number Theory

· Analysis

· Theory of Functions

· Geometry

· Applied Mathematics

· Topology

· Fundamental of Mathematics

· Mathematical Logic

· Mathematical Physics

· Mathematical Statistics

Journal Boards

Editor-in-Chief

Naim Çağman

Department of Mathematics, Tokat Gaziosmanpasa University, Tokat, Turkey.

naim.cagman@gop.edu.tr

Associate Editor-in-Chief

Faruk Karaaslan

Department of Mathematics, Çankırı Karatekin University, Çankırı, Turkey

fkaraaslan@karatekin.edu.tr

Serdar Enginoğlu

Department of Mathematics, Çanakkale Onsekiz Mart University, Çanakkale, Turkey

serdarenginoglu@gmail.com

İrfan Deli

M. R. Faculty of Education, Kilis 7 Aralık University, Kilis, Turkey

irfandeli@kilis.edu.tr

Area Editors

Hari Mohan Srivastava

Department of Mathematics and Statistics, University of Victoria, Victoria, British Columbia V8W 3R4, Canada

harimsri@math.uvic.ca

Muhammad Aslam Noor

COMSATS Institute of Information Technology, Islamabad, Pakistan

noormaslam@hotmail.com

Florentin Smarandache

Mathematics and Science Department, University of New Mexico, New Mexico 87301, USA

fsmarandache@gmail.com

Bijan Davvaz

Department of Mathematics, Yazd University, Yazd, Iran

davvaz@yazd.ac.ir

Pabitra Kumar Maji

Department of Mathematics, Bidhan Chandra College, Asansol 713301, Burdwan (W), West Bengal, India.

pabitra_maji@yahoo.com

Harish Garg

School of Mathematics, Thapar Institute of Engineering & Technology, Deemed University, Patiala-147004, Punjab, India

harish.garg@thapar.edu

Jianming Zhan

Department of Mathematics, Hubei University for Nationalities, Hubei Province, 445000, P. R. China

zhanjianming@hotmail.com

Surapati Pramanik

Department of Mathematics, Nandalal Ghosh B.T. College, Narayanpur, Dist- North 24 Parganas, West Bengal 743126, India

sura_pati@yaho.co.in

Muhammad Irfan Ali

Department of Mathematics, COMSATS Institute of Information Technology Attock, Attock 43600, Pakistan

mirfanali13@yahoo.com

Said Broumi

Department of Mathematics, Hassan II Mohammedia-Casablanca University, Kasablanka 20000, Morocco

broumisaid78@gmail.com

Mumtaz Ali

The University of Southern Queensland, Darling Heights QLD 4350, Australia

Mumtaz.Ali@usq.edu.au

Oktay Muhtaroğlu

Department of Mathematics, Gaziosmanpaşa University, 60250 Tokat, Turkey

oktay.muhtaroglu@gop.edu.tr

Ahmed A. Ramadan

Mathematics Department, Faculty of Science, Beni-Suef University, Beni-Suef, Egypt

aramadan58@gmail.com

Sunil Jacob John

Department of Mathematics, National Institute of Technology Calicut, Calicut 673 601 Kerala, India

sunil@nitc.ac.in

Aslıhan Sezgin

Department of Statistics, Amasya University, Amasya, Turkey

aslihan.sezgin@amasya.edu.tr

Alaa Mohamed Abd El-latif

Department of Mathematics, Faculty of Arts and Science, Northern Border University, Rafha, Saudi Arabia

alaa_8560@yahoo.com

Kalyan Mondal

Department of Mathematics, Jadavpur University, Kolkata, West Bengal 700032, India

kalyanmathematic@gmail.com

Jun Ye

Department of Electrical and Information Engineering, Shaoxing University, Shaoxing, Zhejiang, P.R. China

yehjun@aliyun.com

Ayman Shehata

Department of Mathematics, Faculty of Science, Assiut University, 71516-Assiut, Egypt

drshehata2009@gmail.com

İdris Zorlutuna

Department of Mathematics, Cumhuriyet University, Sivas, Turkey

izorlu@cumhuriyet.edu.tr

Murat Sarı

Department of Mathematics, Yildiz Technical University, İstanbul, Turkey

sarim@yildiz.edu.tr

Daud Mohamad

Faculty of Computer and Mathematical Sciences, University Teknologi Mara, 40450 Shah Alam, Malaysia

daud@tmsk.uitm.edu.my

Tanmay Biswas

Research Scientist, Rajbari, Rabindrapalli, R. N. Tagore Road, P.O.- Krishnagar Dist- Nadia, PIN- 741101, West Bengal, India

tanmaybiswas_math@rediffmail.com

Kadriye Aydemir

Department of Mathematics, Amasya University, Amasya, Turkey

kadriye.aydemir@amasya.edu.tr

Ali Boussayoud

LMAM Laboratory and Department of Mathematics, Mohamed Seddik Ben Yahia
University, Jijel, Algeria

alboussayoud@gmail.com

Muhammad Riaz

Department of Mathematics, Punjab University, Quaid-e-Azam Campus, Lahore-
54590, Pakistan

mriaz.math@pu.edu.pk

Serkan Demiriz

Department of Mathematics, Gaziosmanpaşa University, Tokat, Turkey

serkan.demiriz@gop.edu.tr

Hayati Olğar

Department of Mathematics, Gaziosmanpaşa University, Tokat, Turkey

hayati.olgar@gop.edu.tr

Essam Hamed Hamouda

Department of Basic Sciences, Faculty of Industrial Education, Beni-Suef University,
Beni-Suef, Egypt

ehamouda70@gmail.com

Arooj Adeel (Since 2022)

Department of Mathematics, University of Education Lahore, Pakistan

arooj.adeel@ue.edu.pk

Statistics Editor

Tolga Zaman (Since 2021)

Department of Statistics, Çankırı Karatekin University, Çankırı, Turkey

tolgazaman@karatekin.edu.tr

Foreign Language Editor

Mehmet Yıldız (Since 2021)

Department of Western Languages and Literatures, Çanakkale Onsekiz Mart
University, Çanakkale, Turkey

mehmetyildiz@comu.edu.tr

Layout Editors

Samet Memiş (Since 2022)

Department of Computer Engineering, İstanbul Rumeli University, İstanbul, Turkey

samet.memis@rumeli.edu.tr

Fatih Karamaz (Since 2020)

Department of Mathematics, Çankırı Karatekin University, Çankırı, Turkey

karamaz@karamaz.com

Tuğçe Aydın (2020-2021)

Department of Mathematics, Çanakkale Onsekiz Mart University, Çanakkale, Turkey

aydinttugce@gmail.com

Production Editor

Samet Memiş (Since 2022)

Department of Computer Engineering, İstanbul Rumeli University, İstanbul, Turkey

samet.memis@rumeli.edu.tr

Tuğçe Aydın (2020-2021)

Department of Mathematics, Çanakkale Onsekiz Mart University, Çanakkale, Turkey

aydinttugce@gmail.com

Factorable Surfaces in Pseudo-Galilean Space with Prescribed Mean and Gaussian Curvatures

Sezin Aykurt Sepet[1] , Hülya Gün Bozok[2] , Muhittin Evren Aydın[3]

Abstract — We study the so-called factorable surfaces in the pseudo-Galilean space, the graphs of the product of two functions of one variable. We then classify these surfaces when the mean and Gaussian curvatures are functions of one variable.

1. Introduction

A *Cayley-Klein space* is defined as a real projective space $P(\mathbb{R})$ with a certain absolute figure which is a subset of quadrics and planes. Let $(u_0 : u_1 : u_2 : u_3)$ denote the homogeneous coordinates in $P(\mathbb{R})$. The pseudo-Galilean 3-space G_3^1 that we are interested in is a Cayley-Klein space $P(\mathbb{R})$ with the absolute figure $\{\omega, f, I\}$ such that ω is the absolute plane $u_0 = 0$, f the line $u_0 = u_1 = 0$ and I the fixed hyperbolic involution of points of f. The hyperbolic involution is $(0 : 0 : u_2 : u_3) \mapsto (0 : 0 : u_3 : u_2)$ and $u_2^2 - u_3^2 = 0$ is the absolute conic, [1–5].

Consider the affine coordinates in G_3^1 defined by $(u_0 : u_1 : u_2 : u_3) = (1 : x : y : z)$. Then, a plane of the form $x = d$, $d \in \mathbb{R}$, in G_3^1 is said to be *Lorentzian* since its induced geometry is Lorentzian. We call other planes *isotropic*.

The main purpose of this study, in this special ambient space, is determining the surfaces with prescribed mean (H) and Gaussian (K) curvatures which is a common problem in differential geometry of surfaces. For this, we focus on a graphical surface. Because of the absolute figure of G_3^1, the geometric structure of the surface depends on if it is graph on an isotropic or a Lorentzian plane.

Without lose of generality we may consider the coordinate planes. Hence a graph on the isotropic $xy-$plane (resp. the Lorentzian $yz-$plane) is said to be of *type 1* (*type 2*). Let M be a non-degenerate graph of a smooth function $u = u(s,t)$, $s \in I \subset \mathbb{R}$, $t \in J \subset \mathbb{R}$. If M is of type 1 then it parametrizes $\mathbf{r}(s,t) = (s,t,u(s,t))$ and hence its mean and Gaussian curvatures are given by

$$u_{ss}u_{tt} - u_{st}^2 = -\epsilon K(s,t)\left|1 - u_t^2\right|^2 \tag{1}$$

$$u_{tt} = 2\epsilon H(s,t)2\left|1 - u_t^2\right|^{3/2} \tag{2}$$

[1]sezinaykurt@hotmail.com; [2]hulyagun@osmaniye.edu.tr(Corresponding Author); [3]meaydin@firat.edu.tr
[1]Department of Mathematics, Faculty of Arts and Sciences, Kırşehir Ahi Evran University, Kırşehir, Türkiye
[2]Department of Mathematics, Faculty of Arts and Sciences, Osmaniye Korkut Ata University, Osmaniye, Türkiye
[3]Department of Mathematics, Faculty of Sciences, Fırat University, Elazığ, Türkiye

where ϵ is 1 if $1 - u_t^2 > 0$ and -1 otherwise. Here we notice $u_s = \partial u / \partial s$, $u_{st} = \partial^2 u / \partial s \partial t$, and so. If M is of type 2 then parameterizes $\mathbf{r}(s,t) = (u(s,t), s, t)$ and

$$u_{ss}u_{tt} - u_{st}^2 = -\epsilon K(s,t) \left| u_s^2 - u_t^2 \right|^2 \tag{3}$$

$$u_s^2 u_{tt} - 2u_s u_t u_{st} + u_t^2 u_{ss} = -2\epsilon H(s,t) \left| u_s^2 - u_t^2 \right|^{3/2} \tag{4}$$

We point out that the PDEs (1) and (3) are of Monge-Ampère type and their importance is due to economics, meteorology, oceanography etc. [6–11].

In principle, we will concern with the PDEs (1)-(4). Finding their solutions is complicated and one way to reduce their complexity is to use the technique of separation of variables, namely

$$u(s,t) = f(s) + g(t), \quad u(s,t) = f(s)g(t)$$

for smooth functions f, g. Notice that the graphs $u(s,t) = f(s) + g(t)$ are known as *translation surfaces*. The name is because kinematic point of view, obtained by translating one curve along the other one. If the so-called *generating curves* are denoted by $\alpha(s)$ and $\beta(t)$ then

$$\begin{aligned} \mathbf{r}(s,t) &= \alpha(s) + \beta(t) = (s, t, f(s) + g(t)) \\ \mathbf{r}(s,t) &= \alpha(s) + \beta(t) = (f(s) + g(t), s, t) \end{aligned}$$

Those surfaces were completely obtained in [12–16] when H and K are a constant function.

Most recently, as a generalization, the present authors [17] classified translation surfaces when H and K are a non-constant function of one variable, that is, $K = K(s)$ and $K = K(t)$ (or $H = H(s)$ and $H = H(t)$). The authors found the motivation in Ruiz-Hernández's paper [18] where the translation hypersurfaces in the Euclidean $n-$space $\mathbb{R}^n$ were obtained when mean and Gauss-Kronocker curvatures depend on its first p (or second q) variables, $p + q = n$. This is indeed, in 3-dimensional setting, a well-known framework for surfaces of revolution or, more generally, helicoidal surfaces due to the fact the mean and Gaussian curvatures only depend on the parameter of the profile curve, see [19, 20].

Following Ruiz-Hernández's idea, we will consider the graphs $u(s,t) = f(s)g(t)$ called *factorable* (or *homothetical*) *surfaces* [21]. These surfaces were studied from various point of view in the (pseudo-) Galilean ambient space, see [22–24].

When $u(s,t) = f(s)g(t)$, the PDEs (1)-(4) that we will solve are now

$$fgf''g'' - (f'g')^2 = -\epsilon K \left| 1 - (fg')^2 \right|^2 \tag{5}$$

$$fg'' = 2\epsilon H \left| 1 - (fg')^2 \right|^{3/2} \tag{6}$$

and

$$fgf''g'' - (f'g')^2 = -\epsilon K \left| (f'g)^2 - (fg')^2 \right|^2 \tag{7}$$

$$(f'g)^2 fg'' - 2fg(f'g')^2 + (fg')^2 f''g = -2\epsilon H \left| (f'g)^2 - (fg')^2 \right|^{3/2} \tag{8}$$

where H and K only depend on s or t and a prime denotes the derivative with respect to the related variable. The Equations (5)-(8) were solved in [13, 25, 26] when K and H are a constant.

In Section 3, we will solve (5) and (6), obtaining the graphs are a cylindrical ruled surface of type 3 from geometric point of view. The detailed properties of ruled surfaces may be found in [2, 27]. We remark that K has to be a function of s in (5) while H has to be a function of t in (6). Contrary to this, the solution of (7) is that, up to a change in the roles of the functions f, g, $f(s) = ae^{bs}$, $K(s) = cb^2 f^{-2}(s)$ and $g(t)$ is the solution to the following autonomous differential equation

$$gg'' - g'^2 = c \left(g'^2 - (cg)^2 \right)^2, \ a, b \in \mathbb{R}, \ a, b, c \neq 0$$

We also provide an example admits a solution when H depends on only one variable.

2. Preliminaries

The *pseudo-Galilean distance* between the points $\mathbf{p} = (p_1, p_2, p_3)$ and $\mathbf{q} = (q_1, q_2, q_3)$ is

$$d\left(\mathbf{p}, \mathbf{q}\right) = \begin{cases} |q_1 - p_1|, & p_1 \neq q_1 \\ \sqrt{\left|(q_2 - p_2)^2 - (q_3 - p_3)^2\right|}, & p_1 = q_1 \end{cases}$$

Let $a_1, .., a_5, \varphi$ be some constants. Then, the six-parameter group of motions of G_3^1 which leaves invariant the absolute figure and pseudo-Galilean distance is given in terms of affine coordinates by

$$\begin{aligned} \overline{x} &= a_1 + x \\ \overline{y} &= a_2 + a_3 x + y \cosh \varphi + z \sinh \varphi \\ \overline{z} &= a_4 + a_5 x + y \sinh \varphi + z \cosh \varphi \end{aligned}$$

A line in G_3^1 is said to be *isotropic* if its intersection with the absolute line f is non-empty and *non-isotropic* otherwise. A vector $\mathbf{v} = (v_1, v_2, v_3)$ is said to be *isotropic* (*non-isotropic*) if $v_1 = 0$ ($\neq 0$). Let $\mathbf{w} = (w_1, w_2, w_3)$ and $\langle \cdot, \cdot \rangle_G$ denote the *pseudo-Galilean dot product.* Then, $\langle \mathbf{v}, \mathbf{w} \rangle_G$ is the Lorentzian scalar product if both $\mathbf{v}$ and $\mathbf{w}$ are isotropic. Otherwise, $v_1^2 + w_1^2 \neq 0$, it is defined by $\langle \mathbf{v}, \mathbf{w} \rangle_G = v_1 w_1$. The pseudo-Galilean angle between $\mathbf{v}$ and $\mathbf{w}$ is defined as the Lorentzian angle if $\mathbf{v}$ and $\mathbf{w}$ are isotropic. Otherwise, it is given by the pseudo-Galilean distance. We call $\mathbf{v}$ and $\mathbf{w}$ *orthogonal* if $\langle \mathbf{v}, \mathbf{w} \rangle_G = 0$.

An isotropic vector $\mathbf{v}$ is called *spacelike* if $\langle \mathbf{v}, \mathbf{v} \rangle_L > 0$; *timelike* if $\langle \mathbf{v}, \mathbf{v} \rangle_L < 0$ and *lighlike* if $\langle \mathbf{v}, \mathbf{v} \rangle_L = 0$. Let $\{\mathbf{e}_1, \mathbf{e}_2, \mathbf{e}_3\}$ be standard basis vectors and $\mathbf{v}$ and $\mathbf{w}$ no both isotropic vectors. Then, the *pseudo-Galilean cross-product* is

$$\mathbf{v} \times_G \mathbf{w} = \begin{vmatrix} 0 & -\mathbf{e}_2 & \mathbf{e}_3 \\ v_1 & v_2 & v_3 \\ w_1 & w_2 & w_3 \end{vmatrix}$$

Then, $\langle \mathbf{v} \times_G \mathbf{w}, \mathbf{z} \rangle_G = -\det(\mathbf{v}, \mathbf{w}, \tilde{\mathbf{z}})$, where $\tilde{\mathbf{z}}$ is the projection of $\mathbf{z}$ onto the $yz-$plane. Note that the vector $\mathbf{v} \times_G \mathbf{w}$ is orthogonal to the vectors $\mathbf{v}$ and $\mathbf{w}$.

Let S be a surface in G_3^1 locally given by a regular map

$$(u_1, u_2) \mapsto \mathbf{x}(u_1, u_2) = (x(u_1, u_2), y(u_1, u_2), z(u_1, u_2)), \quad (u_1, u_2) \in D \subset \mathbb{R}^2$$

Denote $x_{,i} = \frac{\partial x}{\partial u_i}$ and $x_{,ij} = \frac{\partial^2 x}{\partial u_i \partial u_j}$ and etc., $1 \leq i, j \leq 2$. Then, S is said to be *admissible* if $x_{,i} \neq 0$ for some $i = 1, 2$. For such an admissible surface S, the *first fundamental form* is

$$\langle d\mathbf{x}, d\mathbf{x} \rangle_G = E du_1^2 + 2F du_1 du_2 + G du_2^2$$

where $E = (x_{,1})^2$, $F = x_{,1} x_{,2}$, $G = (x_{,2})^2$. Since nowhere an admissible surface has Lorentzian tangent plane, up to the absolute figure, the isotropic vector $\mathbf{x}_{,1} \times_G \mathbf{x}_{,2}$ is *normal* to S. Let

$$W = \langle \mathbf{x}_{,1} \times_G \mathbf{x}_{,2}, \mathbf{x}_{,1} \times_G \mathbf{x}_{,2} \rangle_L$$

Then, the surface S is called *spacelike* if $W < 0$; *timelike* if $W > 0$; and *lightlike* if $W = 0$. The spacelike and timelike surfaces are so-called *non-degenerate* and, throughout this study, we deal with the only non-degenerate admissible surfaces. The *unit normal vector* to the non-degenerate surface S is

$$\mathbf{N} = \frac{\mathbf{x}_{,1} \times_G \mathbf{x}_{,2}}{\sqrt{|W|}}$$

Let $\epsilon = \langle \mathbf{N}, \mathbf{N} \rangle_L = \pm 1$ and

$$L_{ij} = \epsilon \frac{1}{x_{,1}} \left\langle x_{,1} \tilde{\mathbf{x}}_{,ij} - (x_{,i})_{,j} \tilde{\mathbf{x}}_{,1}, \mathbf{N} \right\rangle_L = \epsilon \frac{1}{x_{,2}} \left\langle x_{,2} \tilde{\mathbf{x}}_{,ij} - (x_{,i})_{,j} \tilde{\mathbf{x}}_{,2}, \mathbf{N} \right\rangle_L$$

in which one of $x_{,1}$ and $x_{,2}$ is always nonzero due to the admissibility. Then, the *second fundamental form* of S is

$$II = Ldu_1^2 + 2Mdu_1du_2 + Ndu_2^2$$

where $L = L_{11}$, $M = L_{12}$, $N = L_{22}$. Thereby, *the Gaussian and mean curvatures* are defined by

$$K = -\epsilon \frac{LN - M^2}{W} \text{ and } H = -\epsilon \frac{GL - 2FM + EN}{2W}$$

A surface is said to be *minimal* if H vanishes identically.

Let S be a ruled surface in G_3^1 locally given by

$$\mathbf{x}(u_1, u_2) = \gamma(u_1) + u_2 w(u_1)$$

where $\gamma(u_1)$ is a regular curve and $w(u_1)$ is a nonvanishing vector field along $\gamma(u_1)$. There are three types of such surfaces depending on the positions of $\gamma(u_1)$, $w(u_1)$ and the absolute figure:

- **Type 1:** $w(u_1)$ is non-isotropic and $\gamma(u_1)$ does not lie in a pseudo-Euclidean plane.

- **Type 2:** $w(u_1)$ is non-isotropic and $\gamma(u_1)$ lies in a pseudo-Euclidean plane.

- **Type 3:** $w(u_1)$ is isotropic and $\gamma(u_1)$ is an arbitrary curve lying a plane orthogonal to $w(u_1)$.

3. The Graphs of Type 1

Let the graph $z(x, y) = f(x)g(y)$ be of type 1, then

$$\mathbf{r}(x, y) = (x, y, f(x)g(y)), \quad (s, t) \in I \times J \subset \mathbb{R}^2$$

The Gaussian curvature is

$$K = \frac{fgf''g'' - (f'g')^2}{\left[1 - (fg')^2\right]^2} \tag{9}$$

where a prime denotes the derivative with respect to the related variable. We study the case that K is a non-constant function; that is, at least a partial derivative of K with respect to x and y is non-vanishing. It is equivalent to the statement that the first derivatives of both f and g are nonzero on $I \times J$.

In the following we obtain the graphs with $K(x, y) = k(x)$ where $k(x)$ is some smooth function of x.

Theorem 3.1. If the Gaussian curvature $K(x, y)$ of the graph $z(x, y) = f(x)g(y)$ is a non-constant function depending one variable then it is of the form $K(x, y) = k(x)$, where $k(x)$ is some negative smooth function of x. Furthermore, the graph is a cylindrical ruled surface of type 3 such that, up to a translation of y,

$$z(x, y) = \pm y \tanh\left(\pm \int^x \sqrt{-k(s)}ds\right)$$

PROOF. Since there is not a symmetry in Equation (9) up to the functions f and g, we distinguish two cases:

1. **Case** $(\partial K/\partial y)(x, y) = 0$. We set $K(x, y) = k(x)$, for some smooth function $k(x)$. Then,

$$k(x) = \frac{fgf''g'' - (f'g')^2}{\left[1 - (fg')^2\right]^2} \tag{10}$$

Here, if there is a point $y_0 \in J$ such that $g''(y_0) = 0$ then we may assume $g'' = 0$ on a neighborhood of y_0 in J. Letting $g' = c$, $c \neq 0$, (10) is now

$$k(x) = \frac{-c^2 f'^2}{(1 - c^2 f^2)^2}$$

which implies that $k(x)$ is a negative function. Notice that, up to a translation of y, the graph is written by

$$\mathbf{r}(x, y) = (x, 0, 0) + y(0, 1, cf(x))$$

which is a parametrization of a ruled surface of type 3. Here $f(x)$ is the solution to

$$\frac{cf'}{1 - c^2 f^2} = \pm\sqrt{-k(x)}$$

Integrating gives

$$f(x) = |c|^{-1} \tanh\left(\pm \int^x \sqrt{-k(s)} ds\right)$$

which proves the result. Next, we will show that Equation (10) has no a solution provided $g''(y) \neq 0$ on J. In order to overcome difficulties in our calculations we introduce

$$\begin{aligned}
\alpha_1 &= ff'' \\
\alpha_2 &= -f'^2 \\
\alpha_3 &= -f^2
\end{aligned}$$

Then, Equation (10) turns into

$$k(x) = \frac{\alpha_1 gg'' + \alpha_2 g'^2}{(1 + \alpha_3 g'^2)^2} \tag{11}$$

We observe two subcases;

(a) **Subcase** $\alpha_1 \neq 0$. Then,

$$\frac{k(x)}{\alpha_1}\left(1 + \alpha_3 g'^2\right)^2 - \left(\frac{\alpha_2}{\alpha_1}\right) g'^2 = gg'' \tag{12}$$

By taking derivative of Equation (12) with respect to x we obtain

$$\sum_{n=0}^{4} P_n \left(g'\right)^n = 0$$

where

$$\begin{aligned}
P_0 &= \left(k(x)/\alpha_1\right)' \\
P_1 &= 0 \\
P_2 &= 2\left(k(x)/\alpha_1\right)' \alpha_3 + 2\left(k(x)/\alpha_1\right)\alpha_3' - \left(\alpha_2/\alpha_1\right)' \\
P_3 &= 0 \\
P_4 &= \left(k(x)/\alpha_1\right)' \alpha_3^2 + 2\left(k(x)/\alpha_1\right)\alpha_3\alpha_3'
\end{aligned}$$

Because of the fact that g' is a non-constant function of y, $P_0, ..., P_4$ are zero all. From $P_0 = 0$ we get $\left(k(x)/\alpha_1\right)' = 0$, implying the existence of some nonzero constant c such that $k(x) = c\alpha_1$. Then, using this in $P_4 = 0$ we obtain $4cf^3 f' = 0$ which allows $k(x)$ to be zero. This is not possible by our assumption.

(b) **Subcase** $\alpha_1 = 0$. Then, because $\alpha_1 = ff''$, concludes $\alpha_2 = c$, $c \neq 0$. Therefore considering this in Equation (11) and next taking derivative with respect to y we obtain $g'' = 0$, which is a contradiction.

2. **Case** $(\partial K/\partial x)(x, y) = 0$. We set $K(x, y) = k(y)$, for some smooth function $k(y)$. Then, follows

$$k(y) = \frac{\alpha_1 g g'' + \alpha_2 g'^2}{[1 + \alpha_3 g'^2]^2} \tag{13}$$

where if g is a linear function then the left hand side of (13) is a function of y and the other side is a function of x. Thus, g cannot be a linear function by our assumption. Next, let $g'' \neq 0$. Then, by replacing $k(x)$ with $k(y)$ in Equation (12) we may easily show that no (13) has a solution.

$\square$

Example 3.2. Take $z(x, y) = f(x)g(y)$ with $K(x, y) = -4x^2$. By Theorem 3.1, we have $z(x, y) = y \tanh(x^2)$ up to a translation of x. One can be drawn as in Fig. 1.
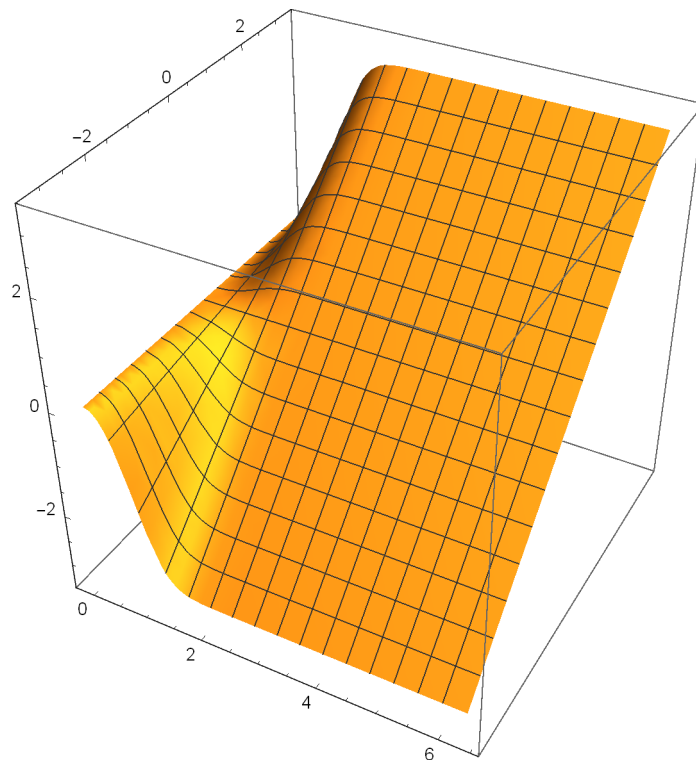
Fig. 1. Graph of $z(x, y) = y \tanh(x^2)$ with $0 \leq x \leq 2\pi$ and $-\pi \leq y \leq \pi$. The Gaussian curvature is $K(x, y) = x^2$.

We are also interested in the graphs $z(x, y) = f(x)g(y)$ whose mean curvature is non-vanishing function of one variable and present the following results:

Theorem 3.3. If the mean curvature H of the graph $z(x, y) = f(x)g(y)$ is a non-constant function depending one variable then it is of the form $H(x, y) = h(y)$, where $h(y)$ is some smooth function of y, and the graph is a cylindrical ruled surface of type 3 such that

$$z(x, y) = cg(y) = 2 \int^y q(s)(1 + 4q(s))^{-1/2} \, ds \tag{14}$$

where $q(y) = \int^y h(s) \, ds$ and c is a non-zero constant.

PROOF. We distinguish two cases:

1. $(\partial H/\partial x)(x,y) = 0$. We set $H(x,y) = h(y)$, for some smooth function $h(y)$. Then, we have

$$h(y) = \frac{fg''}{2\left[1 - (fg')^2\right]^{3/2}} \qquad (15)$$

   Suppose that f is non-constant function. By squaring we write

$$4h^2(y)\left[1 - (fg')^2\right]^3 - f^2 g''^2 = 0$$

   which is a polynomial equation of degree 6 on f whose leading coefficient is $-4h^2(y)g'^6$. Since $h(y)$ is nowhere vanish, we obtain a contradiction. Therefore we have $f = c$, where c is a nonzero constant. So the graph parameterizes as

$$x(1,0,0) + (0,y,cg(y))$$

   which is locally a cylindrical ruled surface of type 3. The result follows by integrating (15).

2. **Case** $(\partial H/\partial y)(x,y) = 0$. We set $H(x,y) = h(x)$, for some smooth function $h(x)$. Then, follows

$$h(x) = \frac{fg''}{2\left[1 - (fg')^2\right]^{3/2}} \qquad (16)$$

   in which f cannot be constant function because otherwise the left hand side is a function of x and the other side is a function of y. In such a case, divide (16) with $f/2$ and derivative with respect to y, obtaining

$$\left(3g'g''^2 - g'^2 g'''\right) f^2 + g''' = 0$$

   Here is clear that the coefficients are not zero all, which is not possible. This completes the proof.

$$\square$$

4. The Graphs of Type 2

Consider the graph $x(y,z) = f(y)g(z)$, $(y,z) \in I \times J$. Then,

$$\mathbf{r}(y,z) = (f(y)g(z), y, z), \quad (s,t) \in I \times J \subset \mathbb{R}^2$$

The Gaussian curvature is

$$K(y,z) = \frac{fgf''g'' - (f'g')^2}{\left[(fg')^2 - (f'g)^2\right]^2} \qquad (17)$$

Here we point out $f', g' \neq 0$ on $I \times J$ because K is a non-constant function in our case.

Thus we present the following result:

Theorem 4.1. If the Gaussian curvature K of the graph $x(y,z) = f(y)g(z)$ is a non-constant function of one variable then, up to a change in the roles of the functions f, g, $f(y) = ae^{by}$ and the following autonomous differential equation holds

$$gg'' - g'^2 = c\left(g'^2 - (cg)^2\right)^2, \quad a, b \in \mathbb{R}, \ a, b, c \neq 0$$

Furthermore, $K = c\left(ab^{-1}e^{by}\right)^{-2}$.

PROOF. Assume K is a non-constant function of one variable. Notice that the roles of f and g in Equation (17) are symmetric and therefore we only focus on the case $K = k(y)$. We previously observe the following cases:

1. **Case** $f(y) = cy + d$, $c, d \in \mathbb{R}$, $c \neq 0$. Then, Equation (17) is now

$$\pm\sqrt{-k(y)} = \frac{cg'}{(fg')^2 - (cg)^2} \tag{18}$$

   The partial derivative of (18) with respect to z is

$$-cg'^2 g'' f^2 - c^3 g^2 g'' + 2c^3 g g'^2 = 0$$

   which is a polynomial equation of degree 2 on f. Because k is nonzero function, the coefficients are not zero all, which is a contradiction. Then, f cannot be a linear function. Similarly, if g is a linear function then we easily arrive the contradiction $f' = 0$. This discussion gives us that f and g must be non-linear functions.

2. **Case** $f' = cf^d$, $c, d \in \mathbb{R}$, $c, d \neq 0$.. Then, the following two sub-cases are provided:

   (a) **Subcase** $d = 1$. Then, $f(y) = ae^{cy}$, $a \in \mathbb{R}$, $a \neq 0$. Equation (17) is

$$c^{-2} f^2 k(y) = \frac{gg'' - g'^2}{[g'^2 - (cg)^2]^2} \tag{19}$$

   where the left hand side is a function of y and the other hand side is a function of z. Then, there exists a nonzero constant λ such that $c^{-2} f^2 k(y) = \lambda$ and

$$gg'' - g'^2 = \lambda \left(g'^2 - (cg)^2\right)^2$$

   which gives the result.

   (b) **Subcase** $d \neq 1$. Equation (17) imply that

$$(c^2 f^{2d-4})^{-1} k(y) = \frac{dgg'' - g'^2}{(g'^2 - c^2 f^{2d-2} g^2)^2} \tag{20}$$

   Letting $dgg'' - g'^2 = T$ and next derivating with respect to z of Equation (20) we obtain

$$T'g'^2 - 4Tg'g'' - c^2 \left(T'g^2 - 4Tgg'\right) f^{2d-2} = 0$$

   which is polynomial equation on f. Using the equality of coefficients we derive following equations

$$T'g'^2 - 4Tg'g'' = 0$$
$$T'g^2 - 4Tgg' = 0$$

   From these equations, we have the contradiction $g' = bg$, $b = const$.

3. **Case** that f is neither a linear function nor of the form $f' = cf^d$. Then, derivating of (17) with respect to z

$$ff'' \left[(g'g'' + gg''') \left(g'^2 - g^2\right) - 4gg'' \left(g'g'' - gg'\right)\right] + 4f'^2 g'^2 \left(g'g'' - gg'\right)$$
$$- 2f'^2 g'g'' \left(g'^2 - g^2\right) = 0$$

   Since $f' \neq 0$, we obtain

$$\frac{ff''}{f'^2} = \frac{-4g'^2 (g'g'' - gg') + 2g'g''(g'^2 - g^2)}{(g'g'' + gg''')(g'^2 - g^2) - 4gg''(g'g'' - gg')}$$

   The left hand side is a function of y while the other side is a function of z. Then, both hand sides are a constant, which contradicts with our assumption.

□

The mean curvature of the graph $x(y, z) = f(y)g(z)$ is given by

$$H = \frac{(fg')^2 f'' g - 2fg(f'g')^2 + (f'g)^2 fg''}{2\left[(fg')^2 - (f'g)^2\right]^{3/2}} \tag{21}$$

Apart from the previous results, we could not completely solve our problem when $H(y, z)$ is nonconstant and

$$\frac{\partial H(y, z)}{\partial y} = 0 \text{ or } \frac{\partial H(y, z)}{\partial z} = 0 \tag{22}$$

But we have an example indicating the existence of the graphs $x(y, z) = f(y)g(z)$ when Equation (22) holds.

Example 4.2. Let $a, b, c \in \mathbb{R} - \{0\}$, up to a change in the roles of the functions f, g, $g(z) = ae^{bz}$ and

$$f(y) = c \exp\left(\pm \int^y \left(\left(2a \int^y h(s)ds\right)^{-2} + a^{-2}\right)^{-1/2} ds\right) \tag{23}$$

Then, the mean curvature of the graph $x(y, z) = f(y)g(z)$ only depends on the variable y.

For the solution of Example, we set $\alpha = \frac{f}{f'}$ and $\beta = \frac{g}{g'}$. Then, Equation (21) is now

$$H(x, y) = -\frac{\alpha\beta(\alpha' + \beta')}{2(\alpha^2 - \beta^2)^{3/2}} \tag{24}$$

Up to a change in the roles of the functions f, g, suppose that β is constant, or equivalently, $g(z) = ae^{bz}$, for some nonzero constants a, b. Equation (24) is

$$-2aH(x, y) = \frac{\alpha\alpha'}{(\alpha^2 - a^{-2})^{3/2}} \tag{25}$$

which means that $H(x, y)$ only depends on the variable y. Put $H(x, y) = h(y)$, for some smooth function $h(y)$. Integrating Equation (25) gives the result of Example.

5. Conclusion

In this paper factorable surfaces are classified when the mean and Gaussian curvatures are functions of one variable in the pseudo-Galilean space. We have obtained that if the Gaussian curvature K of the graph $z(x, y) = f(x)g(y)$ is a non-constant function of one variable then it is a negative function of the form $K = k(x)$. Furthermore, the graph is a cylindrical ruled surface of type 3 and if the mean curvature H of the graph $z(x, y) = f(x)g(y)$ is a non-constant function of one variable then it is of the form $H = h(y)$ and the graph is a cylindrical ruled surface of type 3. Also we have shown that there does not exist a graph $x(y, z) = f(y)g(z)$ in G_3^1 when its mean curvature depends on one variable.

Author Contributions

All authors contributed equally to this work. They all read and approved the last version of the manuscript.

Conflicts of Interest

The authors declare no conflict of interest.

References

[1] O. Giering, Vorlesungen über höhere Geometrie, Friedr Vieweg & Sohn, Braunschweig, Germany, 1982.

[2] B. Divjak and Z. Milin-Sipus, *Special Curves on Ruled Surfaces in Galilean and Pseudo-Galilean Spaces*, Acta Mathematica Hungarica 98 (1) (2003) 203–215.

[3] E. Mólnar, *The Projective Interpretation of the Eight 3-Dimensional Homogeneous Geometries*, Beitrage zur Algebra und Geometrie 38 (2) (1997) 261–288.

[4] A. Onishchick and R. Sulanke, Projective and Cayley-Klein Geometries, Springer, 2006.

[5] I. M. Yaglom, A Simple Non-Euclidean Geometry and Its Physical Basis, Springer-Verlag, New York, 1979.

[6] B. Y. Chen, G. E. Vîlcu, *Geometric Classifications of Homogeneous Production Functions*, Applied Mathematics and Computation 225 (2013) 345–351.

[7] B. Y. Chen, *A Note on Homogeneous Production Models*, Kragujevac Journal of Mathematics 36 (1) (2012) 41–43.

[8] B. Y. Chen, *Solutions to Homogeneous Monge-Ampère Equations of Homothetic Functions and Their Applications to Production Models in Economics*, Journal of Mathematical Analysis and Applications 411 (2014) 223–229.

[9] M. J. P. Cullen, R. J. Douglas, *Applications of the Monge-Ampè re equation and Monge transport problem to meterology and oceanography*, In: L. A. Caffarelli, M. Milman (eds.), NSF-CBMS Conference on the Monge Amp'ere Equation, Applications to Geometry and Optimization, July 9-13, Florida Atlantic University, 1997, pp. 33–54.

[10] D. Gilbarg, N. S. Trudinger, Elliptic Partial Differential Equations of Second Order, Berlin, Springer-Verlag, 1983.

[11] V. Ushakov, *The Explicit General Solution of Trivial Monge-Ampère Equation*, Commentarii Mathematici Helvetici 75 (2000) 125–133.

[12] M. E. Aydın, M. Alyamac Külahcı, A.O. Öğrenmis, *Constant Curvature Translation Surfaces in Galilean 3-Space*, International Electronic Journal of Geometry 12 (1) (2019) 9–19.

[13] A. Kelleci, *Translation-Factorable Surfaces with Vanishing Curvatures in Galilean 3-Spaces,* International Journal of Maps in Mathematics 4 (1) (2021) 14–26.

[14] Z. Milin-Sipus, B. Divjak, *Translation Surface in the Galilean Space*, Glasnik Matematicki 46 (66) (2011) 455–469.

[15] Z. Milin-Sipus, *On a Certain Class of Translation Surfaces in a Pseudo-Galilean Space*, International Mathematical Forum 6 (23) (2011) 1113–1125.

[16] D. W. Yoon, *Some Classification of Translation Surfaces in Galilean 3-Space*, International Journal of Mathematical Analysis 6 (28) (2012) 1355–1361.

[17] M.E. Aydın, S. Aykurt Sepet, H. Gün Bozok, *Translation Surfaces in Pseudo-Galilean Space with Prescribed Mean and Gaussian Curvatures*, Honam Mathematical Journal 44 (1) (2022) 36–51.

[18] G. Ruiz-Hernández, *Translation Hypersurfaces whose Curvature Depends Partially on Its Variables*, Journal of Mathematical Analysis and Applications 497 (2) (2021) 124913.

[19] C. Baikoussis, T. Koufogioros, *Helicoidal Surface with Prescribed Mean or Gauss Curvature*, Journal of Geometry 63 (1998) 25–29.

[20] K. Kenmotsu, *Surface of Revolution with Prescribed Mean Curvature*, Tohoku Mathematical Journal 32 (1980) 147–153.

[21] I. Van de Woestyne, *Minimal Homothetical Hypersurfaces of a Semi-Euclidean Space*, Results in Mathematics 27 (1995) 333–342.

[22] H. S. Abdel-Aziz, M. Khalifa Saad, A. Ali Haytham, *Affine Factorable Surfaces in Pseudo-Galilean Space*, arXiv:1812.00765v1[math.GM].

[23] P. Bansal, M. H. Shahid, *On Classification of Factorable Surfaces in Galilean Space G_3*, Jordan Journal of Mathematics and Statistics 12 (3) (2019) 289–306.

[24] M. S. Lone, *Homothetical Surfaces in Three Dimensional Pseudo-Galilean Spaces Satisfying $\triangle^{II}$* $\mathbf{x}_i = \lambda_i \mathbf{x}_i$, Advances in Applied Clifford Algebras 29 (92) (2019).

[25] M. E. Aydın, A. O. Öğrenmis, M. Ergüt, *Classification of Factorable Surfaces in the Pseudo-Galilean Space*, Glasnik Matematicki 70 (50) (2015) 441–451.

[26] M. E. Aydın, M. Alyamac Külahcı, A. O. Öğrenmis, *Non-Zero Constant Curvature Factorable Surfaces in Pseudo-Galilean Space*, Communications of the Korean Mathematical Society 33 (1) (2018) 247–259.

[27] B. Divjak, Z. Milin-Sipus, *Minding Isometries of Ruled Surfaces in Pseudo-Galilean Space*, Journal of Geometry 77 (2003) 35–47.

New Theory Journal of

Number 40 Year 2022

New Theory Journal of

ISSN: 2149-1402

Editor-in-Chief
Naim Çağman

www.dergipark.org.tr/en/pub/jnt

Salkowski Curves and Their Modified Orthogonal Frames in $\mathbb{E}^3$

Sümeyye Gür Mazlum[1] 🄳 , **Süleyman Şenyurt**[2] 🄳 , **Mehmet Bektaş**[3] 🄳

Abstract — In this study, we examine some properties of Salkowski curves in $\mathbb{E}^3$. We then make sense of the angle (nt) in the parametric equation of the Salkowski curves. We provide the relationship between this angle and the angle between the binormal vector and the Darboux vector of the Salkowski curves. Through this angle, we obtain the unit vector in the direction of the Darboux vector of the curve. Finally, we calculate the modified orthogonal frames with both the curvature and the torsion and give the relationships between the Frenet frame and the modified orthogonal frames of the curve.

Keywords — *Salkowski curves, modified orthogonal frame, Frenet frame*

Mathematics Subject Classification (2020) — 53A04, 53A55

1. Introduction

In differential geometry, the Frenet frame of a continuous differentiable regular curve in Euclidean space $\mathbb{E}^3$ describe the geometric properties of any point moving along the curve. If $\{T(t), N(t), B(t)\}$ is the Frenet frame of any regular curve α in Euclidean space $\mathbb{E}^3$, here, the vector $T(t)$ (resp. $N(t)$ and $B(t)$) is called tangent vector (normal vector and binormal vector) [1, 2]. In Euclidean 3-space, the curves whose principal normal vector makes a constant angle with a fixed direction are called slant helices. Kula et al. [3] studied on the slant helices in Euclidean space $\mathbb{E}^3$. Ali [4] obtained the position vectors of slant helices Euclidean space $\mathbb{E}^3$. In a paper published by Salkowski [5], a curve family, whose curvature is constant but torsion is not, has been defined. In a study done by Monterde [6], it is found out that base normal vectors of Salkowski curves make a constant angle with a constant line. The Frenet vectors and the geodesic curvatures of the spherical indicatrix curves belong to Salkowski curves in $\mathbb{E}^3$ are calculated in [7]. The Smarandache curves according to Frenet frame of Salkowski curves are studied in [8]. Moreover, the modified orthogonal frame of a space curve in Euclidean space $\mathbb{E}^3$ was described by Sasai [9, 10] as a useful tool for investigating analytic curves with singular points where the Frenet frame does not work. The authors in [11–14] obtained the modified orthogonal frame of a space curve and its spherical curves in Euclidean and Minkowski 3-space. Arıkan and Nurkan [15] had a paper on adjoint curve according to modified orthogonal frame with torsion in Euclidean 3-space. Furthermore, there are many studies on the frames of various curves or surfaces in Euclidean 3-space, [16–25]. In another study, we [26] examined the modified frames with both the non-zero curvature and the torsion of the non-unit speed curves in Euclidean space $\mathbb{E}^3$. In

[1]sumeyyegur@gumushane.edu.tr (Corresponding Author); [2]ssenyurt@odu.edu.tr; [3]mbektas@firat.edu.tr
[1]Department of Computer Technology, Kelkit Aydın Doğan Vocational School, Gümüşhane University, Gümüşhane, Türkiye
[2]Department of Mathematics, Faculty of Arts and Sciences, Ordu University, Ordu, Türkiye
[3]Department of Mathematics, Faculty of Science, Fırat University, Elazığ, Türkiye

this study, it has been shown that Salkowski curves in $\mathbb{E}^3$ is not a unit speed curve. Therefore, the torsion of Salkowski curves is investigated. The Frenet derivative formulas are obtained for this curve. Besides, the angle (nt) is made sense and the relationship between this angle and the angle between the binormal vector and the Darboux vector of Salkowski curves is given. By means of this angle, the unit vector in the direction of this vector and the Darboux vector of the curve is calculated. Finally, based on the work [26] done on calculating the modified orthogonal frame of a non-unit speed curve, the modified orthogonal frames with the both curvature and torsion of Salkowski curves are calculated. And relations between the modified orthogonal frames and the Frenet frame of Salkowski curves in Euclidean 3-space are given.

2. Preliminary

Let the curve $\alpha(t)$ be a differentiable space curve in $\mathbb{E}^3$. Frenet vectors (the tangent, binormal and principal normal vectors), the curvature and the torsion of this curve are given as follows:

$$T(t) = \frac{\alpha'(t)}{v(t)}, \quad B(t) = \frac{\alpha'(t) \wedge \alpha''(t)}{\|\alpha'(t) \wedge \alpha''(t)\|}, \quad N(t) = B(t) \wedge T(t) \tag{1}$$

$$\kappa(t) = \frac{\|\alpha'(t) \wedge \alpha''(t)\|}{v^3(t)}, \ and \ \tau(t) = \frac{\det\left(\alpha'(t), \alpha''(t), \alpha'''(t)\right)}{\|\alpha'(t) \wedge \alpha''(t)\|^2} \tag{2}$$

respectively. Here, $v(t) = \|\alpha'(t)\|$. Frenet derivative formulas of this curve [2] are as follows:

$$\begin{bmatrix} T'(t) \\ N'(t) \\ B'(t) \end{bmatrix} = \begin{bmatrix} 0 & v(t)\kappa(t) & 0 \\ -v(t)\kappa(t) & 0 & v(t)\tau(t) \\ 0 & -v(t)\tau(t) & 0 \end{bmatrix} \begin{bmatrix} T(t) \\ N(t) \\ B(t) \end{bmatrix} \tag{3}$$

The Darboux vector $W(t)$ of the non-unit speed curve $\alpha(t)$ is as follows:

$$W(t) = N(t) \wedge N'(t) = v(t)\left(\tau(t)T(t) + \kappa(t)B(t)\right) \tag{4}$$

The unit vector $C(t)$ in direction of the vector $W(t)$ of the non-unit speed curve $\alpha(t)$ is

$$C(t) = v(t) \left(\frac{\tau(t)}{\sqrt{\kappa^2(t) + \tau^2(t)}} T(t) + \frac{\kappa(t)}{\sqrt{\kappa^2(t) + \tau^2(t)}} B(t) \right) \tag{5}$$

or if the angle between of the vectors $B(t)$ and $W(t)$ of the curve $\alpha(t)$ is $\varphi(t)$, then the unit vector [27] is

$$C(t) = \sin\varphi T(t) + \cos\varphi B(t) \tag{6}$$

If $v(t) = 1$, then the curve $\alpha(t)$ is called unit speed curve. Let us create the following vectors for the curve $\alpha(t)$:

$$E_1(t) = \alpha'(t), \quad E_2(t) = E_1'(t), \quad E_3(t) = E_1(t) \wedge E_2(t) \tag{7}$$

These vectors form an orthogonal frame. If $\alpha(t)$ is a unit speed curve and its curvature is non-zero, we can write these vectors in terms of Frenet vectors of the curve as following [9]:

$$E_1(t) = T(t), \quad E_2(t) = \kappa(t)N(t), \quad E_3(t) = \kappa(t)B(t) \tag{8}$$

where,

$$\langle E_1(t), E_1(t)\rangle = 1, \quad \langle E_2(t), E_2(t)\rangle = \langle E_3(t), E_3(t)\rangle = \kappa^2(t) \tag{9}$$

In this case, this frame obtained for the curve is called a modified orthogonal frame with the curvature $\kappa(t)$ of the curve $\alpha(t)$. There are the following relationships between these vectors and them derivative vectors:

$$
\begin{bmatrix} E_1'(t) \\ E_2'(t) \\ E_3'(t) \end{bmatrix} = \begin{bmatrix} 0 & 1 & 0 \\ -\kappa^2(t) & \dfrac{\kappa'(t)}{\kappa(t)} & \tau(t) \\ 0 & -\tau(t) & \dfrac{\kappa'(t)}{\kappa(t)} \end{bmatrix} \begin{bmatrix} E_1(t) \\ E_2(t) \\ E_3(t) \end{bmatrix}
\tag{10}
$$

The parametric equation of Salkowski curves γ_m are as follows:

$$
\begin{aligned}
\gamma_m(t) = \ & \frac{1}{\sqrt{1+m^2}} \left(-\frac{1-n}{4(1+2n)} \sin\left((1+2n)\,t\right) - \frac{1+n}{4(1-2n)} \sin\left((1-2n)\,t\right) - \frac{1}{2}\sin t \ , \right. \\
& \frac{1-n}{4(1+2n)} \cos\left((1+2n)\,t\right) + \frac{1+n}{4(1-2n)} \cos\left((1-2n)\,t\right) + \frac{1}{2}\cos t, \\
& \left. \frac{1}{4m} \cos\left(2nt\right) \right)
\end{aligned}
$$

Figure 1. Here, $m \neq \pm\frac{1}{\sqrt{3}}, 0 \in \mathbb{R}$ and $n = \frac{m}{\sqrt{m^2+1}}$. Moreover, $\left\| \gamma_m'(t) \right\| = \frac{\cos(nt)}{\sqrt{m^2+1}}$; therefore, the curve is regular in the interval of $\left]-\frac{\pi}{2n}, \frac{\pi}{2n}\right[$. The curvature, the torsion and the Frenet vectors of the curve provided in [5,6] are as follows:

$$
\begin{aligned}
\kappa(t) &= 1 \\
\tau(t) &= -\tan\left(nt\right) \\
T(t) &= -\left(\cos t \cos\left(nt\right) + n \sin t \sin\left(nt\right), \cos\left(nt\right)\sin t - n \cos t \sin\left(nt\right), \frac{n}{m}\sin\left(nt\right) \right) \\
N(t) &= \frac{n}{m}\left(\sin t, -\cos t, -m \right) \\
B(t) &= -\left(\cos t \sin\left(nt\right) - n \cos\left(nt\right)\sin t, \sin t \sin\left(nt\right) + n \cos t \cos\left(nt\right), -\frac{n}{m}\cos\left(nt\right) \right)
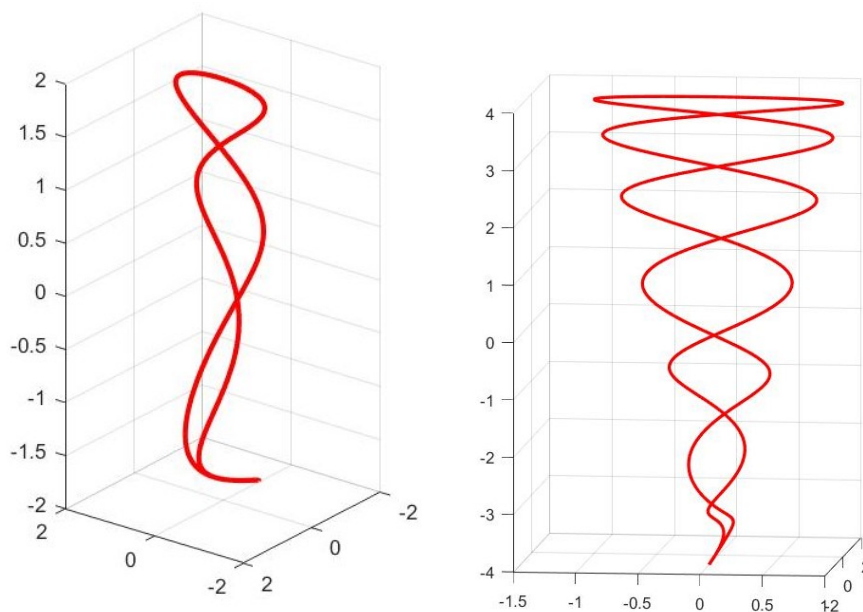\end{aligned}
$$

Fig. 1. Salkowski curves for $m = \frac{1}{8}$ and $m = \frac{1}{16}$

3. The Some Properties of Salkowski Curves in $\mathbb{E}^3$

In this section, we show whether Salkowski curves in $\mathbb{E}^3$ are a unit speed curve. We obtain the its torsion and the Frenet derivative formulas. Also, we make sense the angle (nt) and give the relationship between this angle and the angle between the binormal vector and the Darboux vector of Salkowski curves. By means of this angle, we get the Darboux vector of the curve and the unit vector in the direction of this vector.

3.1. Are Salkowski Curves in $\mathbb{E}^3$ Unit Speed Curves?

First, let us examine whether Salkowski curves are a unit speed curve. If we take first derivative according to the parameter t of Salkowski curves $\gamma_m(t)$, we get

$$\gamma_m'(t) = -\frac{n}{m}\cos(nt)\left(\cos t\cos(nt) + n\sin t\sin(nt), \cos(nt)\sin t - n\cos t\sin(nt), \frac{n}{m}\sin(nt)\right) \quad (11)$$

The norm of the Equation 11 is

$$\left\|\gamma_m'(t)\right\| = v(t) = \frac{n}{m}\cos(nt) = \frac{\cos(nt)}{\sqrt{m^2+1}} \quad (12)$$

If Salkowski curves were a unit speed curve, then we could write

$$\left\|\gamma_m'(t)\right\| = \frac{\cos(nt)}{\sqrt{m^2+1}} = 1$$

Hence, we get

$$\cos(nt) = \sqrt{m^2+1}$$

For the cosine function, since $-1 \leqslant \cos(nt) \leqslant 1$, we have

$$-1 \leqslant \sqrt{m^2+1} \leqslant 1$$

And thus, we obtain

$$-1 \leqslant m^2 \leqslant 0, \quad m^2 = 0, \ \ and \ m = 0$$

But in the definition of Salkowski curves, $m \neq 0$, this is a contradiction.

Corollary 3.1. Salkowski curves are not a unit speed curve.

3.2. The Torsion of Salkowski Curves in $\mathbb{E}^3$

The sign of torsion of Salkowski curves in [6] is regarded as $\tau(t) = \langle B'(t), N(t)\rangle$, thus the torsion of Salkowski curves is stated as $\tau(t) = \tan(nt)$. However, in [5], the torsion of Salkowski curves is given as $\tau(t) = -\tan(nt)$. We know the torsion of the a unit speed curve is found as $\tau(t) = \langle N'(t), B(t)\rangle = -\langle B'(t), N(t)\rangle$. But, we said that Salkowski curves are not a unit speed curve. Thus, to find the torsion of Salkowski curves, we use the following equation:

$$\tau(t) = \frac{\det\left(\gamma_m'(t), \gamma_m''(t), \gamma_m'''(t)\right)}{\left\|\gamma_m'(t) \wedge \gamma_m''(t)\right\|^2} \quad (13)$$

If we take second and third derivatives according to the parameter t of Salkowski curves $\gamma_m(t)$, we get

$$\begin{aligned}
\gamma_m''(t) &= \frac{n}{m}\cos(nt)\left(\cos(nt)\sin t + n\cos t\sin(nt) + n^2\sin t\left(\sin^2(nt) - \cos^2(nt)\right)\right. \\
&\quad - \cos t\cos(nt) + n\sin t\sin(nt) - n^2\cos t\left(\sin^2(nt) - \cos^2(nt)\right) \\
&\quad \left. + \frac{n^2}{m\cos(nt)}\left(\sin^2(nt) - \cos^2(nt)\right)\right)
\end{aligned} \quad (14)$$

$$\gamma_m'''(t) = \frac{n}{m}\cos(nt)\Big(\cos t\cos(nt) - 3n\sin t\sin(nt) + 4n^3\sin t\sin(nt)$$

$$\cos(nt)\sin t + 3n\cos t\sin(nt) - 4n^3\cos t\sin(nt), \frac{4n^3}{m}\sin(nt)\Big) \tag{15}$$

If we apply the vector product to the vectors 11 and 14, we have

$$\gamma_m'(t)\wedge\gamma_m''(t) = -\frac{n^3}{m^3}\cos^3(nt)\big(\cos t\sin(nt) - n\cos(nt)\sin t, \sin t\sin(nt) + n\cos t\cos(nt),$$

$$-\frac{n}{m}\cos(nt)\Big)$$

$$= -\frac{n^3}{m^3}\cos^3(nt)B(t) \tag{16}$$

Then, the norm of the Equation 16 is

$$\big\|\gamma_m'(t)\wedge\gamma_m''(t)\big\| = \frac{n^3}{m^3}\cos^3(nt) \tag{17}$$

If we apply the cross product the vectors 15 and 16, we get

$$\langle\gamma_m'(t)\wedge\gamma_m''(t),\gamma_m'''(t)\rangle = \frac{n^3}{m^3}\Big(-\frac{n}{m}\cos^2 t\cos^5(nt)\sin(nt) + \frac{n^2}{m}\cos t\sin t\cos^6(nt)$$

$$+\frac{3n^2}{m}\cos t\sin t\cos^4(nt)\sin^2(nt) - \frac{3n^3}{m}\sin^2 t\cos^5(nt)\sin(nt)$$

$$-\frac{4n^4}{m}\cos t\sin t\cos^4(nt)\sin^2(nt) + \frac{4n^5}{m}\sin^2 t\cos^5(nt)\sin(nt)$$

$$-\frac{n}{m}\sin^2 t\cos^5(nt)\sin(nt) - \frac{n^2}{m}\cos t\sin t\cos^6(nt)$$

$$-\frac{3n^2}{m}\cos t\sin t\cos^4(nt)\sin^2(nt) - \frac{3n^3}{m}\cos^2 t\cos^5(nt)\sin(nt)$$

$$+\frac{4n^4}{m}\cos t\sin t\cos^4(nt)\sin^2(nt) + \frac{4n^5}{m}\cos^2 t\cos^5(nt)\sin(nt)$$

$$+\frac{4n^5}{m^3}\cos^5(nt)\sin(nt)\Big)$$

$$\langle\gamma_m'(t)\wedge\gamma_m''(t),\gamma_m'''(t)\rangle = \frac{n^3}{m^3}\Big(-\frac{n}{m}\cos^5(nt)\sin(nt) - \frac{3n^3}{m}\cos^5(nt)\sin(nt)$$

$$+\frac{4n^5}{m}\cos^5(nt)\sin(nt) + \frac{4n^5}{m^3}\cos^5(nt)\sin(nt)\Big)$$

$$= -\frac{n^6}{m^6}\cos^5(nt)\sin(nt) \tag{18}$$

Then, if the Equations 17 and 18 are substituted in the Equation 13, we obtain the torsion of Salkowski curves as follows:

$$\tau(t) = -\tan(nt) \tag{19}$$

[5]. But numerous authors take $\tau(t) = \tan(nt)$ in the their studies. In this study, we will use the equality 19 for the torsion of Salkowski curves.

3.3. The Frenet Derivative Formulas of Salkowski Curves in $\mathbb{E}^3$

By using the Equations 12 and 19, the derivative vectors of the Frenet vectors $T(t), N(t), B(t)$ of Salkowski curves are obtained as follows:

$$T'(t) = \frac{n^2}{m^2}\cos(nt)(\sin t, -\cos t, -m)$$

$$= \frac{n}{m}\cos(nt)N(t) \tag{20}$$

$$
\begin{aligned}
N'(t) &= \frac{n}{m} \left(\cos t, \sin t, 0 \right) \\
&= \frac{n}{m} \Big(\cos t \cos^2 (nt) + \cos t \sin^2 (nt) + n \cos (nt) \sin t \sin (nt) - n \cos (nt) \sin t \sin (nt), \\
&\quad \cos^2 (nt) \sin t + \sin t \sin^2 (nt) - n \cos t \cos (nt) \sin (nt) + n \cos t \cos (nt) \sin (nt), \\
&\quad \frac{n}{m} \cos (nt) \sin (nt) - \frac{n}{m} \cos (nt) \sin (nt) \Big) \\
&= \frac{n}{m} \cos (nt) \Big(\cos t \cos (nt) + n \sin t \sin (nt), \cos (nt) \sin t - n \cos t \sin (nt), \frac{n}{m} \sin (nt) \Big) \\
&\quad + \frac{n}{m} \sin (nt) \Big(\cos t \sin (nt) - n \cos (nt) \sin t, \sin t \sin (nt) + n \cos t \cos (nt), -\frac{n}{m} \cos (nt) \Big) \\
&= -\frac{n}{m} \left(\cos (nt) T(t) + \sin (nt) B(t) \right) \tag{21}
\end{aligned}
$$

$$
\begin{aligned}
B'(t) &= \frac{n^2}{m^2} \sin (nt) (\sin t, -\cos t, -m) \\
&= \frac{n}{m} \sin (nt) N(t) \tag{22}
\end{aligned}
$$

We could have obtained these equations using the Equation 3, but we preferred to arrive at these equations by operations.

Corollary 3.2. The Frenet derivative formulas for Salkowski curves are as following:

$$
\begin{bmatrix} T'(t) \\ N'(t) \\ B'(t) \end{bmatrix} = \begin{bmatrix} 0 & \frac{n}{m} \cos (nt) & 0 \\ -\frac{n}{m} \cos (nt) & 0 & -\frac{n}{m} \sin (nt) \\ 0 & \frac{n}{m} \sin (nt) & 0 \end{bmatrix} \begin{bmatrix} T(t) \\ N(t) \\ B(t) \end{bmatrix} \tag{23}
$$

3.4. The Darboux Vector of Salkowski Curves in $\mathbb{E}^3$

Now, let us make sense of the angle (nt) for Salkowski curves. We know that the Darboux vector of any regular curve is found by

$$
W(t) = N(t) \wedge N'(t). \tag{24}
$$

Then, for the Darboux vector of Salkowski curves, we get

$$
\begin{aligned}
W(t) &= \frac{n}{m} (\sin t, -\cos t, -m) \wedge \frac{n}{m} (\cos t, \sin t, 0) \\
&= \frac{n^2}{m} \left(\sin t, -\cos t, \frac{1}{m} \right) \tag{25}
\end{aligned}
$$

Or, we can get it another way. If we use $\tau(t) = -\tan(nt)$, from the Equations 3 and 12, since Salkowski curves are not a unit speed curve, from the Equation

$$
W(t) = v(t) \left(\tau(t) T(t) + \kappa(t) B(t) \right),
$$

the Darboux vector of Salkowski curve is obtained as follows:

$$
\begin{aligned}
W(t) &= \frac{n}{m} \cos (nt) \big(\cos t \sin (nt) + n \sin t \sin (nt) \tan (nt) - \cos t \sin (nt) + n \cos (nt) \sin t, \\
&\quad \sin t \sin (nt) - n \cos t \sin (nt) \tan (nt) - \sin t \sin (nt) - n \cos t \cos (nt), \\
&\quad \frac{n}{m} \sin (nt) \tan (nt) + \frac{n}{m} \cos (nt) \big) \\
&= \frac{n^2}{m} \left(\sin t, -\cos t, \frac{1}{m} \right) \tag{26}
\end{aligned}
$$

Here we see the equality of Equations 25 and 26. Also, the norm of the Darboux vector is

$$\|W(t)\| = \frac{n}{m} \tag{27}$$

3.5. The Angle (nt) of Salkowski Curves in $\mathbb{E}^3$

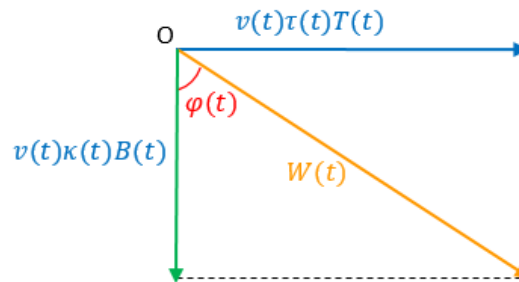Let the angle between the vectors $B(t)$ and $W(t)$ of Salkowski curves be $\varphi(t)$.

Fig. 2. The Darboux vector of Salkowski curves

In this case, from Figure 2, by using the Equation 27, we can write

$$
\begin{aligned}
\langle B(t), W(t) \rangle &= \|B(t)\| \, \|W(t)\| \cos \varphi \\
\\
&= \frac{n}{m} \cos \varphi
\end{aligned}
\tag{28}
$$

Also, if the inner product operation is applied to the vectors $B(t)$ and $W(t)$, we get

$$
\begin{aligned}
\langle B(t), W(t) \rangle &= -\frac{n^2}{m} \Big(\cos t \sin t \sin (nt) - n \sin^2 t \cos (nt) - \cos t \sin t \sin (nt) \\
&\quad - n \cos^2 t \cos (nt) - \frac{n}{m^2} \cos (nt) \Big) \\
&= -\frac{n^2}{m} \Big(-n \cos (nt) - \frac{n}{m^2} \cos (nt) \Big) \\
&= \frac{n}{m} \cos (nt)
\end{aligned}
\tag{29}
$$

From the equality of the Equations 28 and 29, we have

$$\cos \varphi = \cos (nt) \tag{30}$$

On the other hand, from Figure 2, by using the Equation 27, we can write

$$
\begin{aligned}
\langle T(t), W(t) \rangle &= \|T(t)\| \, \|W(t)\| \sin \varphi, \\
\\
&= \frac{n}{m} \sin \varphi
\end{aligned}
\tag{31}
$$

Also, if the inner product operation is applied to the vectors $T(t)$ and $W(t)$, we get

$$
\begin{aligned}
\langle T(t), W(t) \rangle &= -\frac{n^2}{m} \Big(n \sin^2 t \sin (nt) + n \cos^2 t \sin (nt) + \frac{n}{m^2} \sin (nt) \Big) \\
&= -\frac{n^2}{m} \Big(n \sin (nt) + \frac{n}{m^2} \sin (nt) \Big), \\
&= -\frac{n}{m} \sin (nt)
\end{aligned}
\tag{32}
$$

From the equality of the Equations 31 and 32, we have

$$\sin \varphi = -\sin(nt) \tag{33}$$

Hence, from the Equations 30 and 33, we write

$$\begin{aligned}
\cos \varphi - \cos(nt) &= 0 \implies \cos^2 \varphi - 2\cos \varphi \cos(nt) + \cos^2(nt) = 0 \\
\sin \varphi + \sin(nt) &= 0 \implies \sin^2 \varphi + 2\sin \varphi \sin(nt) + \sin^2(nt) = 0
\end{aligned}$$

If these two equations are added side by side, we get

$$\begin{aligned}
2 - 2\left(\cos \varphi \cos(nt) - \sin \varphi \sin(nt)\right) &= 0 \\
\cos \varphi \cos(nt) - \sin \varphi \sin(nt) &= \cos(\varphi + nt) = 1
\end{aligned}$$

And thus, we obtain

$$nt = -\varphi \tag{34}$$

Corollary 3.3. The angle (nt) is the angle opposite sign to the angle between of the binormal vector $B(t)$ and the Darboux vector $W(t)$ of Salkowski curves.

3.6. The Unit Vector in the Direction of Darboux Vector of Salkowski Curves in $\mathbb{E}^3$

Let the unit vector in the direction of Darboux vector $W(t)$ of Salkowski curves be $C(t)$. Then, from the Equations 25 and 27, we have

$$C(t) = \frac{W(t)}{\|W(t)\|} = \left(n \sin t, -n \cos t, \frac{n}{m}\right) \tag{35}$$

On the other hand, from the Figure 2, we write

$$\begin{aligned}
C(t) &= \frac{v(t)}{\|W(t)\|}\left(\tau(t)T(t) + \kappa(t)B(t)\right) \\
&= \sin \varphi T(t) + \cos \varphi B(t) \tag{36}
\end{aligned}$$

[27]. If the Equation 34 is substituted in the Equation 36, we get

$$\begin{aligned}
C(t) &= -\sin(nt)\,T(t) + \cos(nt)\,B(t) \\
&= \left(\cos t \cos(nt)\sin(nt) + n \sin t \sin^2(nt), \cos(nt)\sin t \sin(nt) - n\cos t \sin^2(nt), \frac{n}{m}\sin^2(nt)\right) \\
&\quad - \left(\cos t \cos(nt)\sin(nt) - n\cos^2(nt)\sin t, \cos(nt)\sin t \sin(nt) + n \cos t \cos^2(nt), -\frac{n}{m}\cos^2(nt)\right)
\end{aligned}$$

Then, we indeed obtain

$$C(t) = \left(n \sin t, -\cos t, \frac{n}{m}\right) \tag{37}$$

Here, we see that the Equations 35 and 37 are equal.

4. The Modified Orthogonal Frames of Salkowski Curves in $\mathbb{E}^3$

In this section, we calculate the modified orthogonal frames with the both curvature and torsion of Salkowski curves. And we give the relations between the derivatives of the vectors of these frames and the Frenet vectors or the vectors of the modified orthogonal frames. Let the Frenet frame, the curvature and the torsion of Salkowski curves $\gamma_m(t)$ be $\{T(t), N(t), B(t)\}$, $\kappa(t)$ and $\tau(t)$, respectively.

4.1. The Modified Orthogonal Frame with the Curvature of Salkowski Curves in $\mathbb{E}^3$

Considering the Gram-Schmidt orthogonalization procedure, let us define the orthogonal frame $\{E_1(t),$ $E_2(t), E_3(t)\}$ below for Salkowski curves $\gamma_m(t)$, [26]:

$$E_1(t) = \gamma'_m(t), \quad E_2(t) = E_1'(t) - \frac{\langle E_1'(t), E_1(t)\rangle}{\langle E_1(t), E_1(t)\rangle} E_1(t), \quad E_3(t) = E_1(t) \wedge E_2(t) \tag{38}$$

Here, since Salkowski curves are not a unit speed curve, we can not use the Equation 8. From the Equations 11 and 38, the vector $E_1(t)$ is obtained as follows:

$$E_1(t) = \frac{n}{m}\cos(nt)\,T(t) \tag{39}$$

From the Equation 39, the following equation is gotten:

$$
\begin{aligned}
\frac{\langle E_1'(t), E_1(t)\rangle}{\langle E_1(t), E_1(t)\rangle} &= \frac{\left\langle \left(\frac{n}{m}\cos(nt)\,T(t)\right)', \frac{n}{m}\cos(nt)\,T(t)\right\rangle}{\left\langle \frac{n}{m}\cos(nt)\,T(t), \frac{n}{m}\cos(nt)\,T(t)\right\rangle} \\[2mm]
&= \frac{\left\langle -n\sin(nt)\,T(t) + \frac{n}{m}\cos^2(nt)\,N(t), \cos(nt)\,T(t)\right\rangle}{\cos^2(nt)} \\[2mm]
&= -n\tan(nt)
\end{aligned}
\tag{40}
$$

From the Equations 3, 38 and 40, the vectors $E_2(t)$ and $E_3(t)$ are obtained as follows:

$$
\begin{aligned}
E_2(t) &= -\frac{n^2}{m}\sin(nt)\,T(t) + \frac{n^2}{m^2}\cos^2(nt)\,N(t) + \frac{n^2}{m}\sin(nt)\,T(t) \\[2mm]
&= \frac{n^2}{m^2}\cos^2(nt)\,N(t)
\end{aligned}
\tag{41}
$$

$$E_3(t) = \frac{n^3}{m^3}\cos^3(nt)\,B(t) \tag{42}$$

Since the curvature of Salkowski curves is $\kappa(t) = 1$, using the Equation 12, from the Equations 39, 41 and 42, the modified orthogonal frame $\{E_1(t), E_2(t), E_3(t)\}$ with the curvature $\kappa(t)$ of Salkowski curves $\gamma_m(t)$ is written as follows:

$$E_1(t) = v(t)T(t), \quad E_2(t) = v^2(t)\kappa(t)N(t), \quad E_3(t) = v^3(t)\kappa(t)B(t) \tag{43}$$

where

$$\langle E_1(t), E_2(t)\rangle = \langle E_2(t), E_3(t)\rangle = \langle E_1(t), E_3(t)\rangle = 0 \tag{44}$$

and

$$
\begin{aligned}
\langle E_1(t), E_1(t)\rangle &= v^2(t) = \frac{n^2}{m^2}\cos^2(nt) \\[2mm]
\langle E_2(t), E_2(t)\rangle &= v^4(t)\kappa^2(t) = \frac{n^4}{m^4}\cos^4(nt) \\[2mm]
\langle E_3(t), E_3(t)\rangle &= v^6(t)\kappa^2(t) = \frac{n^6}{m^6}\cos^6(nt)
\end{aligned}
$$

The frame $\{E_1(t), E_2(t), E_3(t)\}$ is indeed orthogonal (from the Equation 44), but is not orthonormal, because the vectors $E_1(t), E_2(t), E_3(t)$ are not unit vectors. Now, let us find the derivative vectors of

the frame, respectively. First, by using the Equation 3, from the Equations 39, 41 and 42, we obtain the derivative vectors $E_1'(t), E_2'(t), E_3'(t)$ in terms of the Frenet vectors $T(t), N(t), B(t)$ as follows:

$$E_1'(t) = -\frac{n^2}{m}\sin(nt)\,T(t) + \frac{n^2}{m^2}\cos^2(nt)\,N(t) \tag{45}$$

$$
\begin{aligned}
E_2'(t) &= -\frac{2n^3}{m^2}\cos(nt)\sin(nt)\,N(t) + \frac{n^2}{m^2}\cos^2(nt)\,N'(t) \\
&= -\frac{2n^3}{m^2}\cos(nt)\sin(nt)\,N(t) + \frac{n^2}{m^2}\cos^2(nt)\left(-\frac{n}{m}\cos(nt)\,T(t) - \frac{n}{m}\sin(nt)\,B(t)\right) \\
&= -\frac{n^3}{m^3}\cos^3(nt)\,T(t) - \frac{2n^3}{m^2}\cos(nt)\sin(nt)\,N(t) - \frac{n^3}{m^3}\cos^2(nt)\sin(nt)\,B(t),
\end{aligned} \tag{46}
$$

$$
\begin{aligned}
E_3'(t) &= -\frac{3n^4}{m^3}\cos^2(nt)\sin(nt)\,B(t) + \frac{n^3}{m^3}\cos^3(nt)\,B'(t) \\
&= \frac{n^4}{m^4}\cos^3(nt)\sin(nt)\,N(t) - \frac{3n^4}{m^3}\cos^2(nt)\sin(nt)\,B(t)
\end{aligned} \tag{47}
$$

Corollary 4.1. From the Equations 45, 46 and 47, we obtain the following equalities between the Frenet vectors and the derivative vectors of the modified orthogonal frame with $\kappa(t)$ of Salkowski curves:

$$
\begin{bmatrix} E_1'(t) \\ E_2'(t) \\ E_3'(t) \end{bmatrix} =
\begin{bmatrix}
-\dfrac{n^2}{m}\sin(nt) & \dfrac{n^2}{m^2}\cos^2(nt) & 0 \\[2ex]
-\dfrac{n^3}{m^3}\cos(nt) & -\dfrac{2n^3}{m^2}\cos(nt)\sin(nt) & -\dfrac{n^3}{m^3}\cos^2(nt)\sin(nt) \\[2ex]
0 & \dfrac{n^4}{m^4}\cos^3(nt)\sin(nt) & -\dfrac{3n^4}{m^3}\cos^2(nt)\sin(nt)
\end{bmatrix}
\begin{bmatrix} T(s) \\ N(s) \\ B(s) \end{bmatrix}
$$

Second, let's get the derivative vectors $E_1'(t), E_2'(t), E_3'(t)$ in terms of the vectors $E_1(t), E_2(t), E_3(t)$. From the Equations 39, 41 and 42, the Frenet vectors are written in terms of the vectors $E_1(t), E_2(t), E_3(t)$ as follows:

$$
\begin{bmatrix} T(t) \\ N(t) \\ B(t) \end{bmatrix} =
\begin{bmatrix}
\dfrac{m}{n\cos(nt)} & 0 & 0 \\[2ex]
0 & \dfrac{m^2}{n^2\cos^2(nt)} & 0 \\[2ex]
0 & 0 & \dfrac{m^3}{n^3\cos^3(nt)}
\end{bmatrix}
\begin{bmatrix} E_1(s) \\ E_2(s) \\ E_3(s) \end{bmatrix} \tag{48}
$$

If the Equation 48 are substituted in the Equations 45, 46 and 47, respectively, we get

$$
\begin{aligned}
E_1'(t) &= -\frac{n^2}{m}\sin(nt)\left(\frac{m}{n\cos(nt)}E_1(t)\right) + \frac{n^2}{m^2}\cos^2(nt)\left(\frac{m^2}{n^2\cos^2(nt)}E_2(t)\right), \\
E_1'(t) &= -n\tan(nt)\,E_1(t) + E_2(t)
\end{aligned} \tag{49}
$$

$$
\begin{aligned}
E_2'(t) &= -\frac{n^3}{m^3}\cos^3\left(nt\right)\left(\frac{m}{n\cos\left(nt\right)}E_1(t)\right) - \frac{2n^3}{m^2}\cos\left(nt\right)\sin\left(nt\right)\left(\frac{m^2}{n^2\cos^2\left(nt\right)}E_2(t)\right) \\
&\quad -\frac{n^3}{m^3}\cos^2\left(nt\right)\sin\left(nt\right)\left(\frac{m^3}{n^3\cos^3\left(nt\right)}E_3(t)\right),
\end{aligned}
$$

$$
= -\frac{n^2}{m^2}\cos^2\left(nt\right)E_1(t) - 2n\tan\left(nt\right)E_2(t) - \tan\left(nt\right)E_3(t) \tag{50}
$$

$$
\begin{aligned}
E_3'(t) &= \frac{n^4}{m^4}\cos^3\left(nt\right)\sin\left(nt\right)\left(\frac{m^2}{n^2\cos^2\left(nt\right)}E_2(t)\right) - \frac{3n^4}{m^3}\cos^2\left(nt\right)\sin\left(nt\right)\left(\frac{m^3}{n^3\cos^3\left(nt\right)}E_3(t)\right)
\end{aligned}
$$

$$
= \frac{n^2}{m^2}\cos\left(nt\right)\sin\left(nt\right)E_2(t) - 3n\tan\left(nt\right)E_3(t) \tag{51}
$$

Corollary 4.2. From the Equations 49, 50 and 51, we obtain the following equalities between the vectors of the modified orthogonal frame with $\kappa(t)$ of Salkowski curves and its derivative vectors:

$$
\begin{bmatrix} E_1'(t) \\[2mm] E_2'(t) \\[2mm] E_3'(t) \end{bmatrix} = \begin{bmatrix} -n\tan\left(nt\right) & 1 & 0 \\[2mm] -\dfrac{n^2}{m^2}\cos^2\left(nt\right) & -2n\tan\left(nt\right) & -\tan\left(nt\right) \\[2mm] 0 & \dfrac{n^2}{m^2}\cos\left(nt\right)\sin\left(nt\right) & -3n\tan\left(nt\right) \end{bmatrix} \begin{bmatrix} E_1\left(s\right) \\[2mm] E_2\left(s\right) \\[2mm] E_3\left(s\right) \end{bmatrix}
$$

4.2. The Modified Orthogonal Frame with the Torsion of Salkowski curves in $\mathbb{E}^3$

Considering the Gram-Schmidt orthogonalization procedure, let us define the orthogonal frame $\{A_1(t), A_2(t), A_3(t)\}$ below for Salkowski curves $\gamma_m(t)$, [26]:

$$
A_1(t) = \gamma_m'(t), \quad A_2(t) = \frac{\tau(t)}{\kappa(t)}\left(A_1'(t) - \frac{\langle A_1'(t), A_1(t)\rangle}{\langle A_1(t), A_1(t)\rangle}A_1(t)\right), \quad A_3(t) = A_1(t) \wedge A_2(t) \tag{52}
$$

From the Equations 11 and 52, the vector $A_1(t)$ is obtained as follows:

$$
A_1(t) = \frac{n}{m}\cos\left(nt\right)T(t) \tag{53}
$$

from the Equations 39 and 53, we see that the vectors $E_1(t)$ and $A_1(t)$ are equal. Therefore, from the Equation 40, we have

$$
\frac{\langle A_1'(t), A_1(t)\rangle}{\langle A_1(t), A_1(t)\rangle} = -n\tan(nt) \tag{54}
$$

From the Equations 3, 52 and 54, the vectors $A_2(t)$ and $A_3(t)$ are obtained as follows:

$$
\begin{aligned}
A_2(t) &= -\tan\left(nt\right)\left(-\frac{n^2}{m}\sin\left(nt\right)T(t) + \frac{n^2}{m^2}\cos^2\left(nt\right)N(t) + \frac{n^2}{m}\sin\left(nt\right)T(t)\right) \\
&= -\frac{n^2}{m^2}\cos\left(nt\right)\sin\left(nt\right)N(t)
\end{aligned} \tag{55}
$$

$$
A_3(t) = -\frac{n^3}{m^3}\cos^2\left(nt\right)\sin\left(nt\right)B(t) \tag{56}
$$

Since the torsion of Salkowski curves is $\tau(t) = -\tan\left(nt\right)$, using the Equation 12, from the Equations 53, 55 and 56, the modified orthogonal frame $\{A_1(t), A_2(t), A_3(t)\}$ with the torsion $\tau(t)$ of Salkowski curves $\gamma_m(t)$ is written as follows:

$$
A_1(t) = v(t)T(t), \quad A_2(t) = v^2(t)\tau(t)N(t), \quad A_3(t) = v^3(t)\tau(t)B(t) \tag{57}
$$

where

$$\langle A_1(t), A_2(t) \rangle = \langle A_2(t), A_3(t) \rangle = \langle A_1(t), A_3(t) \rangle = 0 \tag{58}$$

and

$$\langle A_1(t), A_1(t) \rangle = v^2(t) = \frac{n^2}{m^2} \cos^2(nt)$$

$$\langle A_2(t), A_2(t) \rangle = v^4(t)\tau^2(t) = \frac{n^4}{m^4} \cos^2(nt) \sin^2(nt)$$

$$\langle A_3(t), A_3(t) \rangle = v^6(t)\tau^2(t) = \frac{n^6}{m^6} \cos^4(nt) \sin^2(nt)$$

The frame $\{A_1(t), A_2(t), A_3(t)\}$ is indeed orthogonal (from the Equation 58), but is not orthonormal, because the vectors $A_1(t), A_2(t), A_3(t)$ are not unit vectors. Now, let us find the derivative vectors of the frame, respectively. First, by using the Equation 3, from the Equations 53, 55 and 56, we obtain the derivative vectors $A_1'(t), A_2'(t), A_3'(t)$ in terms of the Frenet vectors as follows:

$$A_1'(t) = -\frac{n^2}{m} \sin(nt) T(t) + \frac{n^2}{m^2} \cos^2(nt) N(t) \tag{59}$$

$$\begin{aligned}
A_2'(t) &= -\frac{n^2}{m^2}\left(-n\sin^2(nt) + n\cos^2(nt)\right) N(t) - \frac{n^2}{m^2} \cos(nt)\sin(nt) N'(t) \\
&= -\frac{n^3}{m^2}\left(-\sin^2(nt) + \cos^2(nt)\right) N(t) \\
&\quad -\frac{n^2}{m^2}\cos(nt)\sin(nt)\left(-\frac{n}{m}\cos(nt) T(t) - \frac{n}{m}\sin(nt) B(t)\right) \\
&= \frac{n^3}{m^3}\cos^2(nt)\sin(nt) T(t) + \frac{n^3}{m^2}\left(2\sin^2(nt) - 1\right) N(t) + \frac{n^3}{m^3}\cos(nt)\sin^2(nt) B(t) \tag{60}
\end{aligned}$$

$$\begin{aligned}
A_3'(t) &= -\frac{n^3}{m^3}\left(\left(-2n\cos(nt)\sin^2(nt) + n\cos^3(nt)\right) B(t) + \cos^2(nt)\sin(nt) B'(t)\right) \\
&= -\frac{n^4}{m^4}\cos^2(nt)\sin^2(nt) N(t) + \frac{n^4}{m^3}\cos(nt)\left(3\sin^2(nt) - 1\right) B(t) \tag{61}
\end{aligned}$$

Corollary 4.3. From the Equations 59, 60 and 61, we obtain the following equalities between the Frenet vectors and the derivative vectors of the modified orthogonal frame with $\tau(t)$ of Salkowski curves:

$$\begin{bmatrix} A_1'(t) \\ A_2'(t) \\ A_3'(t) \end{bmatrix} = \begin{bmatrix} -\dfrac{n^2}{m}\sin(nt) & \dfrac{n^2}{m^2}\cos^2(nt) & 0 \\[2mm] \dfrac{n^3}{m^3}\cos^2(nt)\sin(nt) & \dfrac{n^3}{m^2}\left(2\sin^2(nt) - 1\right) & \dfrac{n^3}{m^3}\cos(nt)\sin^2(nt) \\[2mm] 0 & -\dfrac{n^4}{m^4}\cos^2(nt)\sin^2(nt) & \dfrac{n^4}{m^3}\cos(nt)\left(3\sin^2(nt) - 1\right) \end{bmatrix} \begin{bmatrix} T(s) \\ N(s) \\ B(s) \end{bmatrix}$$

Second, let's get the derivative vectors $A_1'(t), A_2'(t), A_3'(t)$ in terms of the vectors $A_1(t), A_2(t), A_3(t)$. From the Equations 53, 55, and 56, the Frenet vectors are written in terms of the vectors $A_1(t), A_2(t)$, and $A_3(t)$ as follows:

$$\begin{bmatrix} T(t) \\ N(t) \\ B(t) \end{bmatrix} = \begin{bmatrix} \dfrac{m}{n\cos(nt)} & 0 & 0 \\[2mm] 0 & -\dfrac{m^2}{n^2\cos(nt)\sin(nt)} & 0 \\[2mm] 0 & 0 & -\dfrac{m^3}{n^3\cos^2(nt)\sin(nt)} \end{bmatrix} \begin{bmatrix} A_1(s) \\ A_2(s) \\ A_3(s) \end{bmatrix} \tag{62}$$

If the Equation 62 are substituted in the Equations 59, 60 and 61, respectively, we get

$$
\begin{aligned}
A_1'(t) &= -\frac{n^2}{m}\sin(nt)\left(\frac{m}{n\cos(nt)}A_1(t)\right) + \frac{n^2}{m^2}\cos^2(nt)\left(-\frac{m^2}{n^2\cos(nt)\sin(nt)}A_2(t)\right) \\
&= -n\tan(nt)A_1(t) - \frac{1}{\tan(nt)}A_2(t)
\end{aligned}
\tag{63}
$$

$$
\begin{aligned}
A_2'(t) = {}& \frac{n^3}{m^3}\cos^2(nt)\sin(nt)\left(\frac{m}{n\cos(nt)}A_1(t)\right) + \frac{n^3}{m^2}\left(2\sin^2(nt)-1\right)\left(-\frac{m^2}{n^2\cos(nt)\sin(nt)}A_2(t)\right) \\
& + \frac{n^3}{m^3}\cos(nt)\sin^2(nt)\left(-\frac{m^3}{n^3\cos^2(nt)\sin(nt)}A_3(t)\right) \\
= {}& \frac{n^2}{m^2}\cos(nt)\sin(nt)A_1(t) - n\left(\frac{2\sin^2(nt)-1}{\cos(nt)\sin(nt)}\right)A_2(t) - \tan(nt)A_3(t)
\end{aligned}
\tag{64}
$$

$$
\begin{aligned}
A_3'(t) &= -\frac{n^4}{m^4}\cos^2(nt)\sin^2(nt)\left(-\frac{m^2}{n^2\cos(nt)\sin(nt)}A_2(t)\right) \\
&\quad + \frac{n^4}{m^3}\cos(nt)\left(3\sin^2(nt)-1\right)\left(-\frac{m^3}{n^3\cos^2(nt)\sin(nt)}A_3(t)\right) \\
&= \frac{n^2}{m^2}\cos(nt)\sin(nt)A_2(t) - n\left(\frac{3\sin^2(nt)-1}{\cos(nt)\sin(nt)}\right)A_3(t)
\end{aligned}
\tag{65}
$$

Corollary 4.4. From the Equations 63, 64 and 65, we obtain the following equalities between the modified orthogonal frame with $\tau(t)$ of Salkowski curves and its derivative vectors:

$$
\begin{bmatrix} A_1'(t) \\ A_2'(t) \\ A_3'(t) \end{bmatrix} =
\begin{bmatrix}
-n\tan(nt) & -\dfrac{1}{\tan(nt)} & 0 \\[2ex]
\dfrac{n^2}{m^2}\cos(nt)\sin(nt) & -\dfrac{n\left(2\sin^2(nt)-1\right)}{\cos(nt)\sin(nt)} & -\tan(nt) \\[2ex]
0 & \dfrac{n^2}{m^2}\cos(nt)\sin(nt) & -\dfrac{n\left(3\sin^2(nt)-1\right)}{\cos(nt)\sin(nt)}
\end{bmatrix}
\begin{bmatrix} A_1(t) \\ A_2(t) \\ A_3(t) \end{bmatrix}
$$

5. Conclusion

The modified orthogonal frame is a tool that can be used to solve the problem at singular points where the Frenet frame of the analytical or discontinuous curves cannot be calculated. But there is no harm in constructing a modified orthogonal frame of any regular curve. For example, in this study, the modified orthogonal frames of Salkowski curves are calculated and the relationships between the Frenet frame and the modified orthogonal frames are given. The characteristic properties of Salkowski curves can be studied with its modified orthogonal frames, as well as with its Frenet frame.

Author Contributions

All the authors contributed equally to this work. They all read and approved the last version of the paper.

Conflicts of Interest

The authors declare no conflict of interest.

References

[1] M. P. Do Carmo, *Differential Geometry of Curves and Surfaces: Revised and Updated Second Edition*, Courier Dover Publications, 2016.

[2] H. H. Hacısalihoğlu, *Differantial Geometry*, Ankara University Faculty of Science Press, Ankara, Türkiye, 2000.

[3] L. Kula, N. Ekmekci, Y. Yayli, K. İlarslan, *Characterizations of Slant Helices in Euclidean 3-Space*, Turkish Journal of Mathematics 34 (2) (2010) 261–274.

[4] A. T. Ali, *Position Vectors of Slant Helices in Euclidean 3-Space*, Journal of the Egyptian Mathematical Society 20 (1) (2012) 1–6.

[5] E. Salkowski, *Zur Transformation Von Raumkurven* Mathematische Annalen 66 (4) (1909) 517–557.

[6] J. Monterde, *Salkowski Curves Revisited: A Family of Curves with Constant Curvature and Non-Consant Torsion*, Computer Aided Geometric Design 26 (2009) 271–278.

[7] S. Gur, S. Senyurt, *Frenet Vectors and Geodesic Curvatures of Spheric Indicators of Salkowski Curve in* $\mathbb{E}^3$, Hadronic Journal 33 (5) (2010) 485–512.

[8] S. Şenyurt, B. Öztürk, *Smarandache Curves of Salkowski Curve According to Frenet Frame*, Turkish Journal of Mathematics and Computer Science 10 (2018) 190–201.

[9] T. Sasai, *The Fundamental Theorem of Analytic Space Curves and Apparent Singularities of Fuchsian Differential Equations*, Tohoku Math Journal 36 (1984) 17–24.

[10] T. Sasai, *Geometry of Analytic Space Curves with Singularities and Regular Singularities of Differential Equations*, Funkcialaj Ekvacioj 30 (1987) 283–303.

[11] B. Bükcü, M. K. Karacan, *On the Modified Orthogonal Frame with Curvature and Torsion in 3-Space*, Mathematical Sciences and Applications E-Notes 1 (2016) 184–188.

[12] B. Bükcü, M. K. Karacan, *Spherical Curves with Modified Orthogonal Frame*, Journal of New Results in Science 10 (2016) 60–68.

[13] S. Uddin, M. S. Stankovic, M. Iqbal, S. K. Yadav, M. Aslam, *Slant Helices in Minkowski 3-Space* E_1^3 *with Sasai's Modified Frame Fields*, Filomat 36 (2022) 151–164.

[14] H. K. Elsayied, A. A. Altaha, A. Elsharkawy, *On Some Special Curves According to the Modified Orthogonal Frame in Minkowski 3-Space* E_1^3, Kasmera 49 (2021) 2-15.

[15] M. Arıkan, S. K. Nurkan, *Adjoint Curve According to Modified Orthogonal Frame with Torsion in 3-Space*, Uşak University Journal of Science and Natural Sciences 2 (2020) 54–64.

[16] S. Şenyurt, S. Gür Mazlum, L. Grilli, *Gaussian Curvatures of Parallel Ruled Surfaces*, Applied Mathematical Sciences 14 (2020) 171–183.

[17] A. Z. Azak, *Involute-Evolute Curves According to Modified Orthogonal Frame*, Journal of Science and Arts 21(2) (2021) 385–394.

[18] K. Eren, H. H. Kosal, *Evolution of Space Curves and the Special Ruled Surfaces With Modified Orthogonal Frame*, AIMS Mathematics 5 (3) (2020) 2027–2039.

[19] M. S. Lone, H. Es, M. K. Karacan, B. Bükcü, *On Some Curves With Modified Orthogonal Frame in Euclidean 3-Space*, Iranian Journal of Science and Technology, Transactions A: Science 43 (4) (2019) 1905–1916.

[20] M. S. Lone, H. Es, M. K. Karacan, B. Bükcü, *Mannheim Curves with Modified Orthogonal Frame in Euclidean 3-Space*, Turkish Journal of Mathematics 43(2) (2019) 648–663.

[21] Y. Li, S. Y. Liu, Z. G. Wang, *Tangent Developables and Darboux Developables of Framed Curves*, Topology and Its Applications 301 (2021) 107526.

[22] Y. Li, D. Ganguly, S. Dey, A. Bhattacharyya, *Conformal η-Ricci Solitons Within the Framework of Indefinite Kenmotsu Manifolds*, AIMS Mathematics 7 (4) (2022), 5408–5430.

[23] Y. Yayli, I. Gok, H. H. Hacisalihoglu, *Extended Rectifying Curves as New Kind of Modified Darboux Vectors*, TWMS Journal of Pure and Applied Mathematics 9 (2018) 18–31.

[24] A. Kelleci, M. Bektaş, M. Ergüt, *The Hasimoto Surface According to Bishop Frame*, Adıyaman University Journal of Science 9 (1) (2019) 13–22.

[25] S. Gür Mazlum, S. Şenyurt, L. Grilli, *The Dual Expression of Parallel Equidistant Ruled Surfaces in Euclidean 3-Space*, Symmetry 14 (5) (2022) 1062.

[26] S. Gür Mazlum, M. Bektaş, *On the Modified Orthogonal Frames of the Non-Unit Speed Curves in Euclidean Space* $\mathbb{E}^3$, Turkish Journal of Science 7(2) (2022) 58–74.

[27] W. Fenchel, *On the Differential Geometry of Closed Space Curves*, Bulletin of the American Mathematical Society 57 (1951) 44–54.

Random Ensemble MARS: Model Selection in Multivariate Adaptive Regression Splines Using Random Forest Approach

Dilek Sabancı[1] , **Mehmet Ali Cengiz[2]**

Abstract − Multivariate Adaptive Regression Splines (MARS) is a supervised learning model in machine learning, not obtained by an ensemble learning method. Ensemble learning methods are gathered from samples comprising hundreds or thousands of learners that serve the common purpose of improving the stability and accuracy of machine learning algorithms. This study presented REMARS (Random Ensemble MARS), a new MARS model selection approach obtained using the Random Forest (RF) algorithm. 200 training and test data set generated via the Bagging method were analysed in the MARS analysis engine. At the end of the analysis, two different MARS model sets were created, one yielding the smallest Mean Square Error for the test data (Test MSE) and the other yielding the smallest Generalised Cross-Validation (GCV) value. The best model was estimated for both Test MSE and GCV criteria by examining the error of measurement criteria, variable importance averages, and frequencies of the knot values for each model. Eventually, a new model was obtained via the ensemble learning method, i.e., REMARS, that yields result as good as the MARS model obtained from the original data set. The MARS model, which works better in the larger data set, provides more reliable results with smaller data sets utilising the proposed method.

1. Introduction

Machine learning is concerned with designing and analysing models learned from data and developing practical algorithms for prediction [1]. In other words, it suggests using a machine or computer to learn similarly to how the brain learns and predicts [2]. Ensemble learning, another definition of machine learning, refers to a collection of basic models assembled to create a new prediction or classification using the same learning technique. Bagging and Boosting are among the most widely used methods. These methods were designed to improve the stability and accuracy of machine learning algorithms [3]. Random Forest (RF) is an ensemble learning method for classification and regression, representing a significant advancement in machine learning. The method of RF is used to create many individual Classification and Regression Tree (CART) decision trees during the training phase. It aims to find new ways to combine the information from the individual CART trees (the class modes for classification, averaging the predictions of each regression model) [4, 5]. Contrary to the linear and non-linear regression models widely used in practice, Multivariate Adaptive

[1]dilek.kesgin@gop.edu.tr (Corresponding Author); [2]macengiz@omu.edu.tr
[1]Department of Mathematics, Faculty of Arts and Sciences, Tokat Gaziosmanpaşa University, Tokat, Türkiye
[2]Department of Statistics, Faculty of Arts and Sciences, Ondokuz Mayıs University, Samsun, Türkiye

Regression Spline (MARS) is defined as a nonparametric technique that generates different coefficients for different range values of the independent variable and reflects the actual structure better by also adding interaction terms to the model [6]. The model is obtained using the regression models' forward selection and backward elimination algorithms and the essential piecewise functions and combinations [7].

Many studies are conducted in different disciplines using the MARS algorithm. The MARS model was used by [8] in the field of medicine for disease diagnosis, [9] in the field of computer sciences for the quality assessment of web services, by [10] in the field of civil and environmental engineering to estimate pile drivability, by [11] in the field of mechanical engineering to model heat transfer properties and by [12] in the field of accounting and information systems to make financial predictions.

On the other hand, there are other studies in the literature where improvements were made in the model selection of the MARS algorithm. [13] used a genetic algorithm to interfere with knot selection. [14] suggested a new approach to the MARS as CMARS and used a penalised residual sum of squares for the MARS as a Tikhonov regularisation problem. [15] presented the new robust CMARS (RCMARS) in theory and by a robust optimisation technique. [16] proposed a new method for knot selection based on a mapping approach like self-organising maps. [17] applied information measure of complexity (ICOMP) as a powerful model selection criterion for the MARS modelling. [18] used Bootstrapping to obtain the empirical distributions of the parameters and to determine whether they were statistically significant or not in a special case of nonparametric regression.

There were many studies in which Ensemble Learning, Bagging, and Random Forest methods were used together in the literature. We can give the most up to date of these as follows. [19] showed the working mechanism of stacking and bagging on spoof fingerprint detection, which were widely used ensemble learning approaches. [20] offered a quantified way for the standard case when classifiers were aggregated by the majority ("algorithmic variance", i.e., the prediction error variance due only to the randomised training algorithm). A new method was proposed as a multi-objective optimisation approach with the two objectives of accuracy and diversity based on two main challenges in the bagging method provided in [21]. [22] proposed a new classification method for sparse functional data based on functional principal component analysis (FPCA) and bootstrap aggregating.

The present study aims to convert the MARS technique into ensemble learning using the RF algorithm. Moreover, we suggested a new method for selecting the model with superior performance and generalisation from the ensemble of the MARS models. Although there are studies in the literature where the MARS model was used as an ensemble [23-25], there is no method for selecting the best MARS model by creating the MARS models over a random ensemble. Correcting this deficiency in the literature will be attempted with the suggested new method. This study is derived from the first author's PhD dissertation conducted under the supervision of the second author.

2. Method

2.1. Random Forest Algorithm

The article on the RF model published by Leo Breiman in 2001 took its final shape by referring to the studies conducted by [4, 5, 26-31]. The algorithm of the RF method is built by following the steps presented below [8, 32-36]:

i.　k sampling is created by the Bagging method so that the number of observations in the original data set has the same number of observations as n. Also, each sampling represents a CART decision tree.

ii.　While 2/3 of the observations in the original data set are included in the sample as InBag data, 1/3 of them are excluded from the sample as OOB data to test the established internal error rate of the model.

iii. The widest CART decision tree is created with the InBag data. While creating this tree, instead of selecting the best variables out of all existing prediction variables in each node, p out of a total of m independent variables are randomly selected in a split of each node ($p < m$). That is because the tree is not expected to demonstrate excessive growth and overfitting.

iv. The previous steps are repeated until the k number of trees that will form the forest is obtained. Afterwards, a new prediction is made by combining the separate class predictions with k trees. It counts how often an examined observation is classified and in which categories. Each observation is assigned a class with a majority of votes determined through the tree sets.

v. The predictions made with the OOB observations that are not used in individual trees are used to estimate the internal error rate of the forest. The OOB error rate of each decision tree making up the forest is calculated. The percentage of misclassification is determined as the classification error rate of RF.

2.2. Multivariate Adaptive Regression Splines

The MARS technique was developed by the physician and statistician Jerome Harold Friedman in 1991 [37]. According to [38], the MARS is a good innovation in finding suitable conversions to convert the non-linear relationships between dependent and independent variables into a linear structure and determine the interactions between independent variables.

The MARS uses a pair of functions in the form of $[\pm(x-t)]_+$ One is the mirror reflection of the other, as the basis function in linear and non-linear expansions that predict the relationship between dependent and independent variables. These function pairs are also called mirror basis functions. The sign $[.]_+$ states that only the positive results of the related functions will be considered. Otherwise, the related functions are considered zero. The basis function pair representing the variable x and the knot value t is defined as follows [3,6,39]:

$$(x-t)_+ = \begin{cases} x-t, x > t \\ 0, otherwise \end{cases} and \ (t-x)_+ = \begin{cases} t-x, x < t \\ 0, otherwise \end{cases} \tag{1}$$

To find the desired model, the MARS uses a two-step process. Forward selection, the first phase of creating the MARS model, resembles forward stepwise regression. Unlike this method, the MARS uses basis function pairs instead of original inputs [6]. Each step finds the main basis function pair (meaning that both functions of a knot are included in the model) that leads to the most decrease in the SSE (Sum of Squares Error) value using the Greddy algorithm. In forward selection, the process of adding terms continues until the maximum number of terms included in the model is reached. The over fitted MARS model that is established by adding certain basis functions under the conditions and is much bigger than the optimum model is formulated as follows [37]:

$$\hat{f}(x) = a_0 + \sum_{m=1}^{M} a_m B_m(x) = a_0 + \sum_{m=1}^{M} a_m \prod_{m=1}^{K_m} [s_{km}(x_{v(k,m)} - t_{km})]_+ \tag{2}$$

In Equation (2), M is the number of basis functions defined as $m = 1,2,...,M$. While the quantity K_m represents the number of interactions, the quantity s_{km} takes the value ± 1. The constant term in the model is denoted by a_0 while the regression coefficients are denoted by a_m. $B_m(x)$ is the *m-th* basis function. The $v(k,m)$ label the independent variables and the t_{km} present knot value on the corresponding variables [37].

Backward elimination constitutes the second phase of the creation of the MARS model. The main reason this stage is required is the inability to compare the models with the SSE value. That is because when SSE is used to compare the models, backward elimination always selects the biggest model. However, the biggest model does not possess the best generalisation performance; on the contrary, it is over fitted and does not produce good results on new data [6, 40]. The model that became over fitted with forwarding selection is subjected to the elimination process to turn it into a model capable of generalising. The GCV (Generalized Cross Validation) criterion, a goodness of fit index, is used to compare the performance of model subsets and

choose the best subset. GCV considers both the error of residuals and model complexity [3,6,41]. For this reason, lower GCV values are accepted much better. The GCV formula, introduced by [42], is calculated as follows [37]:

$$GCV = \frac{1}{n}\sum_{i=1}^{n}[y_i - \hat{f}_M(x_i)]^2 \Big/ \left[1 - \frac{C(M)}{n}\right]^2 \qquad (3)$$

In Equation (3), the value n gives the number of observations in the data set, y_i gives the observed value of the dependent variable and $\hat{f}(x_i)$ provides the estimated value of the dependent variable. When the numerator of the formula is examined, it can be observed that the mean of the SSE value, i.e., MSE (Mean Square Error), was used. Therefore, the denominator of the formula renders the GCV criterion both different and essential compared to the SSE value. Cost complexity function $C(M)$ is calculated with the formula as follows [37]:

$$C(M) = trace(B(B^T B)^{-1} B^T) + 1 \qquad (4)$$

In Equation (4), B represents the Mxn dimensional data matrix of unconstant M basis functions. The cost complexity function was readapted for the MARS model by [43, 44] and took the form as follows [37]:

$$\tilde{C}(M) = C(M) + dM \qquad (5)$$

Here, d denotes the penalty value used to determine the best knot value. d is also known as Degrees of Freedom (DOF). The most suitable penalty value is in the $2 \leq d \leq 4$ range [37].

2.3. REMARS: Random Ensemble MARS

2.3.1. Difference Between MARS and REMARS

Contrary to linear regression models, in the MARS models, parameter confidence intervals and other controls in the model cannot be directly calculated, as in any nonparametric regression. Techniques related to GCV are used to validate the model. In the model selection of these techniques, the model that gives the lowest value related to the criterion is always selected. Generating hundreds or thousands of the MARS models from an original dataset, selecting the model with the lowest GCV criterion among these models and making predictions with the selected model may appear to be a highly reliable course of action. However, it cannot be deduced that the model with the lowest GCV value, etc., selected from a collection of models will always be the model with the best generalisation ability and performance. This is due to the presence of error measurement criteria such as SSE, MSE, Root Mean Square Error (RMSE), Mean Absolute Error (MAE), Mean Absolute Percent Error (MAPE) and R^2 (Coefficient of Determination), which affect the generalisation ability and performance of the model. Although SSE forms the basis of all error measurement criteria and serves as a subset, the main differences in the formulas make the criteria different from each other. Selecting a model where these differences are not in effect impacts the model's generalisation ability. When choosing the best model, preferring the model with the lowest error measurement criteria, such as RMSE, MSE and SSE, generally increase the R^2 value. Reaching the highest R^2 value with this method causes the error variance of the model to increase in new data. Therefore, when selecting the best model from the MARS models ensemble, a better course of action is observed progressing by considering the confidence interval of the means of different error measurement criteria. This route is not enough on its own. That is because the mean of each error measurement criterion does not correspond to the same model in the MARS models ensemble. Therefore, choosing a model in which knot values and variable importance are not enabled will also affect the validity of the selected model.

2.3.2. REMARS Algorithm

REMARS, a new MARS model selection approach that is obtained using the Random Forest algorithm, 95% confidence interval for the mean of error measurement criteria, knot values and contribution percentages of variables to the model, is created with the following steps.

i. *Sampling:* N samples (SAMPLE 1, SAMPLE 2, …, SAMPLE N) are created by the Bagging method so that the number of observations in the original data set has the same number of observations as *n*. Due to the bagging method, each sample differs in terms of the observations they contain, although they have the same number of observations.

ii. *InBag - Train:* Each sample contains approximately $2n/3$ of the observations in the original data set, and this part is named InBag (InBag 1, InBag 2, …, InBag N). With $n/3$ observation repeated from $2n/3$ observation in InBag, the number of observations of each training dataset (Train 1, Train 2, …, Train N) will be $n(n_1 = n_2 = \cdots = n_N = n)$.

iii. *OOB - Test:* The number of observations in the original data set but non-existent in the samples is approximately $n/3$ and is named OOB (OOB 1, OOB 2, …, OOB N). The remaining $2n/3$ of the test data (Test 1, Test 2, …, Test N) with the number of observations n is made up of repeated observations from the data separated as OOB.

iv. *Analysis:* After the training and test data sets are created, each training data is analysed with its test data in the MARS program. N models (Y_1 = Model 1, Y_2 = Model 2, …, Y_N = Model N) are obtained at the end of the analysis. The results of these models were examined using two different selection criteria (Test MSE and GCV).

v. *Results:* After obtaining a total of *N* models according to Test MSE and GCV criteria, mean – standard deviation – 95% confidence interval for the mean of error measurement criteria (RMSE, MSE, GCV, MAE, MAPE, SSE and R^2) are firstly calculated. Secondly, the number of times each variable's knot is repeated in the models, i.e., their frequency, is determined. Thirdly, each variable's minimum, mean and maximum contribution percentages to the model are obtained.

Fig. 1 shows the flowchart for the REMARS algorithm, which is a new approach for model selection from the randomly generated MARS models ensemble.
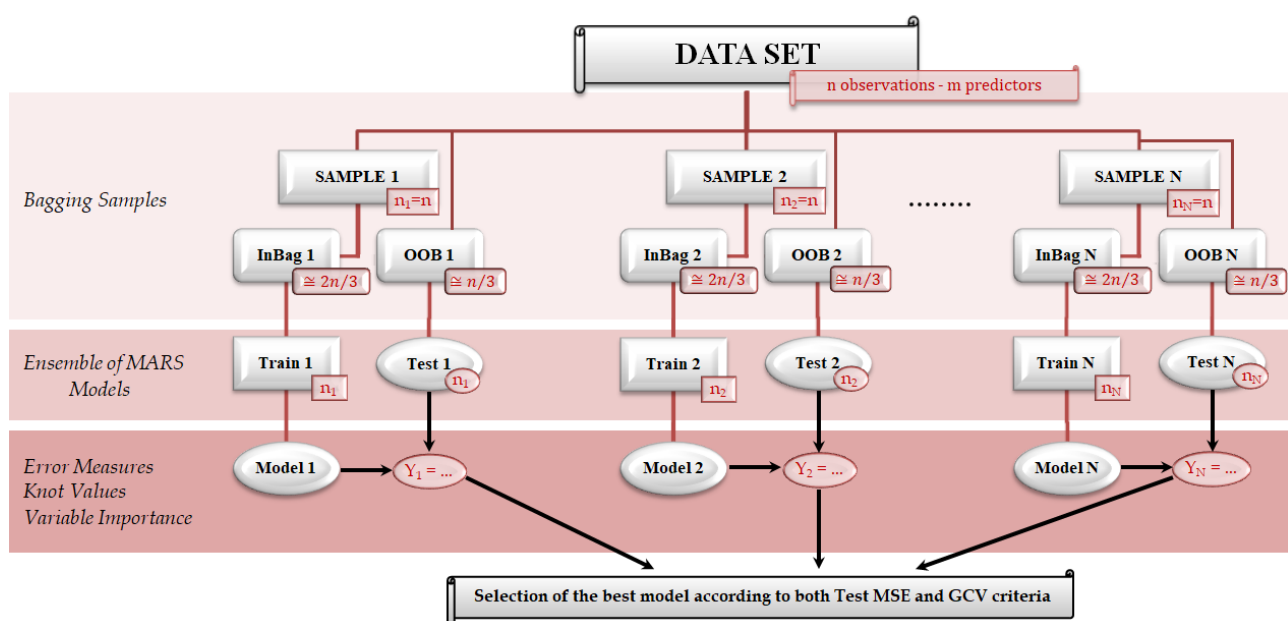

Fig. 1. The flowchart of the REMARS (Random Ensemble MARS) algorithm

2.3.3. REMARS Model Selection

The information obtained from the results is respectively used for model selection. The first model elimination is performed by selecting the models that fall within the lower and upper bound values of the 95% confidence interval for the mean of each error measurement criterion among Test MSE and GCV models, respectively. Afterwards, the models with the highest frequency in the 95% confidence interval for the mean of each error measurement criterion are determined. Determined models are examined separately by considering the frequency of the knot values obtained from all models (the ensemble) and the descriptive statistics of the contribution percentages of the variables to the model. The model that best predicts the dependent variable is selected among the N models. The model set with REMARS will be as good as the MARS model to be obtained from the original data. That is, because the MARS models obtained from randomly generated samples, combined in 95% confidence limits of the mean of all error measurement criteria of these models, the knot values obtained from all of the models in the ensemble, and the use of the contribution percentages to models of the variables will ensure that the selected model is highly consistent.

3. Application

In this section, the application for the selection of the most suitable MARS model using the REMARS method is presented. The MARS analysis engine in the Salford Predictive Modeller version 8.3 by the company Salford System was used in these analyses. the MARS analysis engine, instead of presenting a single MARS model at the end of the analysis, provides a tab including MARS models with several numbers of basis functions. The tab also separately indicates two different models with different selection criteria. The first of these models is the training model that gives the lowest MSE value based on the test data in the backward elimination phase, while the second model is the training model that offers the lowest GCV value in the backward elimination phase. In the application, Test MSE and GCV models were examined separately, and the results were combined.

3.1. Data Set

The research of the data set used in the application was conducted in 1970 in East Boston–Massachusetts. The FEV (Forced Expiratory Volume) values of children of different ages, heights and sexes in smoking and non-smoking environments were measured. [45, 46], who conducted the aforesaid research, examined the effects of parents smoking habits on the respiratory functions of children in East Boston–Massachusetts. [47] presented a section of the data from the study, conducted with Tager, for another analysis. This data set used by [48] was published on the website of [49] and used in the application section of the present study. In the FEV data set, there are measurements of 654 children in smoking/non-smoking environments, aged between 3–19 and height vary between 46–74 inches. Their age means is ten and their height mean 61.1 inches. The FEV measurement values of the children range from 0.791–5.793 litres, and the mean FEV value was calculated as 2.637 litres.

3.2. Analysis Results

At the end of the analysis, the Salford Predictive Modeller 8.3 MARS program presents various criteria for each model obtained by Test MSE and GCV criteria. These criteria, which will be used to determine the best model, can be listed as RMSE, MSE, GCV, SSE, MAE, MAPE, SSE and R^2. Each criterion was obtained separately from the 200 different MARS models created by Test MSE and GCV criteria. Table 1 shows the descriptive statistical findings of each criterion's mean values, standard deviation and 95% confidence interval for the mean (lower limit - upper limit) obtained from 200 models.

Table 1. Descriptive statistics of error measurements of GCV and Test MSE models

Model Selection Criteria	Descriptive Statistics of Measurements		RMSE	MSE	GCV	MAD	MAPE	SSE	R²
Test MSE	**Mean**		0.388	0.151	0.157	0.293	0.116	98.555	0.798
	Standard Deviation		0.018	0.014	0.013	0.012	0.005	9.017	0.018
	95% Confidence Interval for Mean	**Lower Bound**	0.385	0.149	0.156	0.291	0.115	97.555	0.796
		Upper Bound	0.390	0.153	0.159	0.294	0.117	99.812	0.801
GCV	**Mean**		0.373	0.139	0.150	0.284	0.1128	90.974	0.814
	Standard Deviation		0.014	0.010	0.011	0.010	0.004	6.624	0.015
	95% Confidence Interval for Mean	**Lower Bound**	0.371	0.138	0.149	0.282	0.112	90.050	0.811
		Upper Bound	0.375	0.141	0.152	0.285	0.1134	91.898	0.816

When Table 1 is examined, it is clearly observed that the descriptive statistics values of each error criterion of the Test MSE models are higher than the descriptive statistics values of each error criterion of the GCV models. This situation is due to the fact that the number of basis functions in the Test MSE models is generally lower than the number of basis functions in GCV models. On the other hand, while GCV is based on a formula that considers both residuals and model complexity, the formula of the Test MSE is based only on residuals. For this reason, GCV selects the models with more complex structures in the backward elimination phase. In the results, the GCV values obtained from the Test MSE models are generally higher than those in GCV models.

The knot values accompanying the basis functions that constitute each of the 200 Test MSE and GCV models are also included in determining the best model using REMARS method. As a result, the number of each knot belonging to a variable in the 200 models was determined. Frequencies of the top ten knot values most commonly observed in the models were determined for the height and age variables. Also, frequencies of knot values for the sex and smoker variables in the models were found. All of these results for the Test MSE and GCV models are shown in Table 2. When Table 2 was examined for the height variable, it was observed that the top five most commonly observed knot values are the same for the Test MSE and GCV models; however, their existence percentages in the models differ. Knot 66 was ranked first in both model ensembles by being present with a rate of 51% in the Test MSE models and 53% in the GCV models. In the Test MSE models, knots 65; 65.5; 57.5; 69 are present with rates of 34.5%, 27%, 25.5% and 19.5%, respectively. In the GCV models, knots 69; 65; 65.5; 57.5 are present with rates of 48.5%, 39.5%, 31% and 29.5%, respectively. Knot 67.5 is present in both model ensembles in different percentages.

The age variable's most common knot value in the Test MSE and GCV models is 8. This value is presented in the Test MSE and GCV models at approximately the same rates. The presence rates of knots other than 8 in both model ensembles were lower than 25%. Knots 1 and 2 for the sex variable are observed in the Test MSE models with rates of 10% and 8%, respectively, and the GCV models with rates of 28.5% and 29%, respectively. From this, it can be concluded that while each knot value of the sex variable is present in both Test MSE and GCV models with approximately the same rates, they were more effective in the GCV models compared to the Test MSE models. When Table 2 was examined for the smoker variable, it was observed that the knot value 1 had little effect in both model ensembles. The knot value 0 was much more effective in the

GCV models with a rate of 54.5% compared to the Test MSE models (16.5%). This is because observation 0 outnumbers observation 1 in the data set. That is because the MARS models are affected by the quantitative amount of any observation of a variable in the data set to include it in the model. It is observed that the GCV values are higher than those of the Test MSE, when the knot values of a variable in the Test MSE and GCV models are the same, as shown in Table 2. Again, this is because fewer basis functions, therefore fewer knot values, are included in the Test MSE models compared to the GCV models.

Table 2. Frequencies of knot values of GCV and Test MSE models

Model Selection Criteria	Variables							
	Height		Age		Sex		Smoker	
	Knot Values	Frequency	Knot Values	Frequency	Knot Values	Frequency	Knot Values	Frequency
Test MSE	66	102	8	112	1	20	0	33
	65	69	9	34				
	65.5	54	10	27				
	57.5	51	7	8				
	69	39	13	8				
	58.5	31	6	6	2	16	1	2
	64.5	27	3	5				
	64	27	11	4				
	67.5	25	14	4				
	67	23	16	3				
GCV	66	106	8	113	1	57	0	109
	69	97	13	49				
	65	79	9	37				
	65.5	62	14	29				
	57.5	59	10	26				
	70	59	17	21	2	58	1	13
	67.5	58	15	19				
	67	47	12	16				
	68.5	44	16	15				
	71	41	11	13				

The MARS analysis engine includes a tab that ranks the predictors based on their contribution percentage to the model at the end of the analysis. In this tab, which is calculated at a 100% scale, variables are ranked according to their importance percentage in a way that the most important variable always scores 100%. Table 3 shows the minimum, mean and maximum value findings of the importance percentages obtained for each variable in the Test MSE and GCV models.

Table 3. Importance percentage of variables of GCV and Test MSE models

Model Selection Criteria	Variables	Variable Importance		
		Minimum	Mean	Maximum
Test MSE	Height	100.00	100.00	100.00
	Age	8.35	23.87	43.59
	Sex	1.25	9.48	18.50
	Smoker	3.15	10.20	22.48
GCV	Height	100.00	100.00	100.00
	Age	14.03	27.20	52.71
	Sex	1.28	8.48	22.57
	Smoker	0.50	8.98	22.53

Table 3 shows that height is the most important variable in the Test MSE and GCV models. It was found to have an importance percentage of 100% in all models. It is followed by the age variable as the variable with the most significant contribution to the models. However, while the age variable is present in all of the GCV models, it was absent in 8 of the Test MSE models. In comparison, the sex and smoker variables had percentages of contribution in the Test MSE models that were calculated as 15.5% and 17%, respectively, and their percentages in the GCV models are 58% and 60.5%. Therefore, while the sex and smoker variables had almost no contribution to the Test MSE models, the situation was the opposite in the GCV models. Thus, the GCV criterion considers model complexity and tends to establish models with too many variables and knots.

3.3. Model Selection

The results obtained from Test MSE and GCV models ensemble using the REMARS approach constitute the building block of the model selection. In addition to being an approach that converts the classical MARS method into an ensemble, REMARS also uses a different technique in model selection. Instead of selecting the models with the lowest Test MSE and GCV values among Test MSE and GCV ensembles, it considers each model's error criteria, knot values, and variable importance.

3.3.1. Test MSE Criteria

To determine the MARS model with the best performance among the 200 models determined by the Test MSE, the analysis results obtained for the Test MSE in Table 1 are used. The first model elimination is performed by selecting the models that fall within the lower and upper bound values of the 95% confidence interval for the mean of each error measurement criterion among the Test MSE models. That is because progressing by determining a value according to the mean of each error criterion prevents us from selecting over fitted or under fitted models. According to their model number order, the models selected under these conditions are shown in Table 4 for the Test MSE error measurement criteria. When Table 4 is examined, it is seen that some error criteria have common models, and some do not. At this stage, it is important that a particular model number is commonly entering in several error measurement criteria. For this reason, in order to determine the best model, the second model elimination was performed by determining which model number is found in the error measurement criteria in Table 4, and how many times at the most. When Table 4 is examined, it is observed that Model 185 is commonly present in six error measurement criteria other than the MAD error measurement criterion, and Model 3, Model 24, Model 90 and Model 140 are commonly present in five different error measurement criteria. Other Test MSE models are present in fewer numbers in different error measurement criteria.

Table 4. Model numbers entering 95% confidence interval for error criterion mean from Test MSE models

	Error Measurements of Test MSE Models						
	RMSE	MSE	GCV	MAE	MAPE	SSE	R^2
Model Number	2	2	3	1	1	3	1
	3	3	7	3	16	6	3
	6	6	17	21	46	24	17
	21	24	21	22	53	36	65
	24	36	24	24	58	56	70
	25	56	25	25	90	59	103
	36	59	36	48	92	64	110
	56	64	39	59	98	83	135
	59	83	51	83	122	90	147
	64	90	62	91	125	97	166
	90	97	83	103	134	127	180
	97	103	90	106	137	133	181
	103	108	92	108	140	140	185
	108	127	97	117	149	150	191
	127	133	108	127	153	152	194
	130	140	109	129	157	185	
	133	150	136	130	166	187	
	138	152	140	137	178	194	
	140	174	144	144	185		
	150	185	152	177			
	152	187	171	180			
	174	190	176	193			
	185	194	180				
	187		183				
	190		185				
	194		187				
			188				

According to these results, the five most common models in the error measurement criteria among the 200 Test MSE models were determined. Table 5 shows the knot values and variable importance percentages of these models.

In the third model elimination to determine the best out of the five models selected from the Test MSE models, the results in Table 2 are used. When Table 2 is examined, it is observed that in the Test MSE models, knot 66 is essential for the height variable while knot 8 is essential for the age variable. These values are not present in Model 3, Model 24, Model 90 and Model 185. The absence of these knots may cause significant problems in the performance of the error measurement criteria of the models for new data. According to Table 3, the importance percentages of the height and age variables in the models indicate that these variables are required to be present in the models while also serving as moderator variables. It is also observed that the smoker variable contributes to the models. However, the smoker variable is not present in any of the models. That is because knot 0 of the smoker variable was found in 33 models while knot 1 was found in 2 models.

Their percentages of contribution to the models they are included in were found to be high. This shows that the knots contribute to the models, however, this contribution is not sufficient to be included in the selected models. The same situation applies to the sex variable. Model 24 includes the sex variable; however, it cannot be selected as the significant knots of the height variable are not included in this model. When all of these results are combined, Model 140 represents the best model among the Test MSE models. That is because Model 140 has produced the most consistent results in terms of the error measurement criteria, knot values and contribution percentages of variables to the model.

Table 5. Knot values and variable importance percentages of selected Test MSE models

Model Number	Particulars	Variables		
		Height	**Age**	**Sex**
3	**Knot Values**	52	6	
		65.5		
		66		
		69		
	Variable Importance (%)	100	25.81	
24	**Knot Values**	57.5	8	1
		58.5		
		59.5		
		65		
	Variable Importance (%)	100	25.05	7.51
90	**Knot Values**	**65**	11	
			13	
	Variable Importance (%)	100	20.10	
140	**Knot Values**	65.5	8	
		66		
		69		
	Variable Importance (%)	100	18.65	
185	**Knot Values**	65	7	
		66		
		67		
	Variable Importance (%)	100	33.88	

65: Knot value entering the model with the mirror basis function

3.3.2. GCV Criteria

To determine the MARS model with the best performance among the 200 models determined in accordance with GCV firstly the analysis results obtained for GCV in Table 1 are used. The first model elimination is performed by selecting the models that fall within the lower and upper bound values of the 95% confidence interval for the mean of each error measurement criterion among the GCV models. That is because progressing by determining a value according to the mean of each error criterion prevents us from selecting over fitted or under fitted models. The models selected under these conditions are, according to their model number order, shown in Table 6 for the GCV error measurement criteria. According to Table 6, Model 59, Model 116 and Model 130 are commonly present in five different error measurement criteria. Other GCV models are present in fewer numbers in different error measurement criteria.

Table 6. Model numbers entering 95% confidence interval for error criterion mean from GCV models

	Error Measurements of GCV Models						
	RMSE	**MSE**	**GCV**	**MAD**	**MAPE**	**SSE**	**R²**
Model Number	23	23	9	7	5	23	6
	34	34	21	21	6	34	8
	46	59	34	52	9	59	12
	59	82	46	61	14	82	14
	79	104	52	79	28	104	18
	82	105	91	98	30	105	25
	104	106	92	108	43	106	27
	105	108	103	115	46	108	28
	106	116	105	127	53	116	30
	108	130	116	130	58	130	35
	116	146	117	144	59	146	48
	130	174	118	151	61	174	57
	146	182	130	171	62	182	59
	174	190	144	174	70	190	63
	190	198	146	183	75	198	69
	198		182	191	79		82
			190	196	91		83
			191	198	94		94
			196		101		99
					119		103
					122		107
					123		116
					128		117
					138		136
					139		138
					160		141
					166		151
					168		191
					172		
					188		
					189		
					193		
					194		
					196		

According to these results, the three most common models in the error measurement criteria among the 200 GCV models were determined. Table 7 shows the knot values and variable importance percentages of these models. The results in Table 2 and Table 3 are used to determine the best out of the three models selected from the GCV models. According to Table 2, knots 66 and 69 for the height variable and knots 8 and 13 for

the age variable repeat a lot in the GCV models. Knot value 69 from the height variable was not included in Model 130 while knot value 8 from the age variable was not included in Model 116. According to the importance percentages of the height and age variables in Table 3, they should be included in the model to be selected. The sex and smoker variables are seen to have similar contributions to the models. However, as knot 0 of the smoker variable has a significantly higher number of repetitions in the models compared to the knot values of the sex variable, knot 0 of the smoker variable should be included in the model. Based on these observations, Model 59 represents the best model among the GCV models.

Table 7. Knot values and variable importance percentages of selected GCV models

Model Number	Particulars	Variables			
		Height	**Age**	**Sex**	**Smoker**
59	Knot Values	**58**	8	2	0
		62	11		
		66	13		
		69	15		
	Variable Importance (%)	100	34.53	15.62	6.60
116	Knot Values	65	9	1	
		66			
		67			
		67.5			
		69			
		70.5			
	Variable Importance (%)	100	31.08	14.71	
130	Knot Values	56.5	8	2	
		60			
		66			
		67.5			
		68.5			
		71			
	Variable Importance (%)	100	25.06	7.13	

58: Knot value entering the model with mirror basis function

4. Discussion

The results related to the error measurement criteria what presented incidental to Model 140 selected from the Test MSE models using the REMARS method, Model 59 selected from the GCV models using the REMARS method and the MARS model obtained from the original data set are shown in Table 8.

Table 8. Error measurement criteria of the MARS models obtained from original data and REMARS

Data Sets	Error Measurement Criteria						
	RMSE	**MSE**	**GCV**	**MAD**	**MAPE**	**SSE**	**R^2**
Original Data Set	0.385	0.149	0.160	0.291	0.115	97.173	0.802
GCV-Model 59	0.372	0.138	0.152	0.277	0.113	90.349	0.813
Test MSE-Model 140	0.389	0.151	0.157	0.298	0.116	98.938	0.788

When each of the values of the error measurement criteria shown in Table 8 is compared individually for both the Test MSE-Model 140 and GCV-Model 59, it is observed that GCV-Model 59 produces more consistent and reliable results compared to the Test MSE-Model 140. That is because the GCV criterion is calculated with a formula that considers both error and the number of effective parameters. For this reason, it tends to create models with a more complex structure and higher variable efficiency compared to the Test MSE criterion. This situation causes the error measurement criteria of the Test MSE models, which have simpler structures, to deteriorate. Therefore, the model created based on the GCV criterion has a better ability to generalise compared to the model created based on the Test MSE criterion. This is clearly observed when the knot values and importance percentages of the variables in the Test MSE-Model 140 and GCV-Model 59 are examined.

When the values of the error measurement criteria of the MARS model obtained from the original data set are compared with the error measurement criteria of GCV-Model 59, it is observed that GCV-Model 59 produces better results. On the other hand, the knot values in the MARS model obtained from the original data set were obtained as 58.5; 59.5; 65; 66; 69 for the height variable, 8 for the age variable, 2 for the sex variable and 0 for the smoker variable. When these knot values are compared with the knot values of GCV-Model 59, it is observed that knots 66 and 69, which are important for the height variable, are present in both models. The age variable entered the model with a higher knot value in GCV-Model 59. This can be an advantage or disadvantage for the model. However, [48] proved that the abundance in age knots is an advantage for the model. That is because it was shown diagrammatically that the FEV distribution of the children in the smoking environment changed direction in knots 11, 13 and 15. The number of smoker parents is very low in the FEV data and when the number of smoker parents is increased in a different sample, these knots in the age variable take on an important role for the model. Both models have the same knot values for the sex and smoker variables. The contribution percentages of the height, age, sex and smoker variables in the MARS model were obtained as 100%, 27.4%, 4.88% and 2.91%, respectively. When these values are compared with GCV-Model 59, it is understood that the age, sex and smoker variables contribute more to GCV-Model 59. In conclusion, Model 59, which was obtained with REMARS method based on the GCV criterion, produced better results than any other model.

All prediction curves for the actual and predicted FEV values shown in Fig. 2 appear to be overlapped. Here, it can be understood that MSE-Model 140 and GCV-Model 59, which were obtained with REMARS method, produce results that are as consistent and reliable as the ones produced by the MARS model obtained from the original data. On the other hand, the Pearson Correlation between the actual and predicted FEV values was calculated as $r = 0.902 \, (p = 0.001)$ for the GCV-Model 59, $r = 0.888 \, (p = 0.001)$ for the Test MSE-Model 140 and $r = 0.896 \, (p = 0.001)$ for the MARS model obtained from the original data set. The fact that the best correlation between the actual and predicted FEV values are produced by GCV-Model 59 is understood from both the Pearson Correlation Coefficient Value and the scattering of the observation values in Fig. 2.
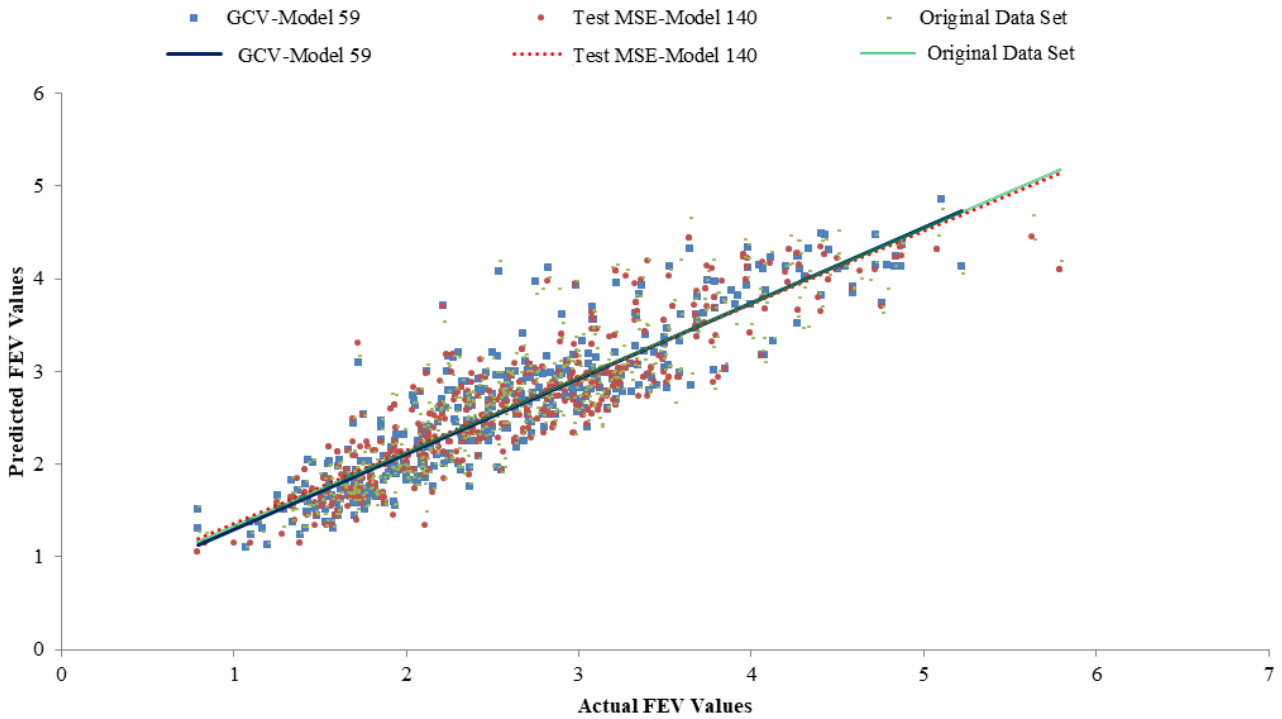
Fig. 2. Distribution of actual and predicted values of the MARS model obtained original data and REMARS

Based on the results obtained, Table 9 shows the basis functions and knot values for Model 59, which was selected with REMARS method based on the GCV criterion, and information on the prediction model.

Table 9. Basis functions and corresponding equations of the MARS model for GCV-Model 59

Basis Functions	Equation	Model
BF1	Max (0, Height-57.5)	
BF2	Max (0, 57.5- Height)	
BF3	Max (0, Age-8)	
BF5	(Sex (2))	
BF7	Max (0, Height -66)	FEV = 1.71963 +0.14058*BF1 - 0.0692608*BF2+0.0754913*BF3 +0.145284*BF5+0.260453*BF7 - 0.280703*BF9-0.106875*BF11 +0.172786*BF13-0.315717*BF23 +0.295305*BF25+0.127262*BF27
BF9	Max (0, Height -69)	
BF11	Max (0, Height -62)	
BF13	(Sex (0))	
BF23	Max (0,Age-13)	
BF25	Max (0, Age -15)	
BF27	Max (0, Age -11)	

5. Conclusion

Model 59, selected from GCV models, produces results more consistent than MARS model created by taking the original data set as training data. It is more suitable to be used for model selection particularly in data set where observations such as FEV data do not demonstrate homogeneity. The MARS model obtained from the original data set was created without being tested with separate test data. Therefore, it is not known whether it is the most useful model for new data. For this reason, the use of the model obtained through ensemble learning instead of the model obtained with a single learner produces more valid and reliable results. The MARS model obtained based on the REMARS method is suggested for this reason. The MARS model works better in big data set. The MARS model obtained using the REMARS method can produce reliable results with smaller data set due to the different samples generated with the Bagging Method. In data set with too many parameters, the procedure of independent variable selection can be carried out, as in the RF method.

Author Contributions

All authors contributed equally to this work. They all read and approved the last version of the manuscript.

Conflict of Interest

The authors declare no conflict of interest.

References

[1] S. Theodoridis, Machine Learning a Bayesian and Optimisation Perspective, Academic Press of Elsevier, 125 London Wall, London, 2015.

[2] S. Suthaharan, Machine Learning Models and Algorithms for Big Data Classification, Springer International Publishing, New York, 2016.

[3] T. Hastie, R. Tibshirani, J. Friedman, The Elements of Statistical Learning: Data Mining, Inference and Prediction, Springer Series in Statistics, Stanford, California, 2001.

[4] T. K. Ho, *Random Decision Forests*, Proceedings of 3rd International Conference on Document Analysis and Recognition (IEEE), Montreal, Canada, 1995, pp. 278–282.

[5] T. K. Ho, *The Random Subspace Method for Constructing Decision Forests*, IEEE Transactions on Pattern Analysis and Machine Intelligence 20 (2) (1998) 832–844.

[6] T. Hill, P. Lewicki, Statistics: Methods and Applications, StatSoft, Tulsa OK, 2006.

[7] J. R. Leathwick, J. Elith, T. Hastie, *Comparative Performance of Generalised Additive Models and Multivariate Adaptive Regression Splines for Statistical Modelling of Species Distributions*, Ecological Modelling 199 (2) (2006) 188–196.

[8] D. Yao, J. Yang, X. Zhan, *A Novel Method for Disease Prediction: Hybrid of Random Forest and Multivariate Adaptive Regression Splines*, Journal of Computers 8 (1) (2013) 170–177.

[9] L. Kumar, S. K. Rath, *Quality Assessment of Web Services Using Multivariate Adaptive Regression Splines*, in: J. Sun, Y. R. Reddy, A. Bahulkar, A. Pasala (Eds.), 22nd Asia-Pacific Software Engineering Conference, New Delhi, India, 2015, pp. 238–245.

[10] W. Zhang, A. T. Goh, *Multivariate Adaptive Regression Splines and Neural Network Models for Prediction of Pile Drivability*, Geoscience Frontiers 7 (1) (2016) 45–52.

[11] P. Dey, A. K. Das, *Application of Multivariate Adaptive Regression Spline-Assisted Objective Function on Optimisation of Heat Transfer Rate Around a Cylinder*, Nuclear Engineering and Technology 48 (6) (2016) 1315–1320.

[12] Y. J. Chen, J. A. Lın, Y. M. Chen, J. H. Wu, *Financial Forecasting with Multivariate Adaptive Regression Splines and Queen Genetic Algorithm-Support Vector Regression*. IEEE Access 7 (2019) 112931–112938.

[13] J. Pittman, *Adaptive Splines and Genetic Algorithms*, Journal of Computational and Graphical Statistics 11 (3) (2002) 615–638.

[14] G. W. Weber, I. Batmaz, G. Köksal, P. Taylan, F. Y. Özkurt, *CMARS: A New Contribution to Nonparametric Regression with Multivariate Adaptive Regression Splines Supported by Continuous Optimisation*, Inverse Problems in Science and Engineering 20 (3) (2012) 371–400.

[15] A. Özmen, G. W. Weber, I. Batmaz, E. Kropat, *RCMARS: Robustification of CMARS with Different Scenarios Under Polyhedral Uncertainty Set*, Communications in Nonlinear Science and Numerical Simulation 16 (12) (2011) 4780–4787.

[16] E. K. Koc, C. Iyigun, *Restructuring Forward Step of MARS Algorithm Using a New Knot Selection Procedure Based on a Mapping Approach*, Journal of Global Optimization 60 (2014) 79–102.

[17] E. K. Koc, H. Bozdogan, *Model Selection in Multivariate Adaptive Regression Splines (MARS) Using Information Complexity as the Fitness Function*, Machine Learning 101 (2015) 35–58.

[18] C. Yazıcı, F. Y. Özkurt, I. Batmaz, *A Computational Approach to Nonparametric Regression: Bootstrapping CMARS Method*, Machine Learnig 101 (2015) 211–230.

[19] S. Agarwal, C. R. Chowdary, C. R., *A-Stacking and A-Bagging: Adaptive Versions of Ensemble Learning Algorithms for Spoof Fingerprint Detection*, Expert Systems with Applications Article ID 113160 (2020) 10 pages.

[20] M. E. Lopes, *Estimating the Algorithmic Variance of Randomised Ensembles via the Bootstrap*, The Annals of Statistics 47 (2) (2019) 1088–1112.

[21] S. E. Roshan, S. Asadi, *Improvement of Bagging Performance for Classification of Imbalanced Datasets Using Evolutionary Multi-Objective Optimization*, Engineering Applications of Artificial Intelligence Article ID 103319 (2020) 19 pages.

[22] H. Kim, Y. Lim, *Bootstrap Aggregated Classification for Sparse Functional Data*, Journal of Applied Statistics 49 (8) (2022) 2052–2063.

[23] W. Pintowati, B. W. Otok, *Pemodelan Kemiskinan di Propinsi Jawa Timur dengan Pendekatan Multivariate Adaptive Regression Splines Ensemble*, Jurnal Sains dan Seni ITS 1 (1) (2012) 283–288.

[24] K. D. Roy, B. Datta, *Multivariate Adaptive Regression Spline Ensembles for Management of Multilayered Coastal Aquifers*, Journal of Hydrologic Engineering 22 (9) (2017) 04017031.

[25] R. Zheng, M. Li, X. Chen, S. Zhao, F. Wu, Y. Pan, J. Wang, *An Ensemble Method to Reconstruct Gene Regulatory Networks Based on Multivariate Adaptive Regression Splines*, IEEE/ACM Transactions on Computational Biology and Bioinformatics 18 (1) (2019) 347–354.

[26] L. Breiman, J. Friedman, C. J. Stone, R. Olshen, Classification and Regression Trees. Belmont: Taylor & Francis, New York, 1984.

[27] E. M. Kleinberg, *Stochastic Discrimination*, Annals of Mathematics and Artificial Intelligence 1 (1990) 207–239.

[28] E. M. Kleinberg, *An Overtraining-Resistant Stochastic Modelling Method for Pattern Recognition*, The Annals of Statistics 24 (6) (1996) 2319–2349.

[29] E. M. Kleinberg, *On the Algorithmic Implementation of Stochastic Discrimination*, IEEE Transactions on Pattern Analysis and Machine Intelligence 22 (5) (2000) 473–490.

[30] L. Breiman, Bagging Predictors (Report No. 421). Department of Statistics University of California. Berkeley, California, 1994.

[31] Y. Amit, D. Geman, *Shape Quantization and Recognition with Randomised Trees*, Neural Computation 9 (7) (1997) 1545–1588.

[32] L. Breiman, *Random Forest*, Machine Learning 45 (1) (2001) 5–32.

[33] M. Akman, Y. Genç, H. Ankaralı, *Random Forests Methods and an Application in Health Science*, Turkiye Klinikleri Journal of Biostatistics 3 (1) (2011) 36–48.

[34] J. Abellán, C. J. Mantas, J. G. Castellano, *A Random Forest Approach Using Imprecise Probabilities*, Knowledge-Based Systems 134 (2017) 72–84.

[35] A. Liaw, M. Wiener, R Project. The R Project for Statistical Computing: https://cran.r-project.org/web/packages/randomForest/randomForest.pdf. Accessed on April 9, 2019.

[36] Minitab, Minitab: http://www.minitab.com/uploadedFiles/Content/Products/SPM/IntroRF_v_8_2.pdf. Accessed on April 9, 2019.

[37] J. H. Friedman, *Multivariate Adaptive Regression Splines*, The Annals of Statistics 19 (1) (1991) 1–67.

[38] J. Deichmann, A. Eshghi, D. Haughton, S. Sayek, N. Teebagy, *Application of Multiple Adaptive Regression Splines (MARS) in Direct Response Modeling*, Journal of Interactive Marketing 16 (4) (2002) 15–27.

[39] G. O. Temel, H. Ankaralı, A. C. Yazıcı, *An Alternative Approach to Regression Models: MARS,* Turkiye Klinikleri Journal of Biostatistics 2 (2) (2010) 58–66.

[40] J. Strickland, Predictive Analytics Using R. Lulu Press (Lulu.com), Morrisville, North Carolina, USA, 2015.

[41] L. C. Briand, B. Freimut, F. Vollei, Using Multiple Adaptive Regression Splines to Understand Trends in Inspection Data and Identify Optimal Inspection Rates (Report No. 062.00/E). Fraunhofer IESE, Kaiserslautern, 2001.

[42] P. Craven, G. Wahba, *Smoothing Noisy Data with Spline Functions: Estimating the Correct Degree of Smoothing by the Method of Generalised Cross-Validation*, Numerische Mathematik 31 (4) (1978) 377–403.

[43] J. H. Friedman, Fitting Functions to Noisy Data in High Dimensions (Technical Report No. LCS 101). Stanford University, Department of Statistics, Stanford, CA, 1988.

[44] J. H. Friedman, B. W. Silverman, *Flexible Parsimonious Smoothing and Additive Modelling*, Technometrics 31 (1) (1989) 3–21.

[45] I. B. Tager, S. T. Weiss, B. Rosner, F. E. Speizer, *Effect of Parental Cigarette Smoking on the Pulmonary Function of Children*, American Journal of Epidemiology 110 (1) (1979) 15–26.

[46] I. B. Tager, S. T. Weiss, A. Munoz, B. Rosner, F. E. Speizer, *Longitudinal Study of the Effects of Maternal Smoking on Pulmonary Function in Children*, New England Journal of Medicine 309 (12) (1983) 699–703.

[47] B. Rosner, Fundamentals of Biostatistics. Duxbury Press, Pacific Grove, CA, 1999.

[48] M. Kahn, *An Exhalent Problem for Teaching Statistics*, Journal of Statistics Education 13 (2) (2005) 1–11.

[49] Journal of Statistics Education, JSE Data Archive. http://jse.amstat.org/datasets /fev.dat.txt. Accessed on October 10, 2017.

4-Dimensional 2-Crossed Modules

Elis Soylu Yılmaz[1] (ID)

Abstract − In this work, we defined a new category called 4-Dimensional 2-crossed modules. We identified the subobjects and ideals in this category. The notion of the subobject is a generalization of ideas like subsets from set theory, subspaces from topology, and subgroups from group theory. We then exemplified subobjects and ideals in the category of 4-Dimensional 2-crossed modules. A quotient object is the dual concept of a subobject. Concepts like quotient sets, spaces, groups, graphs, etc. are generalized with the notion of a quotient object. Using the ideal, we obtain the quotient of two subobjects and prove that the intersection of finite ideals is also an ideal in this category.

1. Introduction

In order to generalize the well-known conclusion that the category of crossed modules is equivalent to the category of simplicial groups with a Moore complex of length 2, Conduché introduced 2-crossed modules of groups in [1] demonstrating that the category of simplicial groups with a three-dimensional Moore complex and the category of 2-crossed modules are equivalent. Therefore, 2-crossed modules also serve as algebraic models for connected homotopy 3-types or pointed CW-complexes X such that $\pi(X) = 0$ if $i > 3$. The idea of 2-crossed modules is adapted for algebras by Grandjean and Vale [2].

The homotopy 3-types can also be represented by crossed squares [3] and quadratic modules [4]. The categories of braided regular crossed modules [5] and Gray 3-groupoids with a single object [6], are other categories that are equivalent to the category of 2-crossed modules. The category of 2-crossed modules is also shown in [7] to be equivalent to the categories of neat crossed squares and neat maps.

For the algebraic description of pointed relative CW–complexes with cells in dimensions 4, Baues and Bleile introduced the concept of 4–dimensional quadratic complexes [8] to investigate the presentation of a space X as mapping cone of a map $\partial(X)$ under a space D. The need for a proper understanding of the relevant algebraic and categorical structure of the 4-Dimensional 2-crossed modules are motivated by studies and examples [9–15] for higher categorical structures. In this work, we defined the notion of 4-Dimensional 2-crossed modules in order to look into any potential equivalence between homotopy 4-types, which was inspired by the work of Baues and Bleile. Examining how 4-Dimensional 2-crossed modules relate to an algebraic structure resembling 2-crossed modules is the main goal of this paper. In order to achieve this, we first introduce the category of 4-Dimensional 2-crossed modules before describing subobjects and ideals in full detail. In conclusion, we demonstrate that the quotient of the objects in this category is a 4-Dimensional 2-crossed module.

---

[1]esoylu@ogu.edu.tr (Corresponding Author)
[1]Department of Mathematics and Computer Science, Faculty of Sciences, Eskişehir Osmangazi University, Eskişehir, Türkiye

The main ideas of this work can be given as:
- To construct a new category weaker than homotopy 4-types and stronger than homotopy 3-types,
- To fully describe the subobjects and ideals within this category,
- To construct the quotient object by using ideals in this category.

2. 4-Dimensional 2-Crossed Modules

Grandjeán and Vale [2] have given a definition of 2-crossed modules of algebras. The following is an equivalent formulation of that concept.

A 2-*crossed module* of k-algebras consists of a complex of P-algebras $L \xrightarrow{\partial_2} M \xrightarrow{\partial_1} P$ together with an action of P on all three algebras and a P-linear mapping

$$\{-, -\} : M \times M \to L$$

which is often called the Peiffer lifting such that the action of P on itself is by multiplication, ∂_2 and ∂_1 are P-equivariant.

PL1 : $\partial_2 \{m_0, m_1\} = m_0 m_1 - \partial_1 (m_1) \cdot m_0$
PL2 : $\{\partial_2 (l_0), \partial_2 (l_1)\} = l_0 l_1$
PL3 : $\{m_0, m_1 m_2\} = \{m_0 m_1, m_2\} + \partial_1 (m_2) \cdot \{m_0, m_1\}$
PL4 : $\{m, \partial_2 (l)\} + \{\partial_2 (l), m\} = \partial_1 (m) \cdot l$
PL5 : $\{m_0, m_1\} \cdot p = \{m_0 \cdot p, m_1\} = \{m_0, m_1 \cdot p\}$

for all $m, m_0, m_1, m_2 \in M, l, l_0, l_1 \in L$ and $p \in P$. Note that we have not specified that M acts on L. We could have done that as follows: if $m \in M$ and $l \in L$, define

$$m \cdot l = \{m, \partial_2 (l)\}$$

From this equation (L, M, ∂_2) becomes a crossed module. We can split **PL4** into two pieces:
PL4 :
$$\begin{aligned} (a) \quad \{m, \partial_2 (l)\} &= m \cdot l \\ (b) \quad \{\partial_2 (l), m\} &= m \cdot l - \partial_1 (m) \cdot l \end{aligned}$$

We denote such a 2-crossed module of algebras by $\{L, M, P, \partial_2, \partial_1\}$.

A morphism of 2-crossed modules is given by the following diagram

$$\begin{array}{ccccc} L & \xrightarrow{\partial_2} & M & \xrightarrow{\partial_1} & P \\ \downarrow{\scriptstyle f_2} & & \downarrow{\scriptstyle f_1} & & \downarrow{\scriptstyle f_0} \\ L' & \xrightarrow{\partial_2'} & M' & \xrightarrow{\partial_1'} & P' \end{array}$$

where $f_0 \partial_1 = \partial_1' f_1, f_1 \partial_2 = \partial_2' f_2$

$$f_1 (p \cdot m) = f_0 (p) \cdot f_1 (m) \quad , \quad f_2 (p \cdot l) = f_0 (p) \cdot f_2 (l)$$

for all $m \in M, l \in L, p \in P$ and

$$\{-, -\} (f_1 \times f_1) = f_2 \{-, -\}$$

We thus get the category of 2-crossed modules denoting it by $\mathsf{X_2Mod}$. In [4], Baues developed the concept of 4-dimensional quadratic modules after defining quadratic modules. Adapting this definition for 2-crossed modules we get a complex of algebras

$$\sigma : K \xrightarrow{\partial_4} L \xrightarrow{\partial_3} M \xrightarrow{\partial_2} P$$

such that

1. $(L, M, P, \partial_2, \partial_3)$ is a 2-crossed module with Peiffer lifting $\{-, -\} : M \times M \to L$;

2. K is a L–module such that $\partial_2(M)$ acts trivially and

3. ∂_4 is a homomorphism of Q_1–modules, such that $\partial_3\partial_4 = 0$.

A *morphism of 4–dimensional 2-crossed modules*, $f : \sigma \to \sigma'$, is a sequence of morphisms

$$
\begin{array}{ccccccc}
\sigma : K & \xrightarrow{\partial_4} & L & \xrightarrow{\partial_3} & M & \xrightarrow{\partial_2} & P \\
f_4 \downarrow & & f_3 \downarrow & & f_2 \downarrow & & f_1 \downarrow \\
\sigma' : K' & \xrightarrow{\partial_4} & L' & \xrightarrow{\partial_3'} & M' & \xrightarrow{\partial_2'} & P'
\end{array}
$$

such that (f_3, f_2, f_1) yields a morphism of 2-crossed modules, f_4 is an f_1–equivariant homomorphism of modules and $\partial_4 f_4 = f_3 \partial_4$. We denote the category of 4-Dimensional 2-crossed modules by X_2Mod^{4D}.

Next, we will define the subobjects in X_2Mod^{4D}.

Definition 2.1. Let

$$
\sigma : Q_4 \xrightarrow{\partial_4} Q_3 \xrightarrow{\partial_3} Q_2 \xrightarrow{\partial_2} Q_1
$$

be an object in X_2Mod^{4D}. Then we say that

$$
\sigma' : Q_4' \xrightarrow{\partial_4'} Q_3' \xrightarrow{\partial_3'} Q_2' \xrightarrow{\partial_2'} Q_1'
$$

is a subobject of σ if

1. Q_4' is a subalgebra of Q_4, Q_3' is a subalgebra of Q_3 and Q_2' is a subring of Q_2;

2. $\partial_2' : Q_2 \to Q_1$ is a subpre-crossed module of $\partial_2 : Q_2 \to Q_1$;

3. The actions of Q_2' on Q_4' and Q_3' via Q_1' is induced from the actions of Q_2 on Q_4 and Q_3 via Q_1;

4. σ' is an object in X_2Mod^{4D} and

5. The diagram

is commutative where for i=1, 2, 3 μ_i are injections.

Example 2.2. Let

$$
\sigma : Q_2 \otimes Q_2 \xrightarrow{\partial_4} Q_2 \otimes Q_2 \xrightarrow{\partial_3} Q_2 \xrightarrow{\partial_2} Q_1
$$

be an object in X_2Mod^{4D} with $Id : Q_2 \otimes Q_2 \to Q_2 \otimes Q_2$ as Peiffer lifting. If K_2 is ideal of Q_2 and K_1 is a subring of Q_1 that is $\delta_2 : K_2 \to K_1$ is a subpre-crossed module of $\partial_2 : Q_2 \to Q_1$ then

$$
\sigma' : K_2 \otimes K_2 \xrightarrow{Id} K_2 \otimes K_2 \xrightarrow{\delta_3} K_2 \xrightarrow{\delta_2} K_1
$$

is a subobject of σ with $Id : K_2 \otimes K_2 \to K_2 \otimes K_2$ as Peiffer lifting.

Example 2.3. Let R be a k-algebra and

$$R/R^2 \otimes R/R^2$$

$$\{-,-\}=Id \downarrow$$

$$\sigma : R/R^2 \otimes R/R^2 \xrightarrow{Id} R/R^2 \otimes R/R^2 \xrightarrow{\partial} R \xrightarrow{Id} R$$

be an object in $X_2 Mod^{4D}$. If I is an ideal of R and J is a subring of I then,

$$I/I^2 \otimes I/I^2$$

$$\{-,-\}=Id \downarrow$$

$$\sigma' : I/I^2 \otimes I/I^2 \xrightarrow{Id} I/I^2 \otimes I/I^2 \xrightarrow{\partial'} I \xrightarrow{i} J$$

is a subobject of σ.

3. Ideals in $X_2 Mod^{4D}$

In this section we will define ideals in $X_2 Mod^{4D}$ and intersections of two ideals is an ideal in this category.

Definition 3.1. Let

$$\sigma : K \xrightarrow{\partial_4} L \xrightarrow{\partial_3} M \xrightarrow{\partial_2} P$$

be an object in $X_2 Mod^{4D}$. Then we say that

$$\sigma' : K' \xrightarrow{\partial'_4} L' \xrightarrow{\partial'_3} M' \xrightarrow{\partial'_2} P'$$

is an ideal of σ if

1. Let $L'L \subseteq L'$, $K'K \subset K'$ and M' be an ideal of M;

2. (a) $M'M \subset M$ and P' is an ideal of P;
    (b) for $p \in P'$ and $m \in M$, $p \cdot m \in M'$;
    (c) for $m' \in M'$ and $p \in P$, $p \cdot m' \in M'$;

3. For $m' \in M'$, $l \in L$, $k \in K$ $\partial_1(m') \cdot l \in L'$, $\partial_1(m') \cdot k \in K'$;

4. For $l' \in L'$, $m \in M$ and $k' \in K'$, $\partial_1(m) \cdot l' \in L'$, $\partial_1(m) \cdot k' \in K'$;

5. K' and L' are P-algebras. That is,

    (a) For $p' \in P'$, $l \in L$ and $k \in K$, $p' \cdot l \in L'$, $p' \cdot k \in K'$;

    (b) For $l' \in L'$, $p \in P$ and $k' \in K'$, $p \cdot l' \in L'$, $p \cdot k' \in K'$;

Example 3.2. Let I be an ideal of R if

$$\theta : K \longrightarrow L \longrightarrow I \xrightarrow{id} I$$

is an object in $X_2 Mod^{4D}$ then θ is an ideal of the 4-Dimensional 2-crossed module σ in Example 2.3.

Example 3.3. Let I and I' be ideals of R and $(I, R, \mu), (I', R, \mu')$ be two nil(2)-modules. Since $(I \cap I', I, \vartheta)$ is a nil(2)-module we have,

i)

$$\sigma' : K \xrightarrow{\partial_2} L \xrightarrow{\pi} I \cap I' \xrightarrow{\vartheta'} I'$$

is an ideal of

$$\sigma : K \xrightarrow{\delta_2} I \times I \xrightarrow{\pi} I \xrightarrow{\mu} R$$

ii)

$$\theta' : K \xrightarrow{\partial_2} L \xrightarrow{\pi} I \cap I' \xrightarrow{\vartheta} I$$

is an ideal of

$$\theta : K \xrightarrow{\delta_2'} I' \times I' \xrightarrow{\pi} I' \xrightarrow{\mu'} R$$

where $L = (I \cap I') \times (I \cap I')$ with Peiffer liftings as identities and π as projection.

Theorem 3.4. The intersection of finite ideals is an ideal in $X_2 Mod^{4D}$.

PROOF. Let

$$\sigma : K \xrightarrow{\partial_3} L \xrightarrow{\partial_2} M \xrightarrow{\partial_1} P$$

be an object in $X_2 Mod^{4D}$. If

$$\sigma_1 : K_1 \xrightarrow{\partial_3'} L_1 \xrightarrow{\partial_2'} M_1 \xrightarrow{\partial_1'} P_1$$

and

$$\sigma_2 : K_2 \xrightarrow{\partial_3''} L_2 \xrightarrow{\partial_2''} M_2 \xrightarrow{\partial_1''} P_2$$

be two subobjects of σ. Then we have,

1. Since $L_1 L \subset L_1, L_2 L \subset L_2$ and $K_1 K \subset K_1, K_2 K \subset K_2$ we get

$$(L_1 \cap L_2) L \subseteq L_1 \cap L_2$$

and

$$(K_1 \cap K_2) K \subset K_1 \cap K_2$$

2. a. Since $M_1 M \subseteq M_1$ and $M_2 M \subseteq M_2$ we get

$$(M_1 \cap M_2) M \subseteq M_1 \cap M_2$$

where $N_1 \trianglelefteq P$ and $P_2 \trianglelefteq P$ imply $P_1 \cap N_2 \trianglelefteq P$.

b. Since σ_1 is an ideal of σ for $x \in P_1$ we have $x \cdot m \in M_1$ and σ_2 is an ideal of σ for $x \in P_2$ we have $x \cdot m \in M_2$. Then we get $x \cdot m \in M_1 \cap M_2$.

c. Since σ_1 and σ_2 are ideals of σ, for $y \in M_1, y \in M_2$, and $p \in P$ we have $p \cdot y \in M_1$ and $p \cdot y \in M_2$ which implies $p \cdot y \in M_1 \cap M_2$.

3. Since σ_1 is an ideal of σ for $y \in M_1$ and $l \in L$ we have $\partial(y) \cdot l \in L_1$ and since ∂_2 is an ideal of σ for $\partial(y) \in M_2$ and $l \in L$ we have $\partial(y) \cdot l \in L_2$. Then we get $\partial(y) \cdot l \in L_1 \cap L_2$. Similarly for $y \in M_1 \cap M_2$ and $k \in K$ we get $\partial(y) \cdot k \in K_1 \cap K_2$.

4. Since for $z \in L_1$ and $m \in M$ $\partial_1(m) \cdot z \in L_1$ and for $z \in L_2, m \in M$ $\partial_1(m) \cdot z \in L_2$ we have $\partial_1(m) \cdot z \in L_1 \cap L_2$. Similarly for $t \in K_1 \cap K_2$ we get $\partial_1(m) \cdot t \in K_1 \cap K_2$.

5. a. Let $x \in P_1 \cap P_2$ for $x \in P_1$ and $l \in L$ we have $x \cdot l \in L_1$ and for $x \in P_2$ and $l \in L$ we have $x \cdot l \in L_2$. Then we get $x \cdot l \in L_1 \cap L_2$. Simlarly for $x \in P_1 \cap P_2$ and $k \in K$ we have $x \cdot k \in K_1 \cap K_2$.

b. Let $z \in L_1 \cap L_2$ for $p \in P$ and $z \in L_1$ we have $p \cdot z \in L_1$ and for $z \in L_2$ and $p \in P$ we have $p \cdot z \in L_2$. Then we have $p \cdot z \in L_1 \cap L_2$. Similarly for $t \in K_1 \cap K_2$ we have $p \cdot k \in K_1 \cap K_2$.

As a result the object

$$K_1 \cap K_2 \xrightarrow{(\partial_3', \partial_3'')} L_2 \cap L_2 \xrightarrow{(\partial_2', \partial_2'')} M_1 \cap M_2 \xrightarrow{(\partial_1', \partial_1'')} P_1 \cap P_2$$

in $X_2 Mod^{4D}$ is an ideal of

$$K \xrightarrow{\partial_3} L \xrightarrow{\partial_3} M \xrightarrow{\partial_3} P$$

$\square$

4. Quotient object in $X_2 Mod^{4D}$

In this section using the ideal σ' of an object σ in $X_2 Mod^{4D}$, we prove that the quotient σ/σ' is an object in $X_2 Mod^{4D}$.

Let

$$\sigma' : K' \xrightarrow{\partial_3'} L' \xrightarrow{\partial_2'} M' \xrightarrow{\partial_1'} P'$$

be an ideal of

$$\sigma : K \xrightarrow{\partial_3} L \xrightarrow{\partial_2} M \xrightarrow{\partial_1} P$$

in $X_2 Mod^{4D}$. Since $M \trianglelefteq M$ and $P' \trianglelefteq P$, the action of P/P' on M/M' can be given as

$$(x + P') \cdot (y + M') = x \cdot y + M'$$

and for $p' \in P'$

$$
\begin{aligned}
p' \cdot (y + M') &= p' \cdot y + M' \\
&= 0 + M' \qquad (\because p' \cdot y \in M)
\end{aligned}
$$

P' acts on M/M' trivially. Next, we will show that

$$
\begin{aligned}
\delta : M/M' &\rightarrow P/P' \\
y + M' &\mapsto \partial_1(y) + P'
\end{aligned}
$$

is a well defined nil(2)-module morphism.

∂_1' is the restriction of ∂_1 to M' implies $\partial_1' \subset P'$. For $m' \in M'$ we have $\partial_1'(m') \cdot (l + L') = \partial_1'(m') \cdot l + L' = L'$ (σ' is an ideal of σ then $\partial_1'(m') \cdot l \in L'$). That is the action of M' on L/L' via P' must be trivial. Therefore M/M' acts on L/L' via P/P'. This action can be defined as:

$$(\partial_1(m) + M) \cdot (l + L') = \partial_1(m) \cdot l + L'$$

for $l + L' \in L/L'$ and $m + M' \in M/M'$.

Theorem 4.1. Let

$$\sigma' : K' \xrightarrow{\partial_3'} L' \xrightarrow{\partial_2'} M' \xrightarrow{\partial_1'} P'$$

be an ideal of

$$\sigma : K \xrightarrow{\partial_3} L \xrightarrow{\partial_2} M \xrightarrow{\partial_1} P$$

in $X_2 Mod^{4D}$. Then

$$\sigma/\sigma' : K/K' \xrightarrow{\delta_3} L/L' \xrightarrow{\delta_2} M/M' \xrightarrow{\delta_1} P/P'$$

is an object in $X_2 Mod^{4D}$.

PROOF. 1. PL1. For $x_1 + M', x_2 + M' \in M/M'$:

$$
\begin{aligned}
\delta\{x_1 + M', x_2 + M'\}_\delta &= \partial_2\{x_1, x_2\}_\sigma + L' \\
&= x_1 x_2 - x_1 \cdot \partial_1(x_2) + L'
\end{aligned}
$$

PL2. For $y_1 + M', y_2 + M' \in L/L'$:

$$
\begin{aligned}
\{\delta_2(y_1 + L'), \delta(y_2 + L')\}_\delta &= \{\partial_2(y_1) + M', \partial_2(y_2) + M'\}_\sigma \\
&= \{\partial_2(y_1), \partial_2(y_2)\}_\sigma + M' \\
&= y_1 y_2 + M' \\
&= (y_1 + M')(y_2 + M')
\end{aligned}
$$

PL3. For $x_o + M', x_1 + M', x_2 + M' \in M/M'$:

$$
\begin{aligned}
\{x_0 + M', x_1 x_2 + M'\}_\delta &= \{x_0, x_1 x_2\}_\sigma + M' \\
&= \{x_0 x_1, x_2\}_\sigma + \partial_1(x_2)\{x_0, x_1\}_\sigma + M' \\
&= \{x_0 x_1, x_2\}_\sigma + M' + \partial_1(x_2)\{x_0, x_1\}_\sigma + M' \\
&= \{x_0 x_1 + M', x_2 + M'\}_\delta + \partial_1(x_2)\{x_0 + M', x_1 + M'\}_\delta
\end{aligned}
$$

PL4. a. For $y + L' \in L/L'$ and $x + M' \in M/M'$:

$$
\begin{aligned}
\{\delta_2(y + L'), x + M'\}_\delta &= \{\partial_2(y) + M', x + M'\}_\delta \\
&= \{\partial_2(y), x\}_\sigma + M' \\
&= (x \cdot y - \partial_1(x) \cdot y) + M'
\end{aligned}
$$

b. For $y + L' \in L/L'$ and $x + M' \in M/M'$:

$$
\begin{aligned}
\{x + M', \delta_2(y + L')\}_\delta &= \{x + M', \partial_2(y) + M'\}_\delta \\
&= \{x, \partial_2(y)\}_\sigma + M' \\
&= (x \cdot y) + M'
\end{aligned}
$$

PL5. For $x_o + M', x_1 + M' \in M/M'$ and $t + P' \in P/P'$:

$$
\begin{aligned}
\{x_0 + M', x_1 + M'\}_\delta \cdot (t + P') &= (\{x_0, x_1\}_\sigma \cdot (t + P')_\delta) + M' \\
&= (\{x_0 \cdot t, x_1\}_\sigma) + M' \\
&= \{(x_0 \cdot t) + M', x_1 + M'\}_\delta
\end{aligned}
$$

and

$$
\begin{aligned}
\{x_0 + M', x_1 + M'\}_\delta \cdot (t + P') &= (\{x_0, x_1\}_\sigma \cdot (t + P')_\delta) + M' \\
&= (\{x_0, x_1 \cdot t\}_\sigma) + M' \\
&= \{x_0 + M', (x_1 \cdot t) + M'\}_\delta
\end{aligned}
$$

2. Since σ' is an ideal of σ/σ' for $m + M' \in M/M'$ we have $\delta_1(m + M') \cdot (k + K') = \delta_1(m + M') \cdot (k + K') = K'$. That is M/M' acts on K/K' via P' trivially. Therefore K/K' is a P/P'-module.

3. For $k + K' \in K/K'$:

$$
\begin{aligned}
\delta_2 \delta_3(k + K') &= \delta_2(\partial_3(k) + L') \\
&= \partial_2(\partial_3(k) + M') \\
&= 0 + M' \\
&= 0_{M/M'}
\end{aligned}
$$

$\square$

5. Conclusion

In this work, we introduced a new category weaker than homotopy 4-types and stronger than homotopy 3-types. As an intriguing result 4–dimensional 2-crossed modules serve as a bridge to investigate categorical equivalences between homotopy 3-types and homotopy 4-types. The categorical equivalences of the category $X_2 Mod^{4D}$ and other homotopy 3–4 types from the various models can be explored as further research. The research presented in this study has addressed fundamentals of the category $X_2 Mod^{4D}$, and these provide guidance for future work in the following:

- Constructing categorical properties such as limit, product, pullback, pushout, etc.,
- Embedding theorem can be adapted for the category $X_2 Mod^{4D}$,
- Freeness conditions and simplicial properties can be examined.

In addition, categorical equivalences and properties are also reference points for further work of $X_2 Mod^{4D}$.

Author Contributions

The author read and approved the last version of the paper.

Conflicts of Interest

The author declares no conflict of interest.

References

[1] D. Conduché, *Modules Croisés Généralisés de Longueur 2*, Journal of Pure and Applied Algebra 34 (2-3) (1984) 155–178.

[2] A. R. Grandjeán, M. J. Vale, *2-Modulos Cruzados en la Cohomologia de André-Quillen*, Memorias de la Real Academia de Ciencias 22 (1986) 1–28.

[3] G. Ellis, *Crossed Squares and Combinatorial Homotopy*, Mathematische Zeitschrift 214 (1) (1993) 93–110.

[4] H. J. Baues, Combinatorial Homotopy and 4-Dimensional Complexes, Berlin, De Gruyter, 2011.

[5] R. Brown, N. D. Gilbert, *Algebraic Models of 3-Types and Automorphism Structures for Crossed Modules*, In Proceedings of the London Mathematical Society 59 (1) (1989) 51–73.

[6] K. H. Kamps, T. Porter, *2-Groupoid Enrichments in Homotopy Theory and Algebra*, K-theory 25 (4) (2002) 373–409.

[7] J. F. Martins, *The Fundamental 2-Crossed Complex of a Reduced CW-Complex*, Homology, Homotopy and Applications 13 (2) (2011) 129–157.

[8] H. J. Baues, B. Bleile, *Presentation of Homotopy Types Under a Space*, ArXiv Preprint, ArXiv:1005.4810, 2010.

[9] U. E. Arslan, S. Kaplan, *On Quasi 2-Crossed Modules for Lie Algebras and Functorial Relations*, Ikonion Journal of Mathematics 4 (1) (2022) 17–26.

[10] R. Brown, I. Içen, *Homotopies and Automorphisms of Crossed Modules of Groupoids*, Applied Categorical Structures 11 (2) (2003) 185–206.

[11] P. Carrasco, J. M. Moreno, *Categorical G-Crossed Modules and 2-Fold Extensions*, Journal of Pure and Applied Algebra 163 (3) (2001) 235–257.

[12] A. Mutlu, T. Porter, *Freeness Conditions for 2-Crossed Codules and Complexes*, Theory and Applications of Categories 4 (8) (1998) 174–194.

[13] A. Mutlu, *Free 2-Crossed Complexes of Simplicial Algebras*, Mathematical and Computational Applications 5 (1) (2000) 13–22.

[14] F. Wagemann, *2 Crossed Modules of Lie Algebras*, Communications in Algebra 34 (5) (2006) 1699–1722.

[15] K. Yılmaz, E. Ulualan, *Construction of Higher Groupoids via Matched Pairs Actions*, Turkish Journal of Mathematics 43 (3) (2019) 1492-–1503.

On the Characterisations of Curves with Modified Orthogonal Frame in $\mathbb{E}^3$

Şeyda Özel[1] 🆔 **, Mehmet Bektaş[2]** 🆔

Abstract − This study analyses (k, m)-type slant helices in compliance with the modified orthogonal frame in 3-dimensional Euclidean space ($\mathbb{E}^3$). Furthermore, we perform some characterisations of curves with modified orthogonal frames in $\mathbb{E}^3$.

1. Introduction

Certain particular curves and surfaces have notable importance in differential geometry. Frenet equality and curvatures of the curve are important in works related to curves. Frenet equations are employed in the structure of plenty of curve theories. One of the primary importance of these curves is the helix curve. The characterisations of curvature and torsion of helix curves perform a remarkable role in describing particular curve types. A helix is a curve whose tangent makes a constant angle with a fixed direction [1]. There is an essential categorisation of a helix. In such a way, a curve is called a helix if $\frac{\kappa}{\tau} = constant$ [2]. The curve is a (k, m)-type slant helix. Then, there is a non-zero fixed vector field, and with this constant vector field, the vector fields that have the identical index of a parallel transport frame do a constant angle. Lately, many search works related to this concept. The slant helix notion in 3-dimensional Euclidean space ($\mathbb{E}^3$) is described by Takeuchi and Izumiya [3]. Soliman et al. [4] investigated the progression of space curves using the type 3-Bishop frame. Bektaş and Yılmaz [5,6] described (k, m)-type slant helices in $\mathbb{E}^4$ and null curves in 4-dimensional Minkowski space.

Additionally, Bulut and Bektaş [7] acquired particular helices upon isomorphic differential geometry of spacelike curves in Minkowski spacetime. Furthermore, Bükcü et al. [8] investigated the spherical curves according to two types of modified orthogonal frames in $\mathbb{E}^3$. Besides, Eren and Köksal [9] investigated the development of space curves with modified orthogonal frames. Azak [10] described the notion of involute-evolute curve according to modified orthogonal frames in $\mathbb{E}^3$. This paper studies (k, m)-type slant helices in compliance with the aforesaid frame in $\mathbb{E}^3$.

---

[1]s_demir2323@outlook.com (Corresponding Author); [2]mbektaş@firat.edu.tr

[1,2]Department of Mathematics, Faculty of Science, Fırat University, Elazığ, Türkiye

2. Preliminaries

This section presents some basic definitions to be employed in the following sections.

Definition 2.1. The curve formed by making a fixed angle in a fixed direction is called a helix. If ratio $\frac{\tau}{\kappa}$ is constant, it means that the curves are helices [13].

Throughout this paper, let C^∞ denote the curves with continuous partial derivatives of every order ∞. Suppose that $\varphi(s) \in C^3$ is parameterised by arc length s in $\mathbb{E}^3$ and its curvature $\kappa(s)$ is different from zero. Thus, an orthonormal frame $\{t, n, b\}$ provides the Serret-Frenet equations

$$\begin{bmatrix} t'(s) \\ n'(s) \\ b'(s) \end{bmatrix} = \begin{bmatrix} 0 & \kappa & 0 \\ -\kappa & 0 & \tau \\ 0 & -\tau & 0 \end{bmatrix} \begin{bmatrix} t(s) \\ n(s) \\ b(s) \end{bmatrix} \tag{2.1}$$

Here, t is the unit tangent vector, n is the unit principal normal, b is the unit binormal. $\tau(s)$ is also the torsion of the curve. Besides a provided C^1 function $\kappa(s)$ as well as a continuous function $\tau(s)$, there is a curve C^3 with an orthonormal frame $\{t, n, b\}$ that provides the Serret-Frenet frame given in Equation (2.1) [11].

Suppose that $\varphi(t)$ is a common analytic curve that may be reparameterised by its arc length s. Herein, $s \in I$ and I is a non-empty open interval. Suggesting that the curvature function has discrete zero points or $\kappa(s)$ is not identically zero, we have an orthogonal frame $\{T, N, B\}$ named as noted below:

$$T = \frac{d\varphi}{ds}, \qquad N = \frac{dT}{ds}, \qquad \text{and} \qquad B = T \times N$$

Here, $T \times N$ is the vector multiplying T and N. The relation between $\{T, N, B\}$ and former Frenet frame vectors at non-zero spots of κ are as follows:

$$T = t, \qquad N = \kappa n, \qquad \text{and} \qquad B = \kappa b \tag{2.2}$$

Hence, we find out that $N(s_0) = B(s_0) = 0$ while $\kappa(s_0) = 0$ and squares of the length of N and B change analytically according to s. By way of Equation (2.2), it is simply to be calculated

$$\begin{bmatrix} T'(s) \\ N'(s) \\ B'(s) \end{bmatrix} = \begin{bmatrix} 0 & 1 & 0 \\ -\kappa^2 & \frac{\kappa'}{\kappa} & \tau \\ 0 & -\tau & \frac{\kappa'}{\kappa} \end{bmatrix} \begin{bmatrix} T(s) \\ N(s) \\ B(s) \end{bmatrix} \tag{2.3}$$

where the whole of the differentiations are executed according to the arc length (s) and

$$\tau = \tau(s) = \frac{det(\varphi', \varphi'', \varphi''')}{\kappa^2}$$

is the torsion of φ. By way of the Serret-Frenet Equation, we acknowledge that whichever spot in which $\kappa^2 = 0$ is a removable singularity of τ. Suggesting that $\langle, \rangle$ be the standard inner multiplying of $\mathbb{E}^3$, in that case $\{T, N, B\}$ provide for

$$\langle T, T \rangle = 1, \qquad \langle N, N \rangle = \langle B, B \rangle = \kappa^2, \qquad \text{and} \qquad \langle T, N \rangle = \langle T, B \rangle = \langle N, B \rangle = 0 \tag{2.4}$$

The orthogonal frame described in Equation (2.3) providing Equation (2.4) is called modified orthogonal frames [8,11]. Then, we acknowledge that for $\kappa = 1$, the Serret-Frenet frame matches up with the modified orthogonal frames.

Suppose that I be an open interval of real line $\mathbb{R}$ and M be a n-dimensional Riemannian manifold and $T_p(M)$ be a tangent space of M at a point $p \in M$. A curve on M is a smooth mapping $\psi: I \to M$. I, a submanifold of $\mathbb{R}$, has a coordinate system consisting of the identity map u of I. The velocity vector of ψ at $s \in I$ is noted by

$$\psi'(s) = \frac{d\psi(u)}{du}\bigg|_s \in T_{\psi(s)}(M)$$

If $\psi'(s) \neq 0$ for whichever s, then a curve $\psi(s)$ is the regular curve. Suppose that $\psi(s)$ is a space curve on M and $\{t, n, b\}$ the moving Frenet frame along ψ, thus we have the below-mentioned features

$$
\begin{aligned}
\psi'(s) &= t \\
D_t t &= \kappa n \\
D_t n &= -\kappa t + \tau b \\
D_t b &= -\tau n
\end{aligned}
\tag{2.5}
$$

where D indicates the covariant differentiation on M [12].

In the following, let vectors $V_K, K \in \{1,2,3\}$ be given as $V_1 = T, V_2 = N, V_3 = B$ and let a fixed direction vector u define the axis for the helix.

Definition 2.2. A curve $\alpha(s)$ is said to be a K-type slant helix if there exists a non-zero fixed direction vector u such that $\langle V_K, u \rangle = c$, where c is a real constant and $K \in \{1,2,3\}$ [14].

Definition 2.3. Let α be a regular unit speed curve $\mathbb{E}^3$ with Frenet frame $\{V_1, V_2, V_3\}$. We call α is a (k, m)-type slant helices if there exists a non-zero constant vector field $u \in \mathbb{E}^3$ satisfies $\langle V_k, u \rangle = a$ and $\langle V_m, u \rangle = b$. Here, a and b are constant concerning Frenet frame $\{V_1, V_2, V_3\}$ [5,6].

3. On the Characterisations of Curves with Modified Orthogonal Frame in $\mathbb{E}^3$

This section presents (k, m)-type slant helices in compliance with the modified orthogonal frame in $\mathbb{E}^3$. Furthermore, we get some characterisations of curves with modified orthogonal frames in $\mathbb{E}^3$.

Theorem 3.1. A unit speed curve ψ is a helix in compliance with orthonormal frame $\{t, n, b\}$ necessary and sufficient condition ψ is a helix in compliance with the modified orthogonal framework $\{T, N, B\}$.

PROOF. $\Rightarrow$ Let ψ be a helix in compliance with the orthonormal framework $\{t, n, b\}$, we know that

$$\langle t, u \rangle = cos\theta = constant \tag{3.1}$$

On the other hand, we write from Equations (2.2) and (3.1),

$$\langle T, u \rangle = cos\theta = constant \tag{3.2}$$

Thus, ψ is a helix in compliance with a modified orthogonal framework $\{T, N, B\}$.

$\Leftarrow$ Suppose that ψ is a helix in compliance with the modified orthogonal framework $\{T, N, B\}$. Thus, we can write

$$\langle T, u \rangle = c = constant. \tag{3.3}$$

Thus, from Equations (3.3) and (2.2), we obtain $\langle t, u \rangle = c = constant$. In this case, ψ is a helix in compliance with the orthonormal framework $\{t, n, b\}$.

Theorem 3.2. There are no (1,2)-type slant helix in compliance with the modified orthogonal framework $\{T, N, B\}$.

Proof. Suppose that ψ is a $(1,2)$-type slant helix. Then, we may write

$$\langle T, u \rangle = c_1 \tag{3.4}$$

and

$$\langle N, u \rangle = c_2 \tag{3.5}$$

where c_1 and c_2 are constants. If we take the derivative of these equations, we obtain $\langle N, u \rangle = 0$. That is to say, u is orthogonal to N. Thus, there are no $(1,2)$-type slant helix in compliance with the modified orthogonal framework $\{T, N, B\}$.

Theorem 3.3. If ψ is a $(1,3)$-type slant helix in compliance with the modified orthogonal framework $\{T, N, B\}$. Then, κ and τ are constants.

Proof. Suppose that ψ is a $(1,3)$-type slant helix in compliance with the modified orthogonal framework $\{T, N, B\}$. Then, we may write

$$\langle T, u \rangle = c_1 \tag{3.6}$$

and

$$\langle B, u \rangle = c_3 \tag{3.7}$$

where c_1 and c_3 are constants.

If we take the derivative of Equations (3.6) and (3.7) and use Equation (2.3), we acquire that κ and τ are constants.

Theorem 3.4. If ψ is a $(2,3)$-type slant helix in compliance with the modified orthogonal framework $\{T, N, B\}$, then

$$\langle T, u \rangle = \frac{\kappa'}{\kappa^3} c_2 + \frac{\tau}{\kappa^2} c_3 \tag{3.8}$$

$$\frac{1}{\tau} (\ln \kappa)' = constant \tag{3.9}$$

where c_2 and c_3 are constants.

Proof. Suppose that ψ is a $(2,3)$-type slant helix in compliance with the modified orthogonal framework $\{T, N, B\}$. Then, we are written as follows:

$$\langle N, u \rangle = c_2 \tag{3.10}$$

and

$$\langle B, u \rangle = c_3 \tag{3.11}$$

Now, if we take the derivative of Equation (3.10) and we use Equation (2.3), we may write

$$\langle T, u \rangle = \frac{\kappa'}{\kappa^3} c_2 + \frac{\tau}{\kappa^2} c_3$$

Similarly, from Equations (3.11) and (2.3), we get

$$\frac{1}{\tau} (\ln \kappa)' = constant$$

Theorem 3.5. If ψ is a 3-type slant helix according to the modified orthogonal frame. Then, the following ordinary differential equation holds

$$\left(\int \frac{\kappa\kappa'}{\tau} ds\right)^2 + \left(\frac{\kappa'}{\kappa\tau}\right)^2 = constant \tag{3.12}$$

PROOF. Supposed that ψ is a 3-type slant helix according to the modified orthogonal framework $\{T, N, B\}$. Thus, we have

$$\langle B, u \rangle = c \tag{3.13}$$

and if we take the derivative of Equation (3.13) and use Equation (2.3), we obtain

$$\langle N, u \rangle = \frac{\kappa'}{\kappa\tau} c \tag{3.14}$$

Moreover, we decompose u as follows

$$u = a_1 T + a_2 N + cB$$

If we take the derivative of constant vector u and use the Equation (2.3), we get

$$a_1'T + a_2'N + a_1 N + a_2\left(-\kappa^2 T + \frac{\kappa'}{\kappa}N + \tau B\right) + c\left(-\tau N + \frac{\kappa'}{\kappa}B\right) = 0 \tag{3.15}$$

and

$$a_1' - a_2\kappa^2 = 0 \tag{3.16}$$

$$a_2' + a_1 + a_2\frac{\kappa'}{\kappa} - c\tau = 0 \tag{3.17}$$

$$a_2\tau + c\frac{\kappa'}{\kappa} = 0 \tag{3.18}$$

From Equations (3.16) and (3.18), we get

$$a_1 = -c\int \frac{\kappa\kappa'}{\tau} ds$$

$$a_2 = \frac{-c\kappa'}{\kappa\tau}$$

We know that u is constant. Moreover, we may select $a_1{}^2 + a_2{}^2 = \|u\|^2 = 1 = constant$. As a result, we are written by the following equations:

$$\left(\int \frac{\kappa\kappa'}{\tau} ds\right)^2 + \left(\frac{\kappa'}{\kappa\tau}\right)^2 = \frac{1}{c^2} = constant$$

4. Conclusion

We analyse (k, m)-form slant helices in compliance with the modified orthogonal frame in $\mathbb{E}^3$. Furthermore, we get some characterisations of curves with modified orthogonal frames in $\mathbb{E}^3$. In the subsequent studies, we will investigate the conformable curves according to a modified orthogonal frame in $\mathbb{E}^3$.

Author Contributions

All authors contributed equally to this work. They all read and approved the last version of the paper.

Conflict of Interest

The authors declare no conflict of interest.

References

[1] M. Barros, *General Helices and a Theorem of Lancret,* Proceedings of the American Mathematical Society 125 (5) (1997), 1503–1509.

[2] D. J. Struik, *Lectures on Classical Differential Geometry*, Addison Wesley, 1988.

[3] S. Izumiya, N. Takeuchi, *New Special Curves and Developable Surfaces*, Turkish Journal of Mathematics 28 (2) (2004), 153–164.

[4] T. Y. Shaker, *Evolution of Space Curves Using Type-3 Bishop Fram*e, Caspian Journal of Mathematical Sciences (CJMS) 8 (1) (2019), 58–73.

[5] M. Bektaş, M. Y. Yılmaz, *(k,m)-Type Slant Helices for Partially Null and Pseudo-Null Curves in Minkowski Space*, Applied Mathematics and Nonlinear Sciences 5(1) (2020) 515–520.

[6] M. Y. Yilmaz, M. Bektaş, *Slant Helices of (k, m)-Type in* $\mathbb{E}^4$, Acta Universitatis Sapientiae, Mathematica 10 (2) (2018) 395–401.

[7] F. Bulut, M. Bektaş, *Special Helices on Equiform Differential Geometry of Spacelike Curves in Minkowski Spacetime*, Communications Faculty of Sciences University of Ankara Series A1 Mathematics and Statistics 69 (2) (2020) 1045–1056.

[8] B. Bükcü, M. K. Karacan, *Spherical Curves with Modified Orthogonal Frame*, Journal of New Results in Science 5 (10) (2016) 60–68.

[9] K. Eren, H. H. Kosal*, Evolution of Space Curves and the Special Ruled Surfaces with Modified Orthogonal Frame,* American Institute of Mathematical Sciences-Aims.

[10] A. Z. Azak, *Involute-Evolute Curves according to Modified Orthogonal Frame,* Journal of Science and Arts 21 (2) (2021) 385–394.

[11] M. S. Lone, H. Es, M. K. Karacan, B. Bükcü, *On Some Curves with Modified Orthogonal Frame in Euclidean 3-Space*, Iranian Journal of Science and Technology, Transactions A: Science 43 (4) (2019) 1905–1916.

[12] N. Ekmekci, *On General Helices and Submanifolds of an Indefinite-Riemannian Manifold*, Analele Stiintifice Universitati Ale I Cuza Lasi Matematica (NS) 46 (2001) 263–270.

[13] T. Ahmad, A. R. Lopez, *Slant Helices in Minkowski Space* E_1^3, Journal of the Korean Mathematical Society 48 (1) (2011) 159–167.

[14] S. Kumar, B. Pal, *K-Type Slant Helices on Spacelike and Timelike Surfaces*, Acta et Commentationes Universitatis Tartuensis de Mathematica 25 (2) (2021) 201–220.

A Novel Operator to Solve Decision-Making Problems Under Trapezoidal Fuzzy Multi Numbers and Its Application

Davut Kesen[1] (ID) , İrfan Deli[2] (ID)

Abstract − This article investigates solutions to multiple attribute decision-making (MADM) problems in which the attribute values take the form of trapezoidal fuzzy multi-numbers. To do this, this paper proposes a kind of mean aggregation operator called the Bonferroni harmonic mean operator for aggregating trapezoidal fuzzy information. Then, an approach that is a solution algorithm has been developed to find a solution to multi-attribute decision-making problems. Afterwards, an illustrative example has been given to verify the developed approach and to show its usefulness and efficiency. Finally, a comparison table has been presented to compare the proposed method with some existing methods.

1. Introduction

As an extension of the classical sets, fuzzy set theory was introduced by Zadeh [1] in 1965 to model uncertain information. Then, a kind of fuzzy sets were introduced by Yager [2] which is called multi-fuzzy sets (fuzzy bags). It is a different generalization of fuzzy sets and provides complete information in some problems as there are situations where each element has different membership values. Miyamoto [3,4] and Sebastian and Ramakrishnan [5,6] expanded and studied the Yager's multi-sets and multi-fuzzy sets in detail. Since some occurrences are with more than one possibility of same or different membership functions, Uluçay et al. [7] developed trapezoidal fuzzy multi-numbers (TFM-numbers) on real number set $\mathbb{R}$ which are extension of both fuzzy numbers and multi-fuzzy sets by allowing the repeated occurrences of any element. Later, various studies have been additionally done by many authors in [8–11].

The Bonferroni mean (BM), primarily proposed by Bonferroni [12] is an aggregation method which is useful to aggregate the crisp data. It can explore the interrelationships among arguments, which have a critical role in multi criteria decision making problems. Therefore, Yager [13] introduced a detailed work of BM and gave some generalizations that enhance its capability. Then, Beliakov et al. [14] made the BM more enhanced by coping with the interrelation of any three aggregated elements instead of any two.

Harmonic mean is a conservative average which give an aggregation locating between the maximum and minimum operators. It is commonly used by scientists as a tool of aggregating data that has tendency to central [15]. In the literature, the harmonic mean is mostly considered as an aggregation

---

[1]kesen66@gmail.com (Corresponding Author); [2]irfandeli@kilis.edu.tr
[1,2]Muallim Rıfat Faculty of Education, Kilis 7 Aralık University, Kilis, Turkiye

method of numerical data information including fuzzy informations. For example, Xu [15] proposed the fuzzy harmonic mean operators named fuzzy weighted harmonic mean (FWHM) operator, fuzzy ordered weighted harmonic mean (FOWHM) operator and fuzzy hybrid harmonic mean (FHHM) operator. Furthermore, he applied these operators to multiple attribute group decision making (MAGDM) problems. Wei [16] developed fuzzy induced ordered weighted harmonic mean (FIOWHM) operator and then, he presented the approach to MAGDM based on the FWHM and FIOWHM operators. Sun and Sun [17] introduced the fuzzy Bonferroni harmonic mean (FBHM) operator and the fuzzy ordered Bonferroni harmonic mean (FOBHM) operator. Then, they applied the FOBHM operator to MADM problems. Until now, Bonferroni harmonic mean aggregation operators based on trapezoidal multi fuzzy numbers have not been studied as we know. In order to fill this gap, this article formed and has five sections. In second section, we give definitions of fuzzy sets, multi-fuzzy sets, and trapezoidal fuzzy multi-numbers and some of their basic properties. In third section, we introduce an aggregation method called weighted Bonferroni harmonic mean operator for aggregating the trapezoidal multi fuzzy information. In addition the section reviews its some special cases and some properties. In fourth section, we propose an algorithm to solve multiple attribute decision making problems under the trapezoidal multi fuzzy numbers. Then, in the section, we apply the proposed operator to a multi attribute decision making problem. In fifth section, we give a brief conclusion. The present paper is derived from the first author's master's thesis under the second author's supervision.

2. Preliminary

In this section, we give some basic concepts such as fuzzy set [1], trapezoidal fuzzy multi numbers [7] and etc. In [8–11, 18–23], readers can find further knowledge.

Definition 2.1. [1] A fuzzy set F on X which is a non-empty set is defined as:

$$F = \{\langle x, \mu_F(x)\rangle : x \in X\}$$

where μ_F is a function from X to $[0,1]$.

Definition 2.2. [24] t-norms are associative, monotonic and commutative two valued functions t that map from $[0,1] \times [0,1]$ into $[0,1]$. These properties are formulated with the following conditions:

  i. $t(0,0) = 0$ and $t(\mu_{X_1}(x), 1) = t(1, \mu_{X_1}(x)) = \mu_{X_1}(x)$

  ii. If $\mu_{X_1}(x) \le \mu_{X_3}(x)$ and $\mu_{X_2}(x) \le \mu_{X_4}(x)$, then $t(\mu_{X_1}(x), \mu_{X_2}(x)) \le t(\mu_{X_3}x), \mu_{X_4}(x))$

  iii. $t(\mu_{X_1}(x), \mu_{X_2}(x)) = t(\mu_{X_2}(x), \mu_{X_1}(x))$

  iv. $t(\mu_{X_1}(x), t(\mu_{X_2}(x), \mu_{X_3}(x))) = t(t(\mu_{X_1}(x), \mu_{X_2})(x), \mu_{X_3}(x))$

Definition 2.3. [24] s-norm are associative, monotonic and commutative two placed functions s which map from $[0,1] \times [0,1]$ into $[0,1]$. These properties are formulated with the following conditions:

  i. $s(1,1) = 1$ *and* $s(\mu_{X_1}(x), 0) = s(0, \mu_{X_1}(x)) = \mu_{X_1}(x)$

  ii. if $\mu_{X_1}(x) \le \mu_{X_3}(x)$ and $\mu_{X_2}(x) \le \mu_{X_4}(x)$, then $s(\mu_{X_1}(x), \mu_{X_2}(x)) \le s(\mu_{X_3}(x), \mu_{X_4}(x))$

  iii. $s(\mu_{X_1}(x), \mu_{X_2}(x)) = s(\mu_{X_2}(x), \mu_{X_1}(x))$

  iv. $s(\mu_{X_1}(x), s(\mu_{X_2}(x), \mu_{X_3}(x))) = s(s(\mu_{X_1}(x), \mu_{X_2})(x), \mu_{X_3}(x))$

  For example, $t_2(\mu_{X_1}(x), \mu_{X_2}(x)) = \mu_{X_1}(x)\mu_{X_2}(x)$ is a t-norm and $s_2(\mu_{X_1}(x), \mu_{X_2}(x)) = \mu_{X_1}(x) + \mu_{X_2}(x) - \mu_{X_1}(x)\mu_{X_2}(x)$ is a s-norm.

Definition 2.4. [7] Let $w_N \in [0,1]$, $x_i, y_i, z_i, t_i \in \mathbb{R}$ and $x_i \leq y_i \leq z_i \leq t_i$. A trapezoidal fuzzy number (TF-number) $N = \langle (x_i, y_i, z_i, t_i); w_N \rangle$ is a special fuzzy set on the real number set $\mathbb{R}$. Its membership function is given as:

$$\mu_N(x) = \begin{cases} (x - x_i)w_N/(y_i - x_i), & x_i \leq x < y_i \\ w_N, & y_i \leq x \leq z_i \\ (t_i - x)w_N/(t_i - z_i), & z_i < x \leq t_i \\ 0, & otherwise \end{cases}$$

Definition 2.5. [5] A multi-fuzzy set G on X which is a non-empty set is defined as:

$$G = \{\langle x, \mu_G^1(x), \mu_G^2(x), ..., \mu_G^i(x), ...\rangle : x \in X\}$$

where $\mu_G^i : X \to [0,1]$ for all $i \in \{1, 2, ..., p\}$ and $x \in X$.

Definition 2.6. [7] Let $\eta_N^s \in [0,1]$ $s \in \{1, 2, ..., p\}$ and $x_i, y_i, z_i, t_i \in \mathbb{R}$ such that $x_i \leq y_i \leq z_i \leq t_i$. Then, trapezoidal fuzzy multi-number (TFM-number) shown by $N = \langle (x_i, y_i, z_i, t_i); \eta_N^1, \eta_N^2, ..., \eta_N^P \rangle$ is a special fuzzy multi-set on the real numbers set $\mathbb{R}$ and its membership functions are defined as:

$$\mu_N^s(x) = \begin{cases} (x - x_i)\eta_N^s/(y_i - x_i) & x_i \leq x \leq y_i \\ \eta_N^s & y_i \leq x \leq z_i \\ (t_i - x)\eta_N^s/(t_i - z_i) & z_i \leq x \leq t_i \\ 0 & otherwise \end{cases}$$

From now on the set of all TFM-number on $\mathbb{R}^+$ will be denoted by $\mho(\mathbb{R}^+)$. Moreover, I_p and I_n will be used instead of $\{1, 2, ..., p\}$ and $\{1, 2, ..., n\}$, respectively.

Definition 2.7. [7] Let $N_1 = \langle (x_1, y_1, z_1, t_1); \eta_{N_1}^1, \eta_{N_1}^2, ..., \eta_{N_1}^P \rangle$, $N_2 = \langle (x_2, y_2, z_2, t_2); \eta_{N_2}^1, \eta_{N_2}^2, ..., \eta_{N_2}^P \rangle \in \mho(\mathbb{R}^+)$ and $\gamma \neq 0$, $\gamma \in \mathbb{R}$. Then,

i. $N_1 + N_2 = (x_1 + x_2, y_1 + y_2, z_1 + z_2, t_1 + t_2);$
$\eta_{N_1}^1 + \eta_{N_2}^1 - \eta_{N_1}^1 \eta_{N_2}^1, \eta_{N_1}^2 + \eta_{N_2}^2 - \eta_{N_1}^2 \eta_{N_2}^2, ..., \eta_{N_1}^P + \eta_{N_2}^P - \eta_{N_1}^P \eta_{N_2}^P \rangle$

ii. $N_1 \times N_2 = \begin{cases} \langle (x_1 x_2, y_1 y_2, z_1 z_2, t_1 t_2); \eta_{N_1}^1 \eta_{N_2}^1, \eta_{N_1}^2 \eta_{N_2}^2, ... \eta_{N_1}^P \eta_{N_2}^P \rangle & (t_1 > 0, t_2 > 0) \\ \langle (x_1 t_2, y_1 z_2, z_1 y_2, t_1 x_2); \eta_{N_1}^1 \eta_{N_2}^1, \eta_{N_1}^2 \eta_{N_2}^2, ... \eta_{N_1}^P \eta_{N_2}^P \rangle & (t_1 < 0, t_2 > 0) \\ \langle (t_1 t_2, z_1 z_2, y_1 y_2, x_1 x_2); \eta_{N_1}^1 \eta_{N_2}^1, \eta_{N_1}^2 \eta_{N_2}^2, ... \eta_{N_1}^P \eta_{N_2}^P \rangle & (t_1 < 0, t_2 < 0) \end{cases}$

iii. $\gamma N_1 = \langle (\gamma x_1, \gamma y_1, \gamma z_1, \gamma t_1); 1 - (1 - \eta_{N_1}^1)^\gamma, 1 - (1 - \eta_{N_1}^2)^\gamma, ..., 1 - (1 - \eta_{N_1}^p)^\gamma \rangle (\gamma \geq 0)$

iv. $N_1^\gamma = \langle (x_1^\gamma, y_1^\gamma, z_1^\gamma, t_1^\gamma); (\eta_{N_1}^1)^\gamma, (\eta_{N_1}^2)^\gamma, ..., (\eta_{N_1}^P)^\gamma \rangle (\gamma \geq 0)$

v. Based on negative exponential of a trapezoidal intuitionistic fuzzy number given by Li [25], we can give following property for TFM-numbers:

$$N_1^{-1} = \left\langle \left(\frac{1}{t_1}, \frac{1}{z_1}, \frac{1}{y_1}, \frac{1}{x_1} \right); \eta_{N_1}^1, \eta_{N_1}^2, ..., \eta_{N_1}^P \right\rangle$$

Definition 2.8. [26] Let $N_1 = \langle (x_1, y_1, z_1, t_1); \eta_{N_1}^1, \eta_{N_1}^2, ..., \eta_{N_2}^P \rangle$, $N_2 = \langle (x_2, y_2, z_2, t_2); \eta_{N_2}^1, \eta_{N_2}^2, ..., \eta_{N_2}^P \rangle \in \mho(\mathbb{R}^+)$. Followings are right:

i. If $x_1 < x_2$, $y_1 < y_2$, $z_1 < z_2$, $t_1 < t_2$, $\eta_{N_1}^1 < \eta_{N_2}^1, \eta_{N_1}^2 < \eta_{N_2}^2, ..., \eta_{N_1}^P < \eta_{N_2}^P$ then $N_1 < N_2$

ii. If $x_1 > x_2$, $y_1 > y_2$, $z_1 > z_2$, $t_1 > t_2$, $\eta_{N_1}^1 > \eta_{N_2}^1, \eta_{N_1}^2 > \eta_{N_2}^2, ..., \eta_{N_1}^P > \eta_{N_2}^P$ then $N_1 > N_2$

iii. If $x_1 = x_2$, $y_1 = y_2$, $z_1 = z_2$, $t_1 = t_2$, $\eta_{N_1}^1 = \eta_{N_2}^1, \eta_{N_1}^2 = \eta_{N_2}^2, ..., \eta_{N_1}^P = \eta_{N_2}^P$ then $N_1 = N_2$

Based on score value for trapezoidal hesitant fuzzy numbers given by Deli [26], we propose following definition.

Definition 2.9. Let $N = \langle (x_i, y_i, z_i, t_i); \eta_N^1, \eta_N^2, ..., \eta_N^P \rangle$ be a TFM-number and P is number of η_N^i. Then, score of N denoted $s(N)$ is defined as:

$$s(N) = \frac{t_i^2 + z_i^2 - x_i^2 - y_i^2}{2P} \sum_{s=1}^{P} \eta_N^s$$

Let $N_i = \langle (x_i, y_i, z_i, t_i); \eta_{N_i}^1, \eta_{N_i}^2, ..., \eta_{N_i}^P \rangle$ $(i \in I_2)$ be a TFM-numbers' collection. Then, comparison of N_1 and N_2 is given as:

i. If $s(N_1) > s(N_2)$, then $N_1 > N_2$

ii. If $s(N_1) < s(N_2)$, then $N_1 < N_2$

iii. If $s(N_1) = s(N_2)$, then $N_1 = N_2$

Definition 2.10. [12] Let σ_i $(i \in I_n)$ be a nonnegative numbers' collection and $p, q \in \mathbb{R}$ such that $p, q \geq 0$. Then, Bonferroni mean (BM) of σ_i $(i \in I_n)$ is defined as:

$$BM^{p,q}(\sigma_1, \sigma_2, ..., \sigma_n) = \left(\frac{1}{n(n-1)} \sum_{i,j=1, i \neq j}^{n} \sigma_i^p \sigma_j^q \right)^{\frac{1}{p+q}}$$

For two collections of nonnegative numbers σ_i and v_i $(i \in I_n)$, the BM has some properties as follows:

i. $BM^{p,q}(0, 0, ..., 0) = 0$

ii. $BM^{p,q}(\sigma, \sigma, ..., \sigma) = \sigma$, if $\sigma_i = \sigma$, for all i

iii. $BM^{p,q}(\sigma_1, \sigma_2, ..., \sigma_n) \geq BM^{p,q}(v_1, v_2, ..., v_n)$,i.e., $BM^{p,q}$ is monotonic, if $\sigma_i \geq v_i$, for all i

iv. $\min\{\sigma_i\} \leq BM^{p,q}(\sigma_1, \sigma_2, ..., \sigma_n) \leq \max\{\sigma_i\}$

Definition 2.11. [17] Let $p, q \geq 0$ and σ_i $(i \in I_n)$ be a collection of nonnegative numbers and $v = (v_1, v_2, ..., v_n)^T$ σ_i's weight vector such that $v_i \geq 0$ $(i \in I_n)$ and $\sum_{i=1}^{n} v_i = 1$. If

$$WBHM^{p,q}(\sigma_1, \sigma_2, ..., \sigma_n) = \frac{1}{\left(\sum_{i,j=1, i \neq j}^{n} \frac{v_i v_j}{\sigma_i^p \sigma_j^q} \right)^{\frac{1}{p+q}}}$$

then $WBHM^{p,q}$ is called the weighted Bonferroni Harmonic Mean (WBHM).

3. Weighted Bonferroni Harmonic Mean Operator on TFM-numbers

In this section we propose TFM weighted Bonferroni harmonic mean based on weighted Bonferroni harmonic mean given by Su et al. [27]. Then, we analyze its properties and review special cases to see how it converts into other operators. In addition, a basic example is presented to see its application to three TFM-numbers.

Definition 3.1. Let $N_i = \langle (x_i, y_i, z_i, t_i); \eta_{N_i}^1, \eta_{N_i}^2, ..., \eta_{N_i}^P \rangle$ $(i \in I_n)$ be a TFM-numbers' collection, $p, q > 0$ and N_i's weight vector is $v = (v_1, v_2, ..., v_n)^T$. Here, v_i is N_i's importance degree, satisfying $v_i \in [0, 1]$, $i \in I_n$ such that $\sum_{i=1}^{n} v_i = 1$. Then,

$$TFMBHM_v^{p,q}(N_1, N_2, ..., N_n) = \frac{1}{\left(\bigoplus_{i,j=1, i \neq j}^{n} \left(\left(\frac{v_i}{N_i^p} \right) \otimes \left(\frac{v_j}{N_j^q} \right) \right) \right)^{\frac{1}{p+q}}}$$

is called TFM weighted Bonferroni harmonic mean operator $(TFMBHM_v)$.

Considering operational laws in Definitions 2.7 of TFM-numbers, we can give following theorem:

Theorem 3.2. Let $N_i = \langle (x_i, y_i, z_i, t_i); \eta_{N_i}^1, \eta_{N_i}^2, ..., \eta_{N_i}^P \rangle$ $(i \in I_n)$ be a TFM-numbers' collection, $p, q > 0$ and N_i's weight vector is $v = (v_1, v_2, ..., v_n)^T$. Here, v_i is N_i's importance degree, satisfying $v_i \in [0, 1]$, $i \in I_n$ such that $\sum_{i=1}^{n} v_i = 1$. Then, $TFMBHM_v^{p,q}(A_1, A_2, ..., A_n)$ is a TFM-number and computed as:

$$
TFMBHM_v^{p,q}(N_1, N_2, ..., N_n) = \left\langle \left(\frac{1}{\left(\sum\limits_{i,j=1,i\neq j}^{n} \frac{v_i v_j}{x_i^p x_j^q} \right)^{\frac{1}{p+q}}}, \frac{1}{\left(\sum\limits_{i,j=1,i\neq j}^{n} \frac{v_i v_j}{y_i^p y_j^q} \right)^{\frac{1}{p+q}}}, \right. \right.
$$

$$
\left. \frac{1}{\left(\sum\limits_{i,j=1,i\neq j}^{n} \frac{v_i v_j}{z_i^p z_j^q} \right)^{\frac{1}{p+q}}}, \frac{1}{\left(\sum\limits_{i,j=1,i\neq j}^{n} \frac{v_i v_j}{t_i^p t_j^q} \right)^{\frac{1}{p+q}}} \right);
$$

$$
1 - \prod_{i,j=1,i\neq j}^{n} [1 - (1 - (1 - (\eta_{N_i}^1)^p)^{v_i})(1 - (1 - (\eta_{N_j}^1)^q)^{v_j})]^{\frac{1}{p+q}},
$$

$$
1 - \prod_{i,j=1,i\neq j}^{n} [1 - (1 - (1 - (\eta_{N_i}^2)^p)^{v_i})(1 - (1 - (\eta_{N_j}^2)^q)^{v_j})]^{\frac{1}{p+q}}, ...,
$$

$$
\left. 1 - \prod_{i,j=1,i\neq j}^{n} [1 - (1 - (1 - (\eta_{N_i}^P)^p)^{v_i})(1 - (1 - (\eta_{N_j}^P)^q)^{v_j})]^{\frac{1}{p+q}} \right\rangle \tag{1}
$$

PROOF. By operation laws in Definition 2.7 of TFM-numbers,

$$
\left(\frac{v_i}{N_i^p} \right) \otimes \left(\frac{v_j}{N_j^q} \right) = \left\langle \left(\frac{v_i v_j}{x_i^p x_j^q}, \frac{v_i v_j}{y_i^p y_j^q}, \frac{v_i v_j}{z_i^p z_j^q}, \frac{v_i v_j}{t_i^p t_j^q} \right); \right.
$$

$$
(1 - (1 - (\eta_{N_i}^1)^p)^{v_i})(1 - (1 - (\eta_{N_j}^1)^q)^{v_j}),
$$

$$
(1 - (1 - (\eta_{N_i}^2)^p)^{v_i})(1 - (1 - (\eta_{N_j}^2)^q)^{v_j}), ...,
$$

$$
\left. (1 - (1 - (\eta_{N_i}^P)^p)^{v_i})(1 - (1 - (\eta_{N_j}^P)^q)^{v_j}) \right\rangle
$$

First of all, we need to show:

$$
\bigoplus_{i,j=1,i\neq j}^{n} \left(\left(\frac{v_i}{N_i^p} \right) \otimes \left(\frac{v_j}{N_j^q} \right) \right) = \left\langle \left(\sum_{i,j=1,i\neq j}^{n} \frac{v_i v_j}{x_i^p x_j^q}, \sum_{i,j=1,i\neq j}^{n} \frac{v_i v_j}{y_i^p y_j^q}, \sum_{i,j=1,i\neq j}^{n} \frac{v_i v_j}{z_i^p z_j^q}, \sum_{i,j=1,i\neq j}^{n} \frac{v_i v_j}{t_i^p t_j^q} \right); \right.
$$

$$
1 - \prod_{i,j=1,i\neq j}^{n} [1 - (1 - (1 - (\eta_{N_i}^1)^p)^{v_i})(1 - (1 - (\eta_{N_j}^1)^q)^{v_j})]^{\frac{1}{p+q}},
$$

$$
1 - \prod_{i,j=1,i\neq j}^{n} [1 - (1 - (1 - (\eta_{N_i}^2)^p)^{v_i})(1 - (1 - (\eta_{N_j}^2)^q)^{v_j})]^{\frac{1}{p+q}}, ...,
$$

$$
\left. 1 - \prod_{i,j=1,i\neq j}^{n} [1 - (1 - (1 - (\eta_{N_i}^P)^p)^{v_i})(1 - (1 - (\eta_{N_j}^P)^q)^{v_j})]^{\frac{1}{p+q}} \right\rangle \tag{2}
$$

If we use mathematical induction on n:
1) when $n = 2$, from Equation (2), we obtain:

$$
\bigoplus_{i,j=1,i\neq j}^{2} \left(\left(\frac{v_i}{N_i^p} \right) \otimes \left(\frac{v_j}{N_j^q} \right) \right) = \left(\frac{v_1}{N_1^p} \otimes \frac{v_2}{N_2^q} \right) \oplus \left(\frac{v_2}{N_2^p} \otimes \frac{v_1}{N_1^q} \right)
$$

$$= \left\langle \left(\frac{v_1 v_2}{x_1^p x_2^q} + \frac{v_2 v_1}{x_2^p x_1^q}, \frac{v_1 v_2}{y_1^p y_2^q} + \frac{v_2 v_1}{y_2^p y_1^q}, \frac{v_1 v_2}{z_1^p z_2^q} + \frac{v_2 v_1}{z_2^p z_1^q}, \frac{v_1 v_2}{t_1^p t_2^q} + \frac{v_2 v_1}{t_2^p t_1^q} \right) ; \right.$$
$$[(1 - (1 - (\eta_{N_1}^1)^p)^{v_1})(1 - (1 - (\eta_{N_2}^1)^q)^{v_2})] \oplus [(1 - (1 - (\eta_{N_2}^1)^p)^{v_2})(1 - (1 - (\eta_{N_1}^1)^q)^{v_1})],$$
$$[(1 - (1 - (\eta_{N_1}^2)^p)^{v_1})(1 - (1 - (\eta_{N_2}^2)^q)^{v_2})] \oplus [(1 - (1 - (\eta_{N_2}^2)^p)^{v_2})(1 - (1 - (\eta_{N_1}^2)^q)^{v_1})], ...,$$
$$\left. [(1 - (1 - (\eta_{N_1}^P)^p)^{v_1})(1 - (1 - (\eta_{N_2}^P)^q)^{v_2})] \oplus [(1 - (1 - (\eta_{N_2}^P)^p)^{v_2})(1 - (1 - (\eta_{N_1}^P)^q)^{v_1})] \right\rangle$$

$$= \left\langle \left(\sum_{i,j=1,i\neq j}^{2} \frac{v_i v_j}{x_i^p x_j^q}, \sum_{i,j=1,i\neq j}^{2} \frac{v_i v_j}{y_i^p y_j^q}, \sum_{i,j=1,i\neq j}^{2} \frac{v_i v_j}{z_i^p z_j^q}, \sum_{i,j=1,i\neq j}^{2} \frac{v_i v_j}{t_i^p t_j^q} \right) ; \right.$$
$$1 - \prod_{i,j=1,i\neq j}^{2} [1 - (1 - (1 - (\eta_{N_i}^1)^p)^{v_i})(1 - (1 - (\eta_{N_j}^1)^q)^{v_j})]^{\frac{1}{p+q}},$$
$$1 - \prod_{i,j=1,i\neq j}^{2} [1 - (1 - (1 - (\eta_{N_i}^2)^p)^{v_i})(1 - (1 - (\eta_{N_j}^2)^q)^{v_j})]^{\frac{1}{p+q}}, ...,$$
$$\left. 1 - \prod_{i,j=1,i\neq j}^{2} [1 - (1 - (1 - (\eta_{N_i}^P)^p)^{v_i})(1 - (1 - (\eta_{N_j}^P)^q)^{v_j})]^{\frac{1}{p+q}} \right\rangle$$

2) Suppose when $n = k$, the Equation (2) is true, i.e.,

$$\bigoplus_{i,j=1,i\neq j}^{k} \left(\left(\frac{v_i}{N_i^p} \right) \otimes \left(\frac{v_j}{N_j^q} \right) \right) = \left\langle \left(\sum_{i,j=1,i\neq j}^{k} \frac{v_i v_j}{x_i^p x_j^q}, \sum_{i,j=1,i\neq j}^{k} \frac{v_i v_j}{y_i^p y_j^q}, \sum_{i,j=1,i\neq j}^{k} \frac{v_i v_j}{z_i^p z_j^q}, \sum_{i,j=1,i\neq j}^{k} \frac{v_i v_j}{t_i^p t_j^q} \right) ; \right.$$
$$1 - \prod_{i,j=1,i\neq j}^{k} [1 - (1 - (1 - (\eta_{N_i}^1)^p)^{v_i})(1 - (1 - (\eta_{N_j}^1)^q)^{v_j})]^{\frac{1}{p+q}},$$
$$1 - \prod_{i,j=1,i\neq j}^{k} [1 - (1 - (1 - (\eta_{N_i}^2)^p)^{v_i})(1 - (1 - (\eta_{N_j}^2)^q)^{v_j})]^{\frac{1}{p+q}}, ...,$$
$$\left. 1 - \prod_{i,j=1,i\neq j}^{k} [1 - (1 - (1 - (\eta_{N_i}^P)^p)^{v_i})(1 - (1 - (\eta_{N_j}^P)^q)^{v_j})]^{\frac{1}{p+q}} \right\rangle$$

(3)

3) Now we will show Equation (2) is true for $n = k + 1$. If we accept $n = k + 1$ in Equation (2):

$$\bigoplus_{i,j=1,i\neq j}^{k+1} \left(\left(\frac{v_i}{N_i^p} \right) \otimes \left(\frac{v_j}{N_j^q} \right) \right) = \left(\bigoplus_{i,j=1,i\neq j}^{k} \left(\left(\frac{v_i}{N_i^p} \right) \otimes \left(\frac{v_j}{N_j^q} \right) \right) \right) \oplus$$
$$\left(\bigoplus_{i=1}^{k} \left(\left(\frac{v_i}{N_i^p} \right) \otimes \left(\frac{v_{k+1}}{N_{k+1}^q} \right) \right) \right) \oplus$$
$$\left(\bigoplus_{j=1}^{k} \left(\left(\frac{v_{k+1}}{N_{k+1}^p} \right) \otimes \left(\frac{v_j}{N_j^q} \right) \right) \right)$$

(4)

$$\bigoplus_{i=1}^{k}\left(\left(\frac{v_i}{N_i^p}\right)\otimes\left(\frac{v_{k+1}}{N_{k+1}^q}\right)\right)=\left\langle\left(\sum_{i=1}^{k}\frac{v_iv_{k+1}}{x_i^px_{k+1}^q},\sum_{i=1}^{k}\frac{v_iv_{k+1}}{y_i^py_{k+1}^q},\sum_{i=1}^{k}\frac{v_iv_{k+1}}{z_i^pz_{k+1}^q},\sum_{i=1}^{k}\frac{v_iv_{k+1}}{t_i^pt_{k+1}^q}\right);\right.$$

$$1-\prod_{i=1}^{k}[1-(1-(1-(\eta_{N_i}^1)^p)^{v_i})(1-(1-(\eta_{N_{k+1}}^1)^q)^{v_{k+1}})]^{\frac{1}{p+q}},$$

$$1-\prod_{i=1}^{k}[1-(1-(1-(\eta_{N_i}^2)^p)^{v_i})(1-(1-(\eta_{N_{k+1}}^2)^q)^{v_{k+1}})]^{\frac{1}{p+q}},...,$$

$$\left.1-\prod_{i=1}^{k}[1-(1-(1-(\eta_{N_i}^P)^p)^{v_i})(1-(1-(\eta_{N_{k+1}}^P)^q)^{v_{k+1}})]^{\frac{1}{p+q}}\right\rangle\qquad(5)$$

and

$$\bigoplus_{j=1}^{k}\left(\left(\frac{v_{k+1}}{N_{k+1}^p}\right)\otimes\left(\frac{v_j}{N_j^q}\right)\right)=\left\langle\left(\sum_{j=1}^{k}\frac{v_{k+1}v_j}{x_{k+1}^px_j^q},\sum_{j=1}^{k}\frac{v_{k+1}v_j}{y_{k+1}^py_j^q},\sum_{j=1}^{k}\frac{v_{k+1}v_j}{z_{k+1}^pz_j^q},\sum_{j=1}^{k}\frac{v_{k+1}v_j}{t_{k+1}^pt_j^q}\right);\right.$$

$$1-\prod_{j=1}^{k}[1-(1-(1-(\eta_{N_{k+1}}^1)^p)^{v_{k+1}})(1-(1-(\eta_{N_j}^1)^q)^{v_j})]^{\frac{1}{p+q}},$$

$$1-\prod_{j=1}^{k}[1-(1-(1-(\eta_{N_{k+1}}^2)^p)^{v_{k+1}})(1-(1-(\eta_{N_j}^2)^q)^{v_j})]^{\frac{1}{p+q}},...,$$

$$\left.1-\prod_{j=1}^{k}[1-(1-(1-(\eta_{N_{k+1}}^P)^p)^{v_{k+1}})(1-(1-(\eta_{N_j}^P)^q)^{v_j})]^{\frac{1}{p+q}}\right\rangle\qquad(6)$$

Finally from Equations (3), (4), (5) and (6), we obtain:

$$TFMBHM_v^{p,q}(N_1,N_2,...,N_n)=\left\langle\left(\sum_{i,j=1,i\neq j}^{k}\frac{v_iv_j}{x_i^px_j^q},\sum_{i,j=1,i\neq j}^{k}\frac{v_iv_j}{y_i^py_j^q},\sum_{i,j=1,i\neq j}^{k}\frac{v_iv_j}{z_i^pz_j^q},\sum_{i,j=1,i\neq j}^{k}\frac{v_iv_j}{t_i^pt_j^q}\right);\right.$$

$$1-\prod_{i,j=1,i\neq j}^{k}[1-(1-(1-(\eta_{N_i}^1)^p)^{v_i})(1-(1-(\eta_{N_j}^1)^q)^{v_j})]^{\frac{1}{p+q}},$$

$$1-\prod_{i,j=1,i\neq j}^{k}[1-(1-(1-(\eta_{N_i}^2)^p)^{v_i})(1-(1-(\eta_{N_j}^2)^q)^{v_j})]^{\frac{1}{p+q}},...,$$

$$\left.1-\prod_{i,j=1,i\neq j}^{k}[1-(1-(1-(\eta_{N_i}^P)^p)^{v_i})(1-(1-(\eta_{N_j}^P)^q)^{v_j})]^{\frac{1}{p+q}}\right\rangle$$

$$\otimes\left\langle\left(\sum_{i=1}^{k}\frac{v_iv_{k+1}}{x_i^px_{k+1}^q},\sum_{i=1}^{k}\frac{v_iv_{k+1}}{y_i^py_{k+1}^q},\sum_{i=1}^{k}\frac{v_iv_{k+1}}{z_i^pz_{k+1}^q},\sum_{i=1}^{k}\frac{v_iv_{k+1}}{t_i^pt_{k+1}^q}\right);\right.$$

$$1-\prod_{i=1}^{k}[1-(1-(1-(\eta_{N_i}^1)^p)^{v_i})(1-(1-(\eta_{N_{k+1}}^1)^q)^{v_{k+1}})]^{\frac{1}{p+q}},$$

$$1-\prod_{i=1}^{k}[1-(1-(1-(\eta_{N_i}^2)^p)^{v_i})(1-(1-(\eta_{N_{k+1}}^2)^q)^{v_{k+1}})]^{\frac{1}{p+q}},...,$$

$$\left.1-\prod_{i=1}^{k}[1-(1-(1-(\eta_{N_i}^P)^p)^{v_i})(1-(1-(\eta_{N_{k+1}}^P)^q)^{v_{k+1}})]^{\frac{1}{p+q}}\right\rangle$$

$$\otimes\left\langle\left(\sum_{j=1}^{k}\frac{v_{k+1}v_j}{x_{k+1}^px_j^q},\sum_{j=1}^{k}\frac{v_{k+1}v_j}{y_{k+1}^py_j^q},\sum_{j=1}^{k}\frac{v_{k+1}v_j}{z_{k+1}^pz_j^q},\sum_{j=1}^{k}\frac{v_{k+1}v_j}{t_{k+1}^pt_j^q}\right);\right.$$

$$1 - \prod_{j=1}^{k}[1 - (1 - (1 - (\eta_{N_{k+1}}^1)^p)^{v_{k+1}})(1 - (1 - (\eta_{N_j}^1)^q)^{v_j})]^{\frac{1}{p+q}},$$

$$1 - \prod_{j=1}^{k}[1 - (1 - (1 - (\eta_{N_{k+1}}^2)^p)^{v_{k+1}})(1 - (1 - (\eta_{N_j}^2)^q)^{v_j})]^{\frac{1}{p+q}}, ...,$$

$$1 - \prod_{j=1}^{k}[1 - (1 - (1 - (\eta_{N_{k+1}}^P)^p)^{v_{k+1}})(1 - (1 - (\eta_{N_j}^P)^q)^{v_j})]^{\frac{1}{p+q}} \Bigg\rangle$$

$$= \Bigg\langle \left(\sum_{i,j=1,i\neq j}^{k+1} \left(\frac{v_i v_j}{x_i^p x_j^q} \right)^{\frac{1}{p+q}}, \sum_{i,j=1,i\neq j}^{k+1} \left(\frac{v_i v_j}{y_i^p y_j^q} \right)^{\frac{1}{p+q}}, \sum_{i,j=1,i\neq j}^{k+1} \left(\frac{v_i v_j}{z_i^p z_j^q} \right)^{\frac{1}{p+q}}, \sum_{i,j=1,i\neq j}^{k+1} \left(\frac{v_i v_j}{t_i^p t_j^q} \right)^{\frac{1}{p+q}} \right);$$

$$1 - \prod_{i,j=1,i\neq j}^{k+1}[1 - (1 - (1 - (\eta_{N_i}^1)^p)^{v_i})(1 - (1 - (\eta_{N_{k+1}}^1)^q)^{v_j})]^{\frac{1}{p+q}},$$

$$1 - \prod_{i,j=1,i\neq j}^{k+1}[1 - (1 - (1 - (\eta_{N_i}^2)^p)^{v_i})(1 - (1 - (\eta_{N_{k+1}}^2)^q)^{v_j})]^{\frac{1}{p+q}}, ...,$$

$$1 - \prod_{i,j=1,i\neq j}^{k+1}[1 - (1 - (1 - (\eta_{N_i}^P)^p)^{v_i})(1 - (1 - (\eta_{N_{k+1}}^P)^q)^{v_j})]^{\frac{1}{p+q}} \Bigg\rangle$$

$\square$

Note 3.3. Let $p, q > 0$ and $N_i = \langle (x_i, y_i, z_i, t_i); \eta_{N_i}^1, \eta_{N_i}^2, ..., \eta_{N_i}^P \rangle$ $(i \in I_n)$ be a TFM-numbers' collection. If $v = \left(\frac{1}{n}, \frac{1}{n}, ..., \frac{1}{n} \right)^T$, then the $TFMBHM_v$ operator converted into the following:

$$TFMBHM_{\frac{1}{n}}^{p,q}(N_1, N_2, ..., N_n) = \cfrac{1}{\left(\bigoplus_{i,j=1,i\neq j}^{n} \left(\left(\frac{1/n}{N_i^p} \right) \otimes \left(\frac{1/n}{N_j^q} \right) \right) \right)^{\frac{1}{p+q}}}$$

Proposition 3.4. Let $p, q > 0$ and $N_i = \langle (x_i, y_i, z_i, t_i); \eta_{N_i}^1, \eta_{N_i}^2, ..., \eta_{N_i}^P \rangle$, $M_i = \langle (k_i, l_i, m_i, n_i); \eta_{M_i}^1, \eta_{M_i}^2, ..., \eta_{M_i}^P \rangle$ $(i \in I_n)$ be TFM-numbers' two collections. $TFMBHM_v$ operator has following properties:

i. **(Idempotency)** If $N_i = N$ for all $(i \in I_n)$, we have

$$TFMBHM_v^{p,q}(N_1, N_2, ..., N_n) = TFMBHM_v^{p,q}(N, N, ..., N) = N$$

ii. **(Monotonicity)** Based on Definition 2.8, if $N_i \geq M_i$ for all $i \in I_n$, then $TFMBHM_v^{p,q}$ is monotonic that is,

$$TFMBHM_v^{p,q}(N_1, N_2, ..., N_n) \geq TFMBHM_v^{p,q}(M_1, M_2, ..., M_n)$$

iii. **(Commutativity)** If $(\dot{N_1}, \dot{N_2}, ..., \dot{N_n})$ be any permutation of $(N_1, N_2, ..., N_n)$ then,

$$TFMBHM_v^{p,q}(N_1, N_2, ..., N_n) = TFMBHM_v^{p,q}(\dot{N_1}, \dot{N_2}, ..., \dot{N_n})$$

iv. **(Boundedness)**
$$N^- \leq TFMBHM_v^{p,q}(N_1, N_2, ..., N_n) \leq N^+$$

where
$$N^+ = \langle (max\{x_i\}_{i\in I_n}, max\{y_i\}_{i\in I_n}, max\{z_i\}_{i\in I_n}, max\{t_i\}_{i\in I_n});$$
$$max\{\eta_{N_i}^1\}_{i\in I_n}, max\{\eta_{N_i}^2\}_{i\in I_n}, ..., max\{\eta_{N_i}^P\}_{i\in I_n} \rangle$$

and
$$N^- = \langle (min\{x_i\}_{i\in I_n}, min\{y_i\}_{i\in I_n}, min\{z_i\}_{i\in I_n}, min\{t_i\}_{i\in I_n});$$
$$min\{\eta_{N_i}^1\}_{i\in I_n}, min\{\eta_{N_i}^2\}_{i\in I_n}, ..., min\{\eta_{N_i}^P\}_{i\in I_n} \rangle$$

By considering different values of p and q, a few specific cases of $TFMBHM_v^{p,q}$ are obtained as follows:

Remark 3.5. If $q = 0$, $TFMBHM_v^{p,q}$ operator converted into TFM weighted generalized harmonic mean operator:

$$TFMBHM_v^{p,0}(N_1, N_2, ..., N_n) = \frac{1}{\left(\bigoplus_{i,j=1,i\neq j}^{n} \left(\frac{v_i v_j}{N_i^p}\right)\right)^{\frac{1}{p}}} = \frac{1}{\left(\bigoplus_{i=1}^{n} \left(\frac{v_i}{N_i^p}\right) \bigoplus_{j=1}^{n} v_j\right)^{\frac{1}{p}}} = \frac{1}{\left(\bigoplus_{i=1}^{n} \left(\frac{v_i}{N_i^p}\right)\right)^{\frac{1}{p}}}$$

which is TFM weighted generalized harmonic mean ($TFMGHM_v$) operator.

Remark 3.6. If $p = 1, q = 0$, $TFMBHM_v^{p,q}$ operator converted into:

$$TFMBHM_v^{1,0}(N_1, N_2, ..., N_n) = \frac{1}{\bigoplus_{i,j=1,i\neq j}^{n} \left(\frac{v_i v_j}{N_i}\right)} = \frac{1}{\left(\bigoplus_{i=1}^{n} \left(\frac{v_i}{N_i}\right) \bigoplus_{j=1}^{n} v_j\right)} = \frac{1}{\bigoplus_{i=1}^{n} \left(\frac{v_i}{N_i}\right)}$$

Remark 3.7. If $p = 2, q = 0$, $TFMBHM_v^{p,q}$ operator converted into:

$$TFMBHM_v^{2,0}(N_1, N_2, ..., N_n) = \frac{1}{\left(\bigoplus_{i,j=1,i\neq j}^{n} \left(\frac{v_i v_j}{N_i^2}\right)\right)^{\frac{1}{2}}} = \frac{1}{\left(\bigoplus_{i=1}^{n} \left(\frac{v_i}{N_i^2}\right) \bigoplus_{j=1}^{n} v_j\right)^{\frac{1}{2}}} = \frac{1}{\left(\bigoplus_{i=1}^{n} \left(\frac{v_i}{N_i^2}\right)\right)^{\frac{1}{2}}}$$

Remark 3.8. If $p = 1, q = 1$, $TFMBHM_v^{p,q}$ operator converted into:

$$TFMBHM_v^{1,1}(N_1, N_2, ..., N_n) = \frac{1}{\left(\bigoplus_{i,j=1,i\neq j}^{n} \left(\frac{v_i v_j}{N_i N_j}\right)\right)^{\frac{1}{2}}}$$

Example 3.9. Suppose we have three TFM-numbers as follows:

$$N_1 = \langle(0.1, 0.4, 0.5, 0.6); 0.5, 0.3, 0.4, 0.2\rangle$$
$$N_2 = \langle(0.1, 0.2, 0.5, 0.8); 0.9, 0.6, 0.3, 0.5\rangle$$
$$N_3 = \langle(0.2, 0.3, 0.3, 0.4); 0.7, 0.8, 0.3, 0.4\rangle$$

Then, based on the operations in Definition 2.7 and Equation (1) for $p, q = 1$, we have

$$N_1^1 \oplus N_2^1 = \langle(0.01, 0.08, 0.25, 0.48); 0.45, 0.18, 0.12, 0.10\rangle$$
$$N_2^1 \oplus N_1^1 = \langle(0.01, 0.08, 0.25, 0.48); 0.45, 0.18, 0.12, 0.10\rangle$$
$$N_1^1 \oplus N_3^1 = \langle(0.02, 0.12, 0.15, 0.24); 0.35, 0.24, 0.12, 0.08\rangle$$
$$N_3^1 \oplus N_1^1 = \langle(0.02, 0.12, 0.15, 0.24); 0.35, 0.24, 0.12, 0.08\rangle$$
$$N_2^1 \oplus N_3^1 = \langle(0.02, 0.06, 0.15, 0.32); 0.63, 0.48, 0.09, 0.20\rangle$$
$$N_3^1 \oplus N_2^1 = \langle(0.02, 0.06, 0.15, 0.32); 0.63, 0.48, 0.09, 0.20\rangle$$

and then we obtain:

$$TFMBHM^{1,1}(N_1, N_2, N_3) = \langle(0.0056, 0.0289, 0.0611, 0.1156); 0.9912, 0.9460, 0.7095, 0.7492\rangle$$

In a similar way, if $p, q = 2$, from Equation (1), we have

$$TFMBHM^{2,2}(N_1, N_2, N_3) = \langle(0.0001, 0.0014, 0.0060, 0.0217); 0.9521, 0.8440, 0.5173, 0.5736\rangle$$

if $p = 1, q = 3$, from Equation (1), we have

$$TFMBHM^{1,3}(N_1, N_2, N_3) = \langle(0.0001, 0.0015, 0.0063, 0.0239); 0.9618, 0.8664, 0.5214, 0.5901\rangle$$

if $p = 3, q = 1$, from Equation (1), we have

$$TFMBHM^{3,1}(N_1, N_2, N_3) = \langle(0.0001, 0.0015, 0.0063, 0.0239); 0.9618, 0.8664, 0.5214, 0.5901\rangle$$

4. An Application of Weighted Bonferroni Harmonic Mean Operator on TFM-numbers

This section developes an algorithm based on weighted Bonferroni harmonic mean operator to solve multi criteria decision making problems.

Algorithm

Here, we firstly give an algorithm to solve decision making problems with multi criteria. Then, to see application of the algorithm, we give an example. As for end of the section, we present a table of $TFMBHM_v^{p,q}$ taken by changing (p,q) values.

Table 1. TFM-numbers for linguistic terms

Linguistic terms	Linguistic values of TFM-numbers
Absolutely low (AL)	$\langle (0.01, 0.05, 0.10, 0.15); 0.1, 0.2, 0.3, 0.4 \rangle$
Very Very Low (VVL)	$\langle (0.05, 0.10, 0.15, 0.20); 0.2, 0.3, 0.4, 0.1 \rangle$
Very Low (VL)	$\langle (0.10, 0.15, 0.15, 0.20); 0.2, 0.4, 0.5, 0.3 \rangle$
Low (L)	$\langle (0.10, 0.20, 0.20, 0.30); 0.3, 0.4, 0.8, 0.1 \rangle$
Fairly low (FL)	$\langle (0.15, 0.20, 0.25, 0.30); 0.4, 0.6, 0.2, 0.5 \rangle$
Medium (M)	$\langle (0.25, 0.30, 0.35, 0.40); 0.4, 0.5, 0.6, 0.8 \rangle$
Fairly high (FH)	$\langle (0.30, 0.35, 0.40, 0.45); 0.6, 0.1, 0.8, 0.4 \rangle$
High (H)	$\langle (0.40, 0.45, 0.50, 0.55); 0.8, 0.9, 0.3, 0.6 \rangle$
Very High (VH)	$\langle (0.45, 0.55, 0.65, 0.75); 0.7, 0.8, 0.6, 0.3 \rangle$
Very Very High (VVH)	$\langle (0.50, 0.60, 0.70, 0.80); 0.1, 0.7, 0.8, 0.9 \rangle$
Absolutely high (AH)	$\langle (0.70, 0.80, 0.90, 1.00); 0.7, 0.8, 0.9, 0.2 \rangle$

Step 1: Build the decision matrix based on experts' decision according to Table 1. Let $X = \{x_i | i \in I_m\}$ be set of alternatives and $C = \{c_j | j \in I_n\}$ be set of criteria whose weight vector is $v = (v_1, v_2, ...v_n)^T$ such that $v_i \geq 0$ and $\sum_{i=1}^{n} v_i = 1$.

Preferable of the alternatives x_i based on the criteria c_j expressed by a linguistic terms is computed by following $TFMBHM_v$:

$$N_{ij} = \langle (x_{ij}, y_{ij}, z_{ij}, t_{ij}); \eta^1_{N_{ij}}, \eta^2_{N_{ij}}, ..., \eta^P_{N_{ij}} \rangle \, (i \in I_m)$$

Step 2: Get preferable for x_i based on N_i $(i \in I_m)$ to aggregate the TFM-numbers $N_{i1}, N_{i2}, ..., N_{in}$ as:

$$N_i = TFMBHM_v^{p,q}(N_{i1}, N_{i2}, ..., N_{in})$$

Step 3: Calculate score value $s(N_i)$ whose formula is given in Definition 2.9 for each N_i to rank alternatives.

Step 4: Rank all score value of N_i according to descending order.

4.1. An Illustrative Example

Example 4.1. An entrepreneur wants to set a factory to a suitable place in the country. There are five alternatives to be chosen to set the factory. The entrepreneur takes into account of following criteria in decision making process :

1. Closeness to raw material (c_1)

2. Facility of transportation (c_2)

3. Regional incentive (c_3)

4. Market breadth (c_4)

There are five candidates x_i $(i \in I_5)$. Besides $v = (0.1, 0.3, 0.1, 0.5)^T$ is weight vector of criteria c_j $(j \in I_4)$. Suppose that the preferability of the alternative x_i with regard to the attribute c_j is measured by a TFM $N_{ij} = \langle (x_{ij}, y_{ij}, z_{ij}, t_{ij}); \eta^1_{N_{ij}}, \eta^2_{N_{ij}}, ..., \eta^P_{N_{ij}} \rangle$ $(i \in I_m)$ and then we build TFM decision matrix $(N_{ij})_{5x4}$ according to decision makers' choices based on linguistic Table 1.

Step 1: Decision matrix is constructed according to decision maker's choices:

Table 2. Decision Matrix N_{ij}

	c_1	c_2	c_3	c_4
N_1	$\langle(0.01,0.05,0.10,0.15);0.1,0.2,0.3,0.4\rangle$	$\langle(0.70,0.80,0.90,1.00);0.7,0.8,0.9,0.2\rangle$	$\langle(0.05,0.10,0.15,0.200.2,0.3,0.4,0.1\rangle$	$\langle(0.70,0.80,0.90,1.000.7,0.8,0.9,0.2\rangle$
N_2	$\langle(0.45,0.55,0.65,0.75);0.7,0.8,0.6,0.3\rangle$	$\langle(0.45,0.55,0.65,0.75);0.7,0.8,0.6,0.3\rangle$	$\langle(0.10,0.20,0.20,0.300.3,0.4,0.8,0.1\rangle$	$\langle(0.01,0.05,0.10,0.150.1,0.2,0.3,0.4\rangle$
N_3	$\langle(0.10,0.20,0.20,0.30);0.3,0.4,0.8,0.1\rangle$	$\langle(0.30,0.35,0.40,0.45);0.6,0.1,0.8,0.4\rangle$	$\langle(0.25,0.30,0.35,0.400.4,0.5,0.6,0.8\rangle$	$\langle(0.50,0.60,0.70,0.800.1,0.7,0.8,0.9\rangle$
N_4	$\langle(0.10,0.15,0.15,0.20);0.2,0.4,0.5,0.3\rangle$	$\langle(0.15,0.20,0.25,0.30);0.4,0.6,0.2,0.5\rangle$	$\langle(0.40,0.45,0.50,0.550.8,0.9,0.3,0.6\rangle$	$\langle(0.05,0.10,0.15,0.200.2,0.3,0.4,0.1\rangle$
N_5	$\langle(0.30,0.35,0.40,0.45);0.6,0.1,0.8,0.4\rangle$	$\langle(0.10,0.15,0.15,0.20);0.2,0.4,0.5,0.3\rangle$	$\langle(0.50,0.60,0.70,0.800.1,0.7,0.8,0.9\rangle$	$\langle(0.45,0.55,0.65,0.750.7,0.8,0.6,0.3\rangle$

Step 2: We aggregate experts' ratings for each alternative, by using TFM-weighted Bonferroni harmonic mean operator. That is,

$$N_1 = TFMBHM_v^{1,1}(N_{11}, N_{12}, N_{13}, N_{14}) = \frac{1}{\left(\bigoplus_{i,j=1,i\neq j}^n \left(\left(\frac{v_i}{N_{1i}^p}\right) \otimes \left(\frac{v_j}{N_{1j}^q}\right) \right) \right)^{\frac{1}{1+1}}}$$

$$= \langle(0.1212, 0.3091, 0.4629, 0.5941); 0.1583, 0.2536, 0.4058, 0.0175\rangle$$

where $$\bigoplus_{i,j=1,i\neq j}^n \left(\left(\frac{v_i}{N_{1i}^p}\right) \otimes \left(\frac{v_j}{N_{1j}^q}\right) \right)$$

$$= \left(\frac{v_1}{N_{11}^p} \otimes \frac{v_2}{N_{12}^q}\right) \oplus \left(\frac{v_1}{N_{11}^p} \otimes \frac{v_3}{N_{13}^q}\right) \oplus \left(\frac{v_1}{N_{11}^p} \otimes \frac{v_4}{N_{14}^q}\right) \oplus \left(\frac{v_2}{N_{12}^p} \otimes \frac{v_1}{N_{11}^q}\right) \oplus \left(\frac{v_2}{N_{12}^p} \otimes \frac{v_3}{N_{13}^q}\right) \oplus \left(\frac{v_2}{N_{12}^p} \otimes \frac{v_4}{N_{14}^q}\right)$$

$$\oplus \left(\frac{v_3}{N_{13}^p} \otimes \frac{v_1}{N_{11}^q}\right) \oplus \left(\frac{v_3}{N_{13}^p} \otimes \frac{v_2}{N_{12}^q}\right) \oplus \left(\frac{v_3}{N_{13}^p} \otimes \frac{v_4}{N_{14}^q}\right) \oplus \left(\frac{v_4}{N_{14}^p} \otimes \frac{v_1}{N_{11}^q}\right) \oplus \left(\frac{v_4}{N_{14}^p} \otimes \frac{v_2}{N_{12}^q}\right) \oplus \left(\frac{v_4}{N_{14}^p} \otimes \frac{v_3}{N_{13}^q}\right)$$

$$N_2 = TFMBHM_v^{1,1}(N_{21}, N_{22}, N_{23}, N_{24})$$
$$= \langle(0.0724, 0.1981, 0.2897, 0.4003); 0.0704, 0.1373, 0.1391, 0.0377\rangle$$

$$N_3 = TFMBHM_v^{1,1}(N_{31}, N_{32}, N_{33}, N_{34})$$
$$= \langle(0.3450, 0.4673, 0.5228, 0.6316); 0.0383, 0.0720, 0.3806, 0.2141\rangle$$

$$N_4 = TFMBHM_v^{1,1}(N_{41}, N_{42}, N_{43}, N_{44})$$
$$= \langle(0.1191, 0.1930, 0.2490, 0.3169); 0.0592, 0.1439, 0.0457, 0.0414\rangle$$

$$N_5 = TFMBHM_v^{1,1}(N_{51}, N_{52}, N_{53}, N_{54})$$
$$= \langle(0.2990, 0.3964, 0.4334, 0.5300); 0.0789, 0.1574, 0.2311, 0.0911\rangle$$

Step 3: Scores of $N_i's$ calculated as:

$$s(N_1) = \frac{0.5941^2 + 0.4629^2 - 0.1212^2 - 0.3091^2}{2.4}(0.1583 + 0.2536 + 0.4058 + 0.0175) = 0.0477,$$

$$s(N_2) = 0.0096, \ s(N_3) = 0.0295, \ s(N_4) = 0.0040, \ s(N_5) = 0.0155$$

Step 4: Alternatives are ranked:

$$x_1 > x_3 > x_5 > x_2 > x_4$$

Finally, the best alternative to choose is x_1. Moreover, rankings for some alternatives in terms of different $TFMBHM_v^{p,q}$ of the example are given in Table 3.

Table 3. Rankings for some alternatives in terms of different $TFMBHM_v^{p,q}$ of Example 4.1

(p,q)	$s(N_1)$	$s(N_2)$	$s(N_3)$	$s(N_4)$	$s(N_5)$	**Ranking**
$(1.0, 2.0)$	0.0139	0.0023	0.0110	0.0010	0.0042	$x_1 > x_3 > x_5 > x_2 > x_4$
$(3.0, 1.0)$	0.0051	0.0007	0.0052	0.0003	0.0014	$x_3 > x_1 > x_5 > x_2 > x_4$
$(3.0, 2.0)$	0.0028	0.0003	0.0025	0.0001	0.0006	$x_1 > x_3 > x_5 > x_2 > x_4$
$(1.0, 0.5)$	0.0932	0.0234	0.0590	0.0106	0.0339	$x_1 > x_3 > x_5 > x_2 > x_4$
$(2.0, 0.5)$	0.0201	0.0043	0.0190	0.0023	0.0071	$x_1 > x_3 > x_5 > x_2 > x_4$
$(3.0, 0.5)$	0.0068	0.0013	0.0084	0.0008	0.0023	$x_3 > x_1 > x_5 > x_2 > x_4$
$(4.0, 0.5)$	0.0031	0.0006	0.0044	0.0004	0.0010	$x_3 > x_1 > x_5 > x_2 > x_4$

5. Comparison Analysis

Table 4. Some rankings in terms of different methods and proposed method of Example 4.1

Methods	Operator	Ranking
Proposed method	$TFMBHM_v^{(1,1)}$	$x_1 > x_3 > x_5 > x_2 > x_1$
Method of Deli and Keleş [8]	$S^i(x_i)$	$x_5 > x_3 > x_4 > x_1 > x_2$
Method of Uluçay et al. [7]	$TFMG_v$	$x_5 > x_3 > x_4 > x_1 > x_2$
Method of Şahin et al. [10]	D_v	$x_3 > x_5 > x_1 > x_4 > x_2$
Method of Uluçay [11]	S_v	$x_4 > x_3 > x_1 > x_5 > x_2$

Table 4 compares introduced method with other existing methods such as distance measure operator proposed by Deli & Keleş [8], TFM weighted geometric operator introduced by Uluçay et al. [7], weighted dice vector similarity operator submitted by Şahin et al. [10] and vector similarity operator given by Uluçay [11] based on Example 4.1. If we check over the comparison table given above, we can see result of the proposed aggregation method presents a new perspective to decision making process. So, proposed method can be readily used to solve decision making problems with multiple criteria.

6. Conclusion

In this article, firstly, Bonferroni harmonic mean was introduced. Then, its some special cases were investigated to see how it converted into other operators. Secondly, to see an application of the operator, a basic example was given. Thirdly, an algorithm was proposed to solve decision making problems. Then, a numerical example was given to show performance of the developed approach and to demonstrate its degree of effectiveness and practicality. Finally, a comparison table was presented to compare proposed method with some existing methods.

In future, the operator will be applied to hesitant fuzzy numbers, intuitionistic fuzzy numbers and neutrosophic fuzzy numbers. In addition, we plan to extend our research to AHP method, ANP method, Topsis method, VIKOR method, QUALIFLEX method, ELECTRE I method, ELECTRE II method, ELECTRE III method, defuzzification techniques and so on.

Author Contributions

All authors contributed equally to this work. They all read and approved the last version of the paper.

Conflicts of Interest

All authors declare no conflict of interest.

References

[1] L. A. Zadeh, *Fuzzy Sets*, Information and Control 8 (1965) 338–353.

[2] R. R. Yager, *On the Theory of Bags*, International Journal of General Systems 13 (1986) 23–37.

[3] S. Miyamoto, *Fuzzy Multi Sets and Their Generalizations*, Workshop on Membrane Computing: Multiset Processing 2235 (2000) 225–235.

[4] S. Miyamoto, *Data Structure and Operations For Fuzzy Multisets*, Transactions on Rough Sets II, Lecture Notes in Computer Science 3135 (2004) 189–200.

[5] S. Sebastian, T. V. Ramakrishnan, *Multi-Fuzzy Sets*, International Mathematical Forum 5 (50) (2010) 2471–2476.

[6] S. Sebastian, T. V. Ramakrishnan, *Multi-Fuzzy Extensions of Functions*, Advances in Adaptive Data Analysis 3 (3) (2011) 339–350.

[7] V. Uluçay, İ. Deli, M. Şahin, *Trapezoidal Fuzzy Multi-Number and Its Application to Multi-Criteria Decision-Making Problems*, Neural Computing and Applications 30 (5) (2018) 1469–1478.

[8] İ. Deli, M. A. Keleş, *Distance Measures on Trapezoidal Fuzzy Multi-Numbers and Application to Multi-Criteria Decision-Making Problems*, Soft Computing 25 (2021) 5979–5992.

[9] M. Şahin, V. Uluçay, F. S. Yılmaz, *Dice Vector Similarity Measure Based on Multi-Criteria Decision Making with Trapezoidal Fuzzy Multi-Numbers*, Neutrosophic Triplet Structures Volume I, Chapter 13 (2017) Pons Editions, Brussels, Belgium.

[10] M. Şahin, V. Uluçay, F. S. Yılmaz, *Improved Hybrid Vector Similarity Measures And Their Applications on Trapezoidal Fuzzy Multi Numbers*, Neutrosophic Triplet Structures Volume I, Chapter 12 (2019) Pons Editions, Brussels, Belgium.

[11] V. Uluçay, *A New Similarity Function of Trapezoidal Fuzzy Multi-Numbers Based on Multi-Criteria Decision Making*, Journal of the Institute of Science and Technology 10 (2) (2020) 1233–1246.

[12] C. Bonferroni, *Sulle Medie Multiple di Potenze*, Bolletino Matematica Italiana, 5 (1950) 267–270.

[13] R. R. Yager, *On Generalized Bonferroni Mean Operators for Multi-Criteria Aggregation*, International Journal of Approximate Reasoning 59 (2009) 1279–1286.

[14] G. Beliakov, S. James, J. Mordelová, T. Rückschlossová, R. R. Yager, *Generalized Bonferroni Mean Operators in Multi-Criteria Aggregation*, Fuzzy Sets and Systems 161 (2010) 2227–2242.

[15] Z. Xu, *Fuzzy Harmonic Mean Operators*, International Journal of Intelligent Systems 24 (2) (2009) 52–172.

[16] G. W. Wei, *FIOWHM Operator and Its Application to Multiple Attribute Group Decision Making*, Expert Systems with Applications 38 (4) (2011) 2984–2989.

[17] H. Sun, M. Sun, *Generalized Bonferroni Harmonic Mean Operators and Their Application to Multiple Attribute Decision Making*, Journal of Computer Information Systems 8 (14) (2012) 5717–5724.

[18] İ. Deli, *A Topsis Method by Using Generalized Trapezoidal Hesitant Fuzzy Numbers and Application to a Robot Selection Problem*, Journal of Intelligent and Fuzzy Systems 38 (1) (2020) 779–793.

[19] İ. Deli, F. Karaaslan, *Generalized Trapezoidal Hesitant Fuzzy Numbers and Their Applications to Multi Criteria Decision-Making Problems*, Soft Computing 25 (2021) 1017–1032.

[20] H. Wang, X. Wang, L. Wang, *Multi-Criteria Decision Making Based on Archimedean Bonferroni Mean Operators of Hesitant Fermatean 2-Tuple Linguistic Terms*, Complexity 4 (2019) 1–19.

[21] V. Torra, Y. Narukawa, *On Hesitant Fuzzy Sets and Decision*, in: H. T. Jeon, K. C. Min, K. W. Oh (Eds.), IEEE International Conference on Fuzzy Systems, Jeju Island, Korea, 2009, pp. 1378–1382.

[22] M. Xia, Z. Xu, *Generalized Intuitionistic Fuzzy Aggregation Based on Hamacher t-conorm and t-norm*, International Journal of Intelligent Systems 27 (2011) 23–47.

[23] Z. Xu, Hesitant Fuzzy Sets Theory, Studies in Fuzziness and Soft Computing, Springer, 2014.

[24] H. J. Zimmermann, Fuzzy Set Theory and Its Applications, Fourth Edition, Kluwer Academic Publishers, Dordrecht, 2001.

[25] D. Li, Decision and Game Theory in Management with Intuitionistic Fuzzy Sets, Studies in Fuzziness and Soft Computing, 308, Springer, 2014.

[26] İ. Deli, *Bonferroni Mean Operators of Generalized Trapezoidal Hesitant Fuzzy Numbers and Their Application to Decision-Making Problems*, Soft Computing 25 (2021) 4925–4949.

[27] W. Su, J. Zhou, S. Zeng, C. Zhang, K. Yu, *A Novel Method for Intuitionistic Fuzzy MAGDM with Bonferroni Weighted Harmonic Means*, Recent Patents on Computer Science 10 (2017) 178–189.

Some New Estimates for Maximal Commutator and Commutator of Maximal Function in $L_{p,\lambda}(\Gamma)$

Merve Esra Türkay[1] ⬤

Abstract — The theory of boundedness of classical operators of real analyses on Morrey spaces defined on Carleson curves has made significant progress in recent years as it allows for various applications. This study obtains new estimates about the boundedness of the maximal commutator operator M_b and the commutator of the maximal function $[M, b]$ in Morrey spaces defined on Carleson curves.

1. Introduction

$L_{p,\lambda}(\mathbb{R}^n)$ Morrey spaces, proposed by Morrey in 1938, were used in the study of the local behavior of the solutions of elliptic partial differential equations. Morrey spaces are quite used for problems in the analysis of variations theory. In addition, Navier-Stokes and Schrödinger's equations have many applications in the potential theory of elliptic problems with discontinuous coefficients. Over the years, many researchers have done various studies on Morrey spaces (For more details, see [1–5]).

In recent years, there has been an increasing interest in various spaces on Carleson curves, such as Lebesgue spaces, Morrey spaces. We only mention [3, 6–9]. There are many applications for Maximal operators, which have a capital place in real and fractional analysis. These nonlinear operators, which are informative in differentiation theory, have inspired the studies of classical operators of harmonic analysis in various spaces. Moreover, they are also featured in many valuable studies (see, for example, [7, 10–12]). Samko [5] studied the boundedness of the M maximal operator in Morrey spaces defined on quasi-metric measure spaces, especially in $L_{p,\lambda}(\Gamma)$ Morrey spaces defined on Carleson curves.

The commutator operation and properties of maximal integrals have been extensively studied in various spaces, and there are many important consequences associated with them (see, for example [13–22]). The maximal commutator M_b is of great importance in studying the commutators of the BMO symbol and singular integral operators. There are important studies on the properties and boundedness of M_b (For more details, see [13, 14, 18, 19]). The commutator of maximal operator $[M, b]$ was studied by many authors (For more details, see [13–15, 18]). This operator is the product of two functions from BMO and H^1 Hardy space. It emerged when it was wanted to give meaning (Let us note that the product of these two functions may not be locally integrable).

---

[1]mesra@cumhuriyet.edu.tr (Corresponding Author)
[1]Department of Mathematics, Faculty of Science, Sivas Cumhuriyet University, Sivas, Türkiye

The fact that the operator M_b is a positive linear operator, unlike the $[M, b]$ operator, indicates that these operators are quite different from each other. However, b is bound to the operator M_b manage the operator $[M, b]$, with some additional conditions.

This study consists of three sections. Section 2 presents preliminaries of the commutator of the maximal operator and maximal commutator on Carleson curves. Section 3 investigates the boundedness of these operators on $L_{p,\lambda}(\Gamma)$.

2. Preliminaries

In this section, before giving the basic definitions and theorems, let us briefly talk about Carleson curves, which are the focus of the paper. For every $t \in \Gamma$ and $r > 0$, if a locally rectifiable Jordan curve Γ satisfies the following condition;

$$\nu\Gamma(t, r) \leq c_0 r$$

it is called the Carleson curve (regular curve), where $\Gamma(t, r) := \Gamma \cap B(t, r)$, $t \in \Gamma$, $r > 0$. Let $\Gamma: \gamma(t) = x(t) + iy(t)$, $a \leq t \leq b$. Length of a regular curve is given with:

$$\nu\Gamma = \ell(\gamma) = \int_{\gamma} |dz| = \int_a^b \sqrt{x'(t)^2 + y'(t)^2} dt$$

Let Γ, equipped with Lebesgue length measure, be a locally rectifiable compound arc. The measure of a measurable subset $\gamma \subset \Gamma$ is displayed with $\gamma \subset \Gamma$. In particular, $|\Gamma(t, r)|$ is the sum of the lengths of the countably many arcs that make up $\Gamma(t, r)$. Let Γ be a locally rectifiable composite curve and $\Gamma_1, \ldots, \Gamma_N$ be a finite number of arcs combined such that $\Gamma = \Gamma_1 \cup \ldots \cup \Gamma_N$. Since

$$\Gamma_j(t, \varepsilon) \subset \Gamma(t, \varepsilon) \subset \Gamma_1(t, \varepsilon) \cup \ldots \cup \Gamma_N(t, \varepsilon)$$

and

$$|\Gamma_j(t, \varepsilon)| \leq |\Gamma(t, \varepsilon)| \leq |\Gamma_1(t, \varepsilon)| + \ldots + |\Gamma_N(t, \varepsilon)|$$

from the above expression

$$\Gamma \text{ is a Carleson curve} \Leftrightarrow \text{Each } \Gamma_j \text{ is a Carleson curve}$$

is obtained. In order to indicate the dependence on t, we shall denote this family by $\{\Gamma_{t,j}\}$. For almost every $\xi \notin \Gamma_{t,j}$ is $f(\xi) \leq t$. Now, we need to give below the necessary definitions for the case of spaces on Carleson curves.

Definition 2.1. [5] $L_{p,\lambda}(\Gamma)$ Morrey spaces with $0 \leq \lambda < 1$, $1 \leq p < \infty$ and $f \in L_p^{loc}(\Gamma)$ is the space of functions such that

$$\|f\|_{L_{p,\lambda}(\Gamma)} = \sup_{r>0,\ t\in\Gamma} r^{-\frac{\lambda}{p}} \|f\|_{L_p(\Gamma(t,r))}$$

$$= \sup_{r>0,\ t\in\Gamma} \left(r^{-\lambda} \int_{\Gamma(t,r)} |f(\tau)|^p \, d\nu(\tau) \right)^{1/p} < \infty$$

When $\lambda < 0$ or $\lambda > 1$, $L_{p,\lambda}(\Gamma) = \theta$ where θ denotes the set of functions on Γ that is equivalent to 0. İf $\lambda = 0$, then $L_{p,0}(\Gamma) = L_p(\Gamma)$ is obtained.

Definition 2.2. [8] The space of functions with bounded mean oscillation $BMO(\Gamma)$ is defined as the set of locally integrable functions f with a finite norm

$$\|f\|_{BMO(\Gamma)} = \sup_{r>0, t\in\Gamma} (v\Gamma(t,r))^{-1} \int_{\Gamma(t,r)} |f(\tau) - f_{\Gamma(t,r)}| \, dv(\tau) < \infty$$

here $f_{\Gamma(t,r)}$ is displayed with;

$$f_{\Gamma(t,r)} := (v\Gamma(t,r))^{-1} \int_{\Gamma(t,r)} f(\tau) \, dv(\tau)$$

Definition 2.3. [8] Let $1 \leq p < \infty$ and Γ be a Carleson curve. Then,

$$L_\infty(\Gamma) = \sup_{t \in \Gamma, r > 0} r^{-\frac{1}{p}} \|f\|_{L_p(\Gamma)}$$

and

$$\|f\|_{L_\infty(\Gamma)} \leq \sup_{t \in \Gamma, r > 0} r^{-\frac{1}{p}} \|f\|_{L_p(\Gamma)} \leq c_0^{1/p} \|f\|_{L_\infty(\Gamma)}$$

The application of the Lebesgue Differentiation Theorem on Carleson curves is as follows:
Let $f \in L_1^{loc}(\Gamma)$, then the following statement applies

$$\lim_{r \to 0} (\nu\Gamma(t,r))^{-1} \int_{\Gamma(t,r)} f(\tau)d\nu(\tau) = f(t) \tag{1}$$

Note that in expression (1) supremum instead of limit and $|f|$ instead of function f is taken, the maximal function is defined.

The definition of the maximal operator on Carleson curves is as follows;

Definition 2.4. [5] Let Γ be a simple Carleson curve and $f \in L_1^{loc}(\Gamma)$. The maximal operator M on Γ defined by

$$Mf(t) = \sup_{t > 0} (v\Gamma(t,r))^{-1} \int_{\Gamma(t,r)} |f(\tau)| \, dv(\tau)$$

The boundedness of the maximal function on $L_p(\Gamma)$ has been studied by Guliyev in [3].

Theorem 2.5. [3] Let Γ be a Carleson curve, $1 \leq p < \infty$ and $t_0 \in \Gamma$. Then, for $p > 1$ and any $r > 0$ in Γ, the inequality

$$\|Mf\|_{L_p(\Gamma(t_0,r))} \precsim r^{\frac{1}{p}} \sup_{\tau > 2r} \tau^{-\frac{1}{p}} \|f\|_{L_p(\Gamma(t_0,r))}$$

holds for all $f \in L_p^{loc}(\Gamma)$.

The definitions of the maximal commutator and commutator of maximal operator on Carleson curves are as follows, respectively.

Definition 2.6. [9] Given a locally integrable function b, the maximal commutator is defined by

$$M_b(f)(t) := \sup_{t > 0} \frac{1}{v\Gamma(t,r)} \int_{\Gamma(t,r)} |b(t) - b(\tau)||f(\tau)|dv(\tau), \; for \; all \; t \in \Gamma$$

Definition 2.7. [9] Given a locally integrable function b, the commutator of the maximal operator is defined by

$$[M,b] f(t) := M(bf)(t) - b(t)Mf(t) \text{ for all } t \in \Gamma$$

Türkay and Mursaleen proved the following statement in [9].

Theorem 2.8. [9] Let $b \in BMO(\Gamma)$ and $0 < \delta < 1$. In this case, there is a positive constant $C = C_\delta$ where the following inequalities holds for all $f \in L_1^{loc}(\Gamma)$;

$$i) M_\delta(M_b(f))(\varsigma) \leq C \|b\|_{BMO(\Gamma)} M^2 f(\varsigma), \; \varsigma \in \Gamma$$

$$ii) M_b(f)(\varsigma) \leq C \|b\|_* M^2 f(\varsigma), \; \varsigma \in \Gamma$$

Lemma 2.9. [9] Let b be any non-negative locally integrable function on Γ. Then for all $f \in L_1^{loc}(\Gamma)$, the following inequalities are provided;

$$|[M,b] f(t)| \leq M_b(f)(t), t \in \Gamma \tag{2}$$

and

$$|[M,b] f(t)| \leq M_b(f)(t) + 2b^-(t)Mf(t), \; t \in \Gamma \tag{3}$$

Theorem 2.10. [9] Let $b \in BMO(\Gamma)$ such that $b^- \in L_\infty(\Gamma)$. Then, there exists a positive constant C such that

$$|[M,b] f(t)| \leq C \left(\|b^+\|_* + \|b^-\|_\infty \right) M^2 f(t) \text{ for all } f \in L_1^{loc}(\Gamma)$$

3. Some New Estimates

This section studies the $L_{p,\lambda}(\Gamma)-$boundedness of the operator M_b and the operator $[M, b]$. Since it is easier to examine the boundedness of the operator M_b than the operator $[M, b]$, we will first investigate the boundedness of the operator M_b. Before the main results are given, the auxiliary theorems that will help in the proof will be reminded. Türkay and Murselen examined the boundedness of the M_b operator in $L_p(\Gamma)$ in [9].

Theorem 3.1. [9] Let $1 < p < \infty$. The operator M_b is bounded on $L_p(\Gamma)$ if and only if $b \in BMO(\Gamma)$.

Inspired by Theorem 3.1, we establish the following theorem.

Theorem 3.2. Let $1 < p < \infty$, $0 \leq \lambda \leq 1$. $b \in BMO(\Gamma)$ if and only if The operator M_b is bounded on $L_{p,\lambda}(\Gamma)$.

PROOF. ($\Rightarrow$) Let $\Gamma(t_0, r_0)$ be a constant Carleson curve. Suppose that $b \in \mathrm{BMO}(\Gamma)$. By Theorem **??** and Theorem 2.5 the following inequality holds for $f \in L_p(\Gamma)$:

$$
\begin{aligned}
||M_b(f)||_{L_{p,\lambda}(\Gamma)} &\approx \sup_{\Gamma(t,r)} \left(|\Gamma(t,r)|^{\lambda-1} \int_{\Gamma(t,r)} M_b(f)(\tau)\, dv(\tau) \right)^{\frac{1}{p}} \\
&= |\Gamma(t_0, r_0)|^{\frac{\lambda-1}{p}} \sup_{\Gamma(t,r) \subset \Gamma(t_0, r_0)} \left(\int_{\Gamma(t,r)} M_b(f)(\tau)\, dv(\tau) \right)^{\frac{1}{p}} \\
&\leq |\Gamma(t_0, r_0)|^{\frac{\lambda-1}{p}} ||b||_* ||f||_{L_p(\Gamma)}
\end{aligned}
$$

($\Leftarrow$) Let the operator M_b be bounded on $L_{p,\lambda}(\Gamma)$, that is, for every $f \in L_{p,\lambda}(\Gamma)$ there is such a positive constant c that the following inequality is obtained;

$$ ||M_b(f)||_{L_{p,\lambda}(\Gamma)} \leq c||f||_{L_{p,\lambda}(\Gamma)} $$

Obviously,

$$ ||f||_{L_{p,\lambda}(\Gamma)} \approx \sup_{\Gamma(t,r)} \left(|\Gamma(t,r)|^{\lambda-1} \int_{\Gamma(t,r)} |f(\tau)|^p dv(\tau) \right)^{\frac{1}{p}} $$

Let $f = \chi_{\Gamma(t_0,r_0)}$ such that $\Gamma(t_0, r_0)$ is a constant Carleson curve. In this case, the following expression is easily written;

$$
\begin{aligned}
||\chi_{\Gamma(t_0,r_0)}||_{L_{p,\lambda}(\Gamma)} &\approx \sup_{\Gamma(t,r)} \left(|\Gamma(t,r)|^{\lambda-1} \int_{\Gamma(t,r)} x_{\Gamma(t_0,r_0)}(\tau)\, dv(\tau) \right)^{\frac{1}{p}} \\
&= \sup_{\Gamma(t,r)} \left(|\Gamma(t,r) \cap \Gamma(t_0, r_0)| \, |\Gamma(t,r)|^{\lambda-1} \right)^{\frac{1}{p}} \\
&= \sup_{\Gamma(t,r) \subset \Gamma(t_0,r_0)} \left(|\Gamma(t,r)| \, |\Gamma(t,r)|^{\lambda-1} \right)^{\frac{1}{p}} \\
&= |\Gamma(t_0, r_0)|^{\frac{\lambda}{p}}
\end{aligned}
\tag{4}
$$

In addition, since

$$ M_b\left(\chi_{\Gamma(t_0,r_0)}\right)(t) \gtrsim \frac{1}{|\Gamma(t_0, r_0)|} \int_{\Gamma(t_0,r_0)} \left| b(\tau) - b_{\Gamma(t_0,r_0)} \right| dv(\tau), \text{ for all } t \in \Gamma(t_0, r_0) $$

then

$$
\begin{aligned}
\left\| M_b\left(\chi_{\Gamma(t_0,r_0)}\right) \right\|_{L_{p,\lambda}(\Gamma)} &\approx \sup_{\Gamma(t,r)} \left(|\Gamma(t,r)|^{\lambda-1} \int_{\Gamma(t,r)} \left| M_b\left(\chi_{\Gamma(t_0,r_0)}\right)(\tau) \right|^p dv(\tau) \right)^{\frac{1}{p}} \\
&\gtrsim |\Gamma(t_0, r_0)|^{\frac{\lambda}{p}} \frac{1}{|\Gamma(t_0,r_0)|} \int_{\Gamma(t_0,r_0)} \left| b(\tau) - b_{\Gamma(t_0,r_0)} \right| dv(\tau)
\end{aligned}
\tag{5}
$$

Since by assumption

$$\left\|M_b\left(\chi_{\Gamma(t_0,r_0)}\right)\right\|_{L_{p,\lambda}(\Gamma)} \lesssim \left\|\chi_{\Gamma(t_0,r_0)}\right\|_{L_{p,\lambda}(\Gamma)}$$

and by (4) and (5), we get that

$$\frac{1}{|\Gamma(t_0,r_0)|}\int_{\Gamma(t_0,r_0)}|b(\tau)-b_{\Gamma(t_0,r_0)}|dv(\tau)\leq c \tag{6}$$

Thus, the desired result is obtained. □

Milman and Schonbek obtained the $L_p(\mathbb{R}^n)$-boundedness of the operator $[M,b]$ with real interpolation techniques in [20]. Inspired by this study, Türkay and Murselen examined the boundedness of the operator $[M,b]$ in $L_p(\Gamma)$ in [9].

Theorem 3.3. [9] Let $1 < p < \infty$. The operator $[M,b]$ is bounded on $L_p(\Gamma)$ if and only if $b \in BMO(\Gamma)$ and $b^- \in L_\infty(\Gamma)$.

Applying Theorem 3.3, the below theorem is obtained.

Theorem 3.4. Let $1 < p < \infty$, $0 \leq \lambda \leq 1$. $b \in BMO(\Gamma)$ such that $b^- \in L_\infty(\Gamma)$ if and only if the operator $[M,b]$ is bounded on $L_{p,\lambda}(\Gamma)$.

PROOF. ($\Rightarrow$) Suppose that $b \in BMO(\Gamma)$ such that $b^- \in L_\infty(\Gamma)$. Thus, the following inequality is obtained from Theorem 2.10;

$$|[M,b]f(t)| \leq C\left(\left\|b^+\right\|_* + \left\|b^-\right\|_\infty\right)M^2f(t) \text{ for all } f \in L_1^{loc}(\Gamma)$$

Moreover, from Theorem 3.3, the operator $[M,b]$ is bounded on $L_p(\Gamma)$, with $1 < p < \infty$, so the following inequality is satisfied for all $f \in L_p(\Gamma)$;

$$\|[M,b]\|_{L_{p,\lambda}(\Gamma)}$$
$$\sup_{\Gamma(t,r)}\left(|\Gamma(t,r)|^{\lambda-1}\int_{\Gamma(t,r)}|[M,b]f(\tau)|^p dv(\tau)\right)^{\frac{1}{p}}$$
$$\leq |\Gamma(t_0,r_0)|^{\frac{\lambda-1}{p}}\sup_{\Gamma(t,r)\subset\Gamma(t_0,r_0)}\left(\int_{\Gamma(t,r)}|[M,b]f(\tau)|^p dv(\tau)\right)^{\frac{1}{p}}$$
$$\leq C|\Gamma(t_0,r_0)|^{\frac{\lambda-1}{p}}\left(\|b^+\|_{BMO(\Gamma)}+\|b^-\|_{L_\infty(\Gamma)}\right)M^2f(t)$$
$$\leq C_\Gamma$$

Hence,

$$\|[M,b]f\|_{L_{p,\lambda}(\Gamma)} \leq C\|f\|_{L_{p,\lambda}(\Gamma)} \tag{7}$$

The inequality (7) gives the desired result easily.

($\Leftarrow$) Assume that $[M,b]$ is bounded on $L_{p,\lambda}(\Gamma)$. Let $\Gamma(t_0,r_0)$ be a fixed Carleson curve. Denote by M_b the local maximal function of f:

$$M_{\Gamma(t_0,r_0)}f(x) := \sup_{t\in\Gamma(t,r):\,\Gamma(t,r)\subset\Gamma(t_0,r_0)}\frac{1}{|\Gamma(t,r)|}\int_{\Gamma(t,r)}|f(y)|\,dv(\tau),\ \ (t\in\Gamma)$$

Since

$$M(b\chi_{\Gamma(t_0,r_0)})\chi_{\Gamma(t_0,r_0)} = M_{\Gamma(t_0,r_0)}(b)$$

and

$$M\left(\chi_{\Gamma(t_0,r_0)}\right)\chi_{\Gamma(t_0,r_0)} = \chi_{\Gamma(t_0,r_0)}$$

then, we get the following inequality

$$
\begin{aligned}
\left| M_{\Gamma(t_0,r_0)}(b) - b\chi_{\Gamma(t_0,r_0)} \right| &= \left| M(b\chi_{\Gamma(t_0,r_0)})\chi_{\Gamma(t_0,r_0)} - bM\left(\chi_{\Gamma(t_0,r_0)}\right)\chi_{\Gamma(t_0,r_0)} \right| \\
&\leq \left| M(b\chi_{\Gamma(t_0,r_0)}) - bM\left(\chi_{\Gamma(t_0,r_0)}\right) \right| \\
&= \left| [M,b]\,\chi_{\Gamma(t_0,r_0)} \right|
\end{aligned}
$$

Hence,

$$
\left\| M_{\Gamma(t_0,r_0)}(b) - b\chi_{\Gamma(t_0,r_0)} \right\|_{L_{p,\lambda}(\Gamma)} \leq \left\| [M,b]\,\chi_{\Gamma(t_0,r_0)} \right\|_{L_{p,\lambda}(\Gamma)} \tag{8}
$$

Thus, from Equation (8), we get

$$
\begin{aligned}
\frac{1}{|\Gamma(t_0,r_0)|} \int_{\Gamma(t_0,r_0)} \left| \left(b - M_{\Gamma(t_0,r_0)}(b)\right)(\tau) \right| dv(\tau) &\leq \left(\frac{1}{\Gamma(t_0,r_0)} \int_{\Gamma(t_0,r_0)} \left| \left(b - M_{\Gamma(t_0,r_0)}(b)\right)(\tau) \right|^p dv(\tau) \right)^{\frac{1}{p}} \\
&\leq |\Gamma(t_0,r_0)|^{-\frac{1}{p}} |\Gamma(t,r)|^{\frac{1-\lambda}{p}} \left\| b\chi_{\Gamma(t_0,r_0)} - M_{\Gamma(t_0,r_0)}(b) \right\|_{L_{p,\lambda}(\Gamma)} \\
&\leq |\Gamma(t_0,r_0)|^{-\frac{1}{p}} |\Gamma(t,r)|^{\frac{1-\lambda}{p}} \left\| [M,b]\,\chi_{\Gamma(t_0,r_0)} \right\|_{L_{p,\lambda}(\Gamma)} \\
&\leq c\,|\Gamma(t_0,r_0)|^{-\frac{1}{p}} |\Gamma(t,r)|^{\frac{1-\lambda}{p}} \left\| \chi_{\Gamma(t_0,r_0)} \right\|_{L_{p,\lambda}(\Gamma)} \\
&\approx c\,|\Gamma(t_0,r_0)|^{-\frac{1}{p}} |\Gamma(t,r)|^{\frac{1-\lambda}{p}} |\Gamma(t_0,r_0)|^{\frac{1}{p}} |\Gamma(t,r)|^{\frac{\lambda-1}{p}} \\
&= c
\end{aligned}
$$

Since

$$
\int_{\Gamma(t_0,r_0)} \left| \left(b - b_{\Gamma(t_0,r_0)}\right)(\tau) \right| dv(\tau) =
\begin{cases}
-\int_{\Gamma(t_0,r_0)} b(\tau) - b_{\Gamma(t_0,r_0)} dv(\tau), & b(t) \leq b_{\Gamma(t_0,r_0)} \text{ and } t \in \Gamma(t_0,r_0) \\
\int_{\Gamma(t_0,r_0)} b(\tau) - b_{\Gamma(t_0,r_0)} dv(\tau), & b(t) > b_{\Gamma(t_0,r_0)} \text{ and } t \in \Gamma(t_0,r_0)
\end{cases}
\tag{9}
$$

for the following sets

$$
I_1 := \left\{ t \in \Gamma(t_0,r_0) : b(t) \leq b_{\Gamma(t_0,r_0)} \right\}
$$

and

$$
I_2 := \left\{ t \in \Gamma(t_0,r_0) : b(t) > b_{\Gamma(t_0,r_0)} \right\}
$$

are valid. Thus, the expression

$$
-\int_{I_1} \left[b(\tau) - b_{\Gamma(t_0,r_0)} \right] dv(\tau) = \int_{I_2} \left[b(\tau) - b_{\Gamma(t_0,r_0)} \right] dv(\tau)
$$

can be written. In view of the inequality

$$
b(x) \leq b_{\Gamma(t_0,r_0)} \leq M_{\Gamma(t_0,r_0)}(b), x \in E
$$

we get that

$$
\begin{aligned}
&\frac{1}{|\Gamma(t_0,r_0)|} \int_{\Gamma(t_0,r_0)} \left| \left(b - b_{\Gamma(t_0,r_0)}\right)(\tau) \right| dv(\tau) \\
&= \frac{2}{|\Gamma(t_0,r_0)|} \int_{I_2} \left[\left(b - b_{\Gamma(t_0,r_0)}\right)(\tau) \right] dv(\tau) \\
&\leq \frac{2}{|\Gamma(t_0,r_0)|} \int_{I_2} \left[\left(b - M_{\Gamma(t_0,r_0)}(b)\right)(\tau) \right] dv(\tau) \\
&\precsim c
\end{aligned}
$$

Consequently, $b \in BMO(\Gamma)$.

Besides, the following expression is valid

$$
0 \leq b^- = |b| - b^+ \leq M_{\Gamma(t_0,r_0)}(b) - b^+ + b^- = M_{\Gamma(t_0,r_0)}(b) - b \tag{10}
$$

where $M_{\Gamma(t_0,r_0)}(b) \geq |b|$. From our assumption, $[M,b]$ is bounded on $L_{p,\lambda}(\Gamma)$, thus the following inequality is valid;

$$
\begin{aligned}
\left\| [M,b]\,f \right\|_{L_{p,\lambda}(\Gamma)} &\leq C \left(\left\| b^+ \right\|_{BMO(\Gamma)} + \left\| b^- \right\|_{L^\infty(\Gamma)} \right) \left\| f \right\|_{L_{p,\lambda}(\Gamma)} \\
&< C_\Gamma
\end{aligned}
$$

Moreover, we obtained $b \in BMO(\Gamma)$ before, with these data we obtain $b^- \in L_\infty(\Gamma)$. $\square$

4. Conclusion

In recent years, studies on Morrey spaces defined in $\mathbb{R}^n$ metric space and their reinterpretation with Carleson curves have presented a different field of study to scientists working on Morrey spaces. In this article, we have given new estimates about the boundedness of the maximal commutator operator M_b and the commutator of the maximal function $[M, b]$ in Morrey spaces defined on Carleson curves. By making some generalizations on Morrey spaces defined on Carleson curves of this study, it is thought that it will inspire the obtaining of new inequalities boundedness of the maximal commutator operator M_b and the commutator of the maximal function $[M, b]$.

Author Contributions

The author read and approved the last version of the paper.

Conflicts of Interest

The author declares no conflict of interest.

References

[1] V. S. Guliyev, J. J. Hasanov, Y. Zeren, *Necessary and Sufficient Conditions for the Boundedness of Riesz Potential in the Modifed Morrey Spaces*, Journal of Mathematical Inequalities 5 (4) (2011) 491–506.

[2] V. S. Guliyev, K. Rahimova, *Parabolic Fractional Integral Operator in Modified Parabolic Morrey Spaces*, Proceedings Razmadze Mathematical Institute 163 (2013) 85–106.

[3] V. Guliyev, H. Armutcu, T. Azeroglu, *Characterizations for the Potential Operators on Carleson Curves in Local Generalized Morrey Spaces*, Open Mathematics 18 (1) (2020), 1317–1331.

[4] C. B. Morrey, *On the Solutions of Quasi-Linear Elliptic Partial Differential Equations*, Transactions of the American Mathematical Society 43 (1938) 126–166.

[5] N. Samko, *Weighted Hardy and Singular Operators in Morrey Spaces*, Journal of Mathematical Analysis and Applications 350 (1) (2009) 56–72.

[6] A. Böttcher, Y. I. Karlovich, Carleson Curves, Muckenhoupt Weights, and Toeplitz Operators, 15, Springer Science Business Media, 1997.

[7] I. B. Dadashova, C. Aykol, Z. Cakir, A. Serbetci, *Potential Operators in Modified Morrey Spaces Defined on Carleson Curves*, Transactions of A. Razmadze Mathematical Institute 172 (1) (2018) 15–29.

[8] J. I Mamedkhanov, I. B. Dadashova, *Some Properties of the Potential Operators in Morrey Spaces Defined on Carleson Curves*, Complex Variables and Elliptic Equations 55 (8-10) (2010) 937–945.

[9] M. E. Türkay, M. Mursaleen, *Some Estimates in $L_p(\Gamma)$ for Maximal Commutator and Commutator of Maximal Function* (2022) In Press.

[10] L. Grafakos, Modern Fourier Analysis, 2nd ed., Graduate Texts in Mathematics, 250, Springer, New York 2009.

[11] A. Kufner, O. John, S. Fucik, Function Spaces, Noordhoff, Leyden, and Academia, Prague 1977.

[12] E. M. Stein, Harmonic Analysis: Real-Variable Methods, Orthogonality, and Oscillatory Integrals, Princeton Mathematical Series, 43, Princeton University Press, Princeton, NJ 1993.

[13] M. Agcayazi, A. Gogatishvili, K. Koca, R. Mustafayev, *A Note on Maximal Commutators and Commutators of Maximal Functions*, Journal of the Mathematical Society of Japan 67 (2) (2015) 581–593.

[14] C. Aykol, H. Armutcu, M. N. Omarova, *Maximal Commutator and Commutator of Maximal Function on Modified Morrey Spaces*, Transactions of NAS of Azerbaijan, Issue Mathematics 36 (2016) 29–35.

[15] J. Bastero, Milman M. and Ruiz F.J., *Commutators for the Maximal and Sharp Functions*, Proceedings of the American Mathematical Society 128 (11) (2000) 3329–3334.

[16] A. Bonami, T. Iwaniec, P. Jones, M. Zinsmeister, *On the Product of Functions in BMO and H_1*, Annales De L'institut Fourier (Grenoble) 57 (5) (2007) 1405–1439.

[17] J. Garcia-Cuerva, E. Harboure, C. Segovia, J. L. Torrea, *Weighted Norm Inequalities for Commutators of Strongly Singular Integrals*, Indiana University Mathematics Journal 40 (4) (1991) 1397–1420.

[18] A. Gogatishvili, R.Ch. Mustafayev, M. Agcayazi, *Weak-Type Estimates in Morrey Spaces for Maximal Commutator and Commutator of Maximal Function* Tokyo Journal of Mathematics 41 (1) (2018) 193–218.

[19] D. Li, G. Hu, X. Shi, *Weighted Norm Inequalities for the Maximal Commutators of Singular Integral Operators*, Journal of Mathematical Analysis and Applications 319 (2) (2006) 509–521.

[20] M. Milman, T.Schonbek, *Second Order Estimates in Interpolation Theory and Applications*, Proceedings of the American Mathematical Society 110 (4) (1990) 961–969.

[21] C. Segovia, J. L. Torrea, *Higher Order Commutators for Vector-Valued Calderon-Zygmund Operators*, Transactions of the American Mathematical Society 336 (2) (1993) 537–556.

[22] C. P. Xie, *Some Estimates of Commutators*, Real Analysis Exchange 36 (2) (2010) 405–415.

On Parametric Surfaces with Constant Mean Curvature Along Given Smarandache Curves in Lie Group

Zühal Küçükarslan Yüzbaşı [1] , **Sevinç Taze** [2]

Abstract − This paper finds sufficient conditions to determine a surface whose mean curvature along a given Smarandache curve is constant in a three-dimensional Lie group. This is accomplished by using the Frenet frames of the specified curve to express surfaces that span the TN, NB, and TB Smarandache curves parametrically. In terms of the curvatures of given Smarandache curves, marching scale functions, and their partial derivatives, the mean curvatures of these surfaces along the given TN, NB, and TB Smarandache curves are determined. Sufficient conditions are found to maintain the provided mean curvatures of the resulting surfaces at a constant value. Finally, some examples are provided.

1. Introduction

The theory of curves is one of the most crucial research areas in classical differential geometry. For a very long time, and even now, special curves and their characterizations have been investigated. The use of special curves can be observed in nature, mechanical devices, computer-aided design, and other things. The Smarandache curve, one of the special curves, has a position vector made up of Frenet frame vectors on another regular curve. Ahmad first presented a few special Smarandache curves to the Euclidean space in [1]. Additionally, some researchers investigated Smarandache curves in the Lie group and Minkowski space [2,3], respectively.

In two ways, Lie groups are made of algebra and geometry, two significant branches of mathematics: first, Lie groups are groups, and second, they are smooth manifolds. As a result, there must be some kind of coherence between the Lie groups' geometric and algebraic structure. The current approach to geometry as a whole is based on the geometry of Lie groups. Additionally, numerous research findings on curves and surfaces in the 3-dimensional Lie group have been published in [4-8].

On the other hand, in differential geometry, surfaces can have a variety of remarkable effects and properties. Researchers later turned their focus to the construction surfaces along a special curve such as a geodesic, an asymptotic, or a line of curvature. Some recently research on these topics was done in [9-12]. The process in these papers is as follows: conditions for that curve to be a geodesic, asymptotic, and line of curvature have been given, and the parametric surface has been constructed as a linear combination of an

[1]zuhal2387@yahoo.com.tr (Corresponding Author); [2]svncatlla@gmail.com

[1,2]Department of Mathematics, Faculty of Science, Fırat University, Elazığ, Türkiye

isoparametric curve and its Frenet frame. A new study on construction surfaces with constant curvatures along a given curve was recently proposed by Bayram et al. [13,14].

We organized our paper as follows: we give some basic information regarding the Smarandache curve and surface theory in the 3-dimensional Lie group in Section 2. We build surfaces along the Smarandache curves of the specified curve in Section 3, and then we derive sufficient conditions for each case where the surfaces have constant mean curvature along the TN, NB, and TB Smarandache curves. This study was derived from the second author's master's thesis under the supervision of the first author.

2. Preliminaries

The Frenet formulas for a unit speed curve $\alpha(s)$ in the Lie group are expressed as follows:

$$\begin{bmatrix} T'(s) \\ N'(s) \\ B'(s) \end{bmatrix} = \begin{bmatrix} 0 & \kappa_1 & 0 \\ -\kappa_1 & 0 & (\kappa_2 - \overline{\kappa_2}) \\ 0 & -(\kappa_2 - \overline{\kappa_2}) & 0 \end{bmatrix} \begin{bmatrix} T(s) \\ N(s) \\ B(s) \end{bmatrix} \tag{1}$$

where κ_1 and κ_2 are the curvature functions of $\alpha(s)$ and $\overline{\kappa_2} = \frac{1}{2}\langle [T,N], B \rangle$ which was introduced [4-7], is the Lie group torsion of $\alpha(s)$. Here, $T = \alpha'(s)$, $\kappa_1(s) = \|D_T T\| = \|T'\|$, $\kappa_2 = \|D_T B\| - \overline{\kappa_2}$, and $D_T X = X' + \frac{1}{2}[T, X]$.

Definition 2.1. [5] $\tilde{h} = \frac{\kappa_2 - \overline{\kappa_2}}{\kappa_1}$ is denoted the harmonic curvature function of $\alpha(s)$.

Theorem 2.2. [4,5] The curve is a general helix in Lie Group G if and only if its harmonic function is a constant function.

Definition 2.3. [15] Let $\varphi = \varphi(s, t)$ be a surface in the 3-dimesional Lie Group, then the mean curvature of the ruled surface φ in three-dimensional Lie group is given by

$$H = \frac{En - 2Fm + lG}{EG - F^2} \tag{2}$$

where the surface normal $N = \frac{\varphi_s \times \varphi_t}{\|\varphi_s \times \varphi_t\|}$, $E = \langle \varphi_s, \varphi_s \rangle$, $F = \langle \varphi_s, \varphi_t \rangle$, $G = \langle \varphi_t, \varphi_t \rangle$, $l = \langle \varphi_{ss}, N \rangle$, $m = \langle \varphi_{st}, N \rangle$, and $n = \langle \varphi_{tt}, N \rangle$.

Definition 2.4. [3] Smarandache curves are defined as regular curves whose position vectors are composed of Frenet frame vectors. This leads us

TN-Smarandache curve is defined as $\alpha_{TN}(s) = \frac{1}{\sqrt{2}}(T(s) + N(s))$,

NB-Smarandache curve is defined as $\alpha_{NB}(s) = \frac{1}{\sqrt{2}}(N(s) + B(s))$,

TB-Smarandache curve is defined as $\alpha_{TB}(s) = \frac{1}{\sqrt{2}}(T(s) + B(s))$,

and

TNB-Smarandache curve is defined as $\alpha_{TB}(s) = \frac{1}{\sqrt{3}}(T(s) + N(s) + B(s))$.

3. Surfaces with Constant Mean Curvature along Given Smarandache Curves

One of the special curves is the Smarandache curve, whose position vector is composed of Frenet frame vectors on another regular curve. Ahmad first presented a few unique Smarandache curves to the Euclidean space in [1]. Then, Değirmen et al. presented a few unique Smarandache curves to the Lie group in [3]. In this section, we will characterize the surfaces whose mean curvatures are constant in the three-dimensional Lie Group.

Consider $\alpha(s)$ to be an arc-length parametrized curve on a surface $P(s,t)$ in G. Then the curve α is called an isoparametric curve if it is a parameter curve, that is, there exists a parameter t_0 such that $\alpha(s) = P(s,t_0)$.

Since $\alpha(s)$ is an isoparametric curve on this surface, there exists a parameter $t = t_0 \in [0,T]$ such that $\alpha(s) = P(s,t_0)$ that leads us

$$f(s,t_0) = g(s,t_0) = h(s,t_0) = 0 \text{ such that } s \in [0,L] \text{ and } t_0 \in [0,T] \tag{3}$$

Hence, if the TN, NB, and TB Smarandache curves are isoparametric curves on this surface, then there exists a parameter $t = t_0 \in [0,T]$ such that $\alpha_{TN}(s) = P(s,t_0)$, $\alpha_{NB}(s) = P(s,t_0)$, $\alpha_{TB}(s) = P(s,t_0)$, respectively.

$P(s,t)$ is defined based on the Smarandache curves of the curve $\alpha(s)$ and using the Frenet frame of the curve in Lie group G, respectively, as follows

$$P(s,t) = \alpha_{TN}(s) + f(s,t)T(s) + g(s,t)N(s) + h(s,t)B(s) \tag{4}$$
$$P(s,t) = \alpha_{NB}(s) + f(s,t)T(s) + g(s,t)N(s) + h(s,t)B(s) \tag{5}$$
$$P(s,t) = \alpha_{TB}(s) + f(s,t)T(s) + g(s,t)N(s) + h(s,t)B(s) \tag{6}$$

Using the Formulation (2) to calculate mean curvatures, one can easily get the mean curvature of the surface provided in Equation (4) as follows:

$$H = \frac{p_0\,p_1 + p_2 - p_3 p_4}{p_5 p_6} \tag{7}$$

where

$$p_0 = \frac{1}{\sqrt{2}}\left(f_t{}^2 + g_t{}^2 + h_t{}^2\right)$$

$$p_1 = \left((\kappa_1 h_t - \tilde{h}\kappa_1 g_t)\left(-\frac{\partial}{\partial s}\kappa_1 - \kappa_1{}^2\right) + (\kappa_1 h_t + \tilde{h}\kappa_1 f_t)\left(-\kappa_1{}^2 + \frac{\partial}{\partial s}\kappa_1 - (\tilde{h}\kappa_1)^2\right) - (\kappa_1 g_t + \kappa_1 f_t)\left(\kappa_1(\tilde{h}\kappa_1) - \frac{\partial}{\partial s}(\tilde{h}\kappa_1)\right)\right)$$

$$p_2 = \left((\kappa_1 h_t - \tilde{h}\kappa_1 g_t)f_{tt} + (\kappa_1 h_t + \tilde{h}\kappa_1 f_t)g_{tt} - (\kappa_1 g_t + \kappa_1 f_t)h_{tt}\right)\left(\kappa_1{}^2 + \frac{(\tilde{h}\kappa_1)^2}{2}\right)$$

$$p_3 = 2\left((\kappa_1 h_t - \tilde{h}\kappa_1 g_t)(f_{ts} - g_t\kappa_1) + (\kappa_1 h_t + \tilde{h}\kappa_1 f_t)(f_t\kappa_1 + g_{ts} - h_t\tilde{h}\kappa_1) - (\kappa_1 g_t + \kappa_1 f_t)(g_t\tilde{h}\kappa_1 + h_{ts})\right)$$

$$p_4 = \left(-\frac{1}{\sqrt{2}}\kappa_1 f_t + \frac{1}{\sqrt{2}}\kappa_1 g_t + \frac{1}{\sqrt{2}}\tilde{h}\kappa_1 h_t\right)$$

$$p_5 = 2\left(\left(\kappa_1{}^2 + \frac{(\tilde{h}\kappa_1)^2}{2}\right)(f_t{}^2 + g_t{}^2 + h_t{}^2) - \frac{1}{2}(-\kappa_1 f_t + \kappa_1 g_t + \tilde{h}\kappa_1 h_t)^2\right)$$

and

$$p_6 = \sqrt{(\kappa_1 h_t - \tilde{h}\kappa_1 g_t)^2 + (\kappa_1 h_t + \tilde{h}\kappa_1 f_t)^2 + (\kappa_1 g_t + \kappa_1 f_t)^2}$$

The mean curvature of the surface provided in Equation (5) is given as follows:

$$H = \frac{q_0 q_1 + q_2 - q_3 q_4}{q_5 q_6} \tag{8}$$

where

$$q_0 = \left(f_t{}^2 + g_t{}^2 + h_t{}^2\right)$$

$$q_1 = \left(\left((-(\tilde{h}\kappa_1))(h_t + g_t)\right)\left(-\frac{\partial}{\partial s}\kappa_1 + \kappa_1(\tilde{h}\kappa_1)\right) + (\kappa_1 h_t + \tilde{h}\kappa_1 f_t)\left(-\kappa_1{}^2 - \frac{\partial}{\partial s}(\tilde{h}\kappa_1) - (\tilde{h}\kappa_1)^2\right) + (-\kappa_1 g_t + \tilde{h}\kappa_1 f_t)\left(-(\tilde{h}\kappa_1)^2 + \frac{\partial}{\partial s}(\tilde{h}\kappa_1)\right)\right)$$

$$q_2 = \left(\left(-(\tilde{h}\kappa_1))(h_t + g_t)\right) f_{tt} + \left(\kappa_1 h_t + \tilde{h}\kappa_1 f_t\right) g_{tt} + (-\kappa_1 g_t + \tilde{h}\kappa_1 f_t) h_{tt}\right)\left(\frac{\kappa_1{}^2}{2} + \frac{(\tilde{h}\kappa_1)^2}{2}\right)$$

$$q_3 = \frac{2}{\sqrt{2}}\left(\left(-(\tilde{h}\kappa_1))(h_t + g_t)\right)(f_{ts} - g_t\kappa_1) + (\kappa_1 h_t + \tilde{h}\kappa_1 f_t)(f_t\kappa_1 + g_{ts} - h_t\tilde{h}\kappa_1) + (-\kappa_1 g_t + \tilde{h}\kappa_1 f_t)(g_t\tilde{h}\kappa_1 + h_{ts})\right)$$

$$q_4 = \left(-\kappa_1 f_t - (\tilde{h}\kappa_1)(h_t + g_t)\right)$$

$$q_5 = \left(\left(\kappa_1{}^2 + (\tilde{h}\kappa_1)^2\right)\left(f_t{}^2 + g_t{}^2 + h_t{}^2\right) - \left(-\kappa_1 f_t - \tilde{h}\kappa_1 g_t + \tilde{h}\kappa_1 h_t\right)^2\right)$$

and

$$q_6 = \sqrt{(-(\tilde{h}\kappa_1)(g_t + h_t))^2 + (\kappa_1 h_t + \tilde{h}\kappa_1 f_t)^2 + (-\kappa_1 g_t + \tilde{h}\kappa_1 f_t)^2}$$

Then, the mean curvature of the surface provided in Equation (6) is given as follows:

$$H = \frac{r_0 r_1 - r_2}{r_3} \tag{9}$$

where

$$r_0 = \left(f_t{}^2 + g_t{}^2 + h_t{}^2\right)$$

$$r_1 = \left((h_t)\left(-\frac{1}{\sqrt{2}}\kappa_1{}^2 + \frac{1}{\sqrt{2}}\kappa_1\tilde{h}\kappa_1\right) - (f_t)\left(\frac{1}{\sqrt{2}}\kappa_1\tilde{h}\kappa_1 - \frac{1}{\sqrt{2}}(\tilde{h}\kappa_1)^2\right)\right) + \frac{1}{2}(h_t f_{tt} - f_t h_{tt})(\kappa_1 - \tilde{h}\kappa_1)^2$$

$$r_2 = 2\left(\frac{1}{\sqrt{2}}(\kappa_1 - \tilde{h}\kappa_1)g_t\right)\left((h_t)(f_{ts} - g_t\kappa_1) - (f_t)(g_t\tilde{h}\kappa_1 + h_{ts})\right)$$

and

$$r_3 = \left(\left((\kappa_1 - \tilde{h}\kappa_1)^2\right)\left(f_t{}^2 + g_t{}^2 + h_t{}^2\right) - \left((\kappa_1 - \tilde{h}\kappa_1)g_t\right)^2\right)\sqrt{\left(h_t{}^2 - f_t{}^2\right)}$$

Therefore, we can give the following main theorems for all the Smaradanche curves of the curve $\alpha(s)$:

Theorem 3.1. Consider that the surface $P(s, t)$ is determined by Equation (4). One of the following six conditions is satisfied if the mean curvature in Equation (7) along the isoparametric Smarandache curve TN of the curve $\alpha(s)$ is constant:

a) $f = g = h = f_t = f_{tt}(s, t_0) = 0,$ $g_t(s, t_0) = constant \neq 0,$ $h_t(s, t_0) = constant \neq 0,$ $\tilde{h}(s) = constant,$ and $\kappa_1(s) = constant.$

b) $f = g = h = g_t = g_{tt}(s, t_0) = 0,$ $f_t(s, t_0) = constant \neq 0,$ $h_t(s, t_0) = constant \neq 0,$ $\tilde{h}(s) = constant,$ and $\kappa_1(s) = constant.$

c) $f = g = h = h_t = h_{tt}(s, t_0) = 0,$ $f_t(s, t_0) = constant \neq 0,$ $g_t(s, t_0) = constant \neq 0,$ $\tilde{h}(s) = constant,$ and $\kappa_1(s) = constant.$

d) $f = g = h = f_t = g_t = f_{tt} = g_{tt}(s, t_0) = 0, h_t(s, t_0) \neq 0, \tilde{h}(s) = constant,$ and $\kappa_1(s) = constant.$

e) $f = g = h = f_t = h_t = f_{tt} = h_{tt}(s, t_0) = 0, g_t(s, t_0) = constant \neq 0, \tilde{h}(s) = constant,$ and $\kappa_1(s) = constant.$

f) $f = g = h = h_t = g_t = h_{tt} = g_{tt}(s, t_0) = 0, f_t(s, t_0) \neq 0, \tilde{h}(s) = constant$, and $\kappa_1(s) = constant$.

Theorem 3.2. Consider that the surface $P(s, t)$ is determined by Equation (5). One of the following six conditions is satisfied if the mean curvature in Equation (8) along the isoparametric Smarandache curve NB of the curve $\alpha(s)$ is constant:

a) $f = g = h = f_t = f_{tt}(s, t_0) = 0,$ $\quad g_t(s, t_0) = constant \neq 0, h_t(s, t_0) = constant \neq 0,$ $\quad \tilde{h}(s) = constant$, and $\kappa_1(s) = constant$.

b) $f = g = h = g_t = g_{tt}(s, t_0) = 0,$ $\quad f_t(s, t_0) = constant \neq 0, h_t(s, t_0) = constant \neq 0,$ $\quad \tilde{h}(s) = constant$, and $\kappa_1(s) = constant$.

c) $f = g = h = h_t = h_{tt}(s, t_0) = 0,$ $\quad f_t(s, t_0) = constant \neq 0, g_t(s, t_0) = constant \neq 0,$ $\quad \tilde{h}(s) = constant$, and $\kappa_1(s) = constant$.

d) $f = g = h = f_t = g_t = f_{tt} = g_{tt}(s, t_0) = 0, h_t(s, t_0) \neq 0, \tilde{h}(s) = constant$, and $\kappa_1(s) = constant$.

e) $f = g = h = f_t = h_t = f_{tt} = h_{tt}(s, t_0) = 0, g_t(s, t_0) \neq 0, \tilde{h}(s) = constant$, and $\kappa_1(s) = constant$.

f) $f = g = h = g_t = h_t = g_{tt} = h_{tt}(s, t_0) = 0, f_t(s, t_0) \neq 0, \tilde{h}(s) = constant$, and $\kappa_1(s) = constant$.

Theorem 3.3. Consider that the surface $P(s, t)$ is determined by Equation (6). One of the following six conditions is satisfied if the mean curvature in Equation (9) along the isoparametric Smarandache curve TB of the curve $\alpha(s)$ is constant:

a) $f = g = h = f_t = f_{tt}(s, t_0) = 0,$ $\quad g_t(s, t_0) = constant \neq 0, h_t(s, t_0) = constant \neq 0,$ $\quad \tilde{h}(s) = constant \neq 1$, and $\kappa_1(s) = constant$.

b) $f = g = h = g_t = g_{tt}(s, t_0) = 0,$ $\quad f_t(s, t_0) = constant \neq 0, h_t(s, t_0) = constant \neq 0,$ $\quad \tilde{h}(s) = constant$, and $\kappa_1(s) = constant$.

c) $f = g = h = h_t = h_{tt}(s, t_0) = 0,$ $\quad f_t(s, t_0) = constant \neq 0, g_t(s, t_0) = constant \neq 0,$ $\quad \tilde{h}(s) = constant \neq 1$, and $\kappa_1(s) = constant$.

d) $f = g = h = f_t = g_t = f_{tt} = g_{tt}(s, t_0) = 0, \quad h_t(s, t_0) \neq 0, \quad \tilde{h}(s) = constant \neq 1, \quad$ and $\quad \kappa_1(s) = constant$.

e) $f = g = h = f_t = h_t = f_{tt} = h_{tt}(s, t_0) = 0, g_t(s, t_0) \neq 0, \tilde{h}(s) = constant$, and $\kappa_1(s) = constant$.

f) $f = g = h = g_t = h_t = h_{tt} = g_{tt}(s, t_0) = 0, \quad f_t(s, t_0) \neq 0, \quad \tilde{h}(s) = constant \neq 1, \quad$ and $\quad \kappa_1(s) = constant$.

Example 3.4. Let $\alpha(s)$ be a parametrized by $\alpha(s) = \left(\frac{1}{\sqrt{2}} \cos s, \frac{1}{\sqrt{2}} \sin s, \frac{s}{\sqrt{2}}\right)$, $0 \leq s \leq 2\pi$. Then, the Frenet vectors in the three dimensional Lie Group are given as

$$T(s) = \left(-\frac{1}{\sqrt{2}} \sin s, \frac{1}{\sqrt{2}} \cos s, \frac{1}{\sqrt{2}}\right)$$

$$N(s) = (-\cos s, -\sin s, 0)$$

and

$$B(s) = \frac{1}{\sqrt{2}} (\sin s, -\cos s, 1)$$

where $\kappa_1 = \frac{1}{\sqrt{2}}, \overline{\kappa_2} = 0, \kappa_2 = \frac{1}{\sqrt{2}}$, and $\tilde{h}(s) = 1$.

Then, we can give the following cases:

Case 1. We can select $f(s,t) = 0$, $g(s,t) = t^3$, $h(s,t) = s \sin t$, and $t_0 = 0$ while taking into account the (d) condition of Theorem 3.1. Consequently, the surface $P_1(s,t)$ of the Lie group is provided by

$$P_1(s,t) = \alpha_{TN}(s) + f(s,t)T(s) + g(s,t)N(s) + h(s,t)B(s)$$

$$P_1(s,t) = \frac{1}{\sqrt{2}}(T(s) + N(s)) + f(s,t)T(s) + g(s,t)N(s) + h(s,t)B(s)$$

and so

$$P_1(s,t) = \left(-\frac{\sin s}{2} - \frac{\cos s}{\sqrt{2}} - t^3 \cos s + \frac{1}{\sqrt{2}} s \sin t \sin s \ , \frac{\cos s}{2} - \frac{\sin s}{\sqrt{2}} - t^3 \sin s - s \sin t \frac{\cos s}{\sqrt{2}}, \frac{1}{2} + \frac{1}{\sqrt{2}} s \sin t\right)$$

which is plotted in Fig. 1, where $0 \le s \le 2\pi$ and $0 \le t \le 1$ with constant mean curvature $H(s,t_0) = -\frac{1}{4}$.
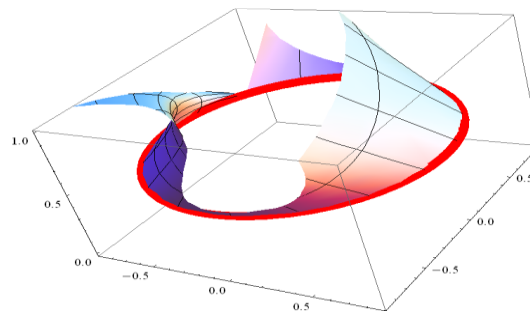
Fig. 1. The surface $P_1(s,t)$ with constant mean curvature along the TN Smarandache curve of the curve $\alpha(s)$

Case 2. We can select $f(s,t) = e^s t$, $g(s,t) = t^3$, $h(s,t) = 0$, and $t_0 = 0$ while taking into account the (f) condition of Theorem 3.2. Consequently, the surface $P_2(s,t)$ of the Lie group is provided by

$$P_2(s,t) = \alpha_{NB}(s) + f(s,t)T(s) + g(s,t)N(s) + h(s,t)B(s)$$

$$P_2(s,t) = \frac{1}{\sqrt{2}}(N(s) + B(s)) + f(s,t)T(s) + g(s,t)N(s) + h(s,t)B(s)$$

and so

$$P_2(s,t) = \left(-\frac{1}{\sqrt{2}}\cos s + \frac{1}{2}\sin s - e^s t \frac{1}{\sqrt{2}}\sin s - t^3 \cos s, -\frac{1}{\sqrt{2}}\sin s - \frac{1}{2}\cos s + e^s t \frac{1}{\sqrt{2}}\cos s - t^3 \sin s, \frac{1}{2} + \frac{1}{\sqrt{2}} e^s t\right)$$

which is plotted in Fig. 2, where $0 \le s \le 2\pi$ and $0 \le t \le 1$ with constant mean curvature $H(s,t_0) = -\frac{1}{2}$.
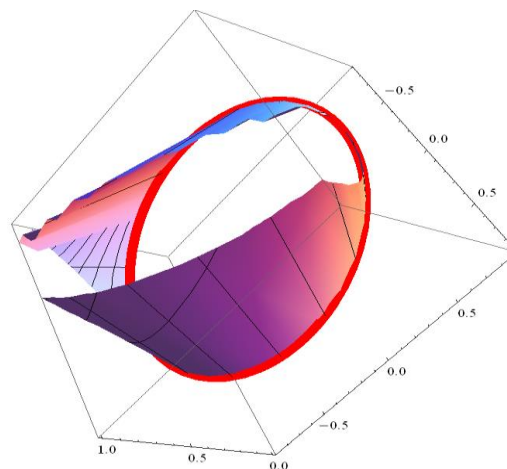
Fig. 2. The surface $P_2(s,t)$ with constant mean curvature along the NB Smarandache curve of the curve $\alpha(s)$

Case 3. We can select $f(s,t) = st^3$, $g(s,t) = s \sin t$, $h(s,t) = 0$, and $t_0 = 0$ while taking into account the (e) condition of Theorem 3.3. Consequently, the surface $P_3(s,t)$ of the Lie group is provided by

$$P_3(s,t) = \alpha_{TB}(s) + f(s,t)T(s) + g(s,t)N(s) + h(s,t)B(s)$$

$$P_3(s,t) = \frac{1}{\sqrt{2}}(T(s) + B(s)) + f(s,t)T(s) + g(s,t)N(s) + h(s,t)B(s)$$

and so

$$P_3(s,t) = \left(-st^3 \frac{1}{\sqrt{2}}\sin s - s\sin t\cos s, st^3 \frac{1}{\sqrt{2}}\cos s - s\sin t\sin s, 1 + \frac{1}{\sqrt{2}}st^3\right)$$

which is plotted in Fig. 3, where $0 \le s \le 2\pi$ and $0 \le t \le 1$ with constant mean curvature $H(s,t_0) = 0$.
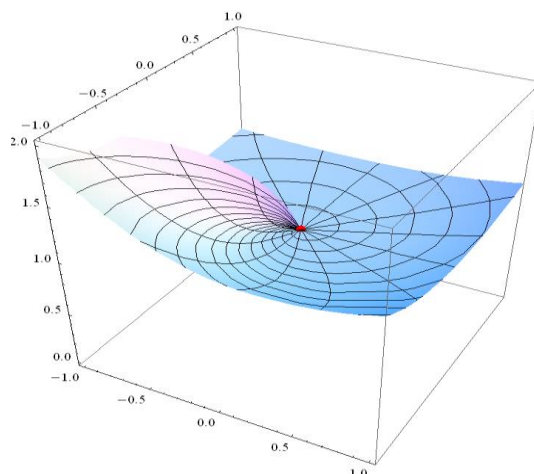

Fig. 3. The surface $P_3(s,t)$ with constant mean curvature along the TB Smarandache curve of the curve $\alpha(s)$

4. Conclusion

In this study, we constructed surfaces along the given TN, NB, and TB Smarandache curves of the curve $\alpha(s)$, and in each case, calculated the mean curvature of the given surfaces. Thus, sufficient conditions were derived to obtain surfaces with constant mean curvature along the TN, NB, and TB Smarandache curves of the curve $\alpha(s)$, respectively. According to the given theorems, we constructed the surfaces $P_i(s,t)$, for $1 \le i \le 3$ with constant mean curvature and illustrated them in Figs. 1-3 for the parameters $0 \le s \le 2\pi$ and $0 \le t \le 1$ by using Mathematica, respectively. In addition to the results shown in the manuscript, the work has also brought up a number of open questions for future studies, such as how to construct surfaces with constant Gauss curvatures along the given TN, NB, and TB Smarandache curves.

Author Contributions

The first author provided the idea and wrote the first draft, and the second author made the calculations and wrote the first draft. They all read and approved the last version of the manuscript.

Conflict of Interest

All the authors declare no conflict of interest.

Acknowledgement

References

[1] A. T. Ali, *Special Smarandache Curves in the Euclidean space*, International Journal of Mathematical Combinatorics 2 (2010) 30–36.

[2] M. Turgut, S. Yılmaz, *Smarandache Curves in Minkowski Space-Time*, International Journal of Mathematical Combinatorics 3 (2008) 51–55.

[3] C. Değirmen, O. Z. Okuyucu, Ö. G. Yıldız, *Smarandache Curves in Three-Dimensional Lie Groups*, Communications Faculty of Sciences University of Ankara Series A1 Mathematics and Statistics 68 (2019) 1175–1185.

[4] Ü. Çiftçi, *A Generalization of Lancret's Theorem*, Journal of Geometry and Physics 59 (2009) 1597–1603.

[5] O. Z. Okuyucu, I. Gök, Y. Yaylı, N. Ekmekci, *Slant Helices in Three Dimensional Lie Groups*, Applied Mathematics and Computation 221 (2013) 672–683.

[6] D. W. Yoon, *General Helices of AW(k)-Type in the Lie Group*, Journal of Applied Mathematics 2012 (2012) Article ID 535123 pp. 10.

[7] D. W. Yoon, Z. K. Yüzbaşı, M. Bektaş, *An Approach for Surfaces Using an Asymptotic Curve in Lie Group*, Journal of Advanced Physics 6 (4) (2017) 586–590.

[8] D. W. Yoon, Z. K. Yüzbaşı, *On Constructions of Surfaces Using A Geodesic in Lie Group*, Journal of Geometry 110 (2) (2019) 1–10.

[9] G. J. Wang, K. Tang, C. L. Tai, *Parametric Representation of a Surface Pencil with a Common Spatial Geodesic*, Computer-Aided Design 36 (2004) 447–459.

[10] C. Y. Li, R. H. Wang, C. G. Zhu, *Parametric Representation of a Surface Pencil with a Common Line of Curvature*, Computer-Aided Design 43 (2011) 1110–1117.

[11] E. Kasap, F. T. Akyıldız, *Surfaces with a Common Geodesic in Minkowski 3-space*, Applied Mathematics and Computation 177 (2006) 260–270.

[12] M. Altın, A. Kazan, H. B. Karadağ, *Hypersurface Families with Smarandache curves in Galilean 4-space*, Communications Faculty of Sciences University of Ankara Series A1 Mathematics and Statistics 70 (2021) 744-761.

[13] E. Bayram, *Construction of Surfaces with Constant Mean Curvature Along a Timelike Curve*, Journal of Polytechnic 1 (2022) pp. 7.

[14] H. Coşanoğlu, E. Bayram, *Construction of Surfaces with Constant Mean Curvature along a Curve in E^3*, Journal of Natural and Applied Sciences 24 (3) (2020) 533–538.

[15] E. Abbena, S. Salamon, A. Gray, Modern Differential Geometry of Curves and Surfaces with Mathematica, Third Edition, 1998.

A New Transformation Method for Solving High-Order Boundary Value Problems

Merve Yücel[1] 🔘 **, Fahreddin Muhtarov** 🔘 **, Oktay Mukhtarov** 🔘

Abstract − The main purpose of this work is to provide a new approximation method, the so-called parameterised differential transform method (PDTM), for solving high-order boundary value problems (HOBVPs). Our method differs from the classical differential transform method by calculating the coefficients of the solution, which has the form of a series. We applied the proposed new method to fourth-order boundary value problems to substantiate it. The resulting solution is graphically compared with the exact solution and the solutions obtained by the classical DTM and ADM methods.

1. Introduction

High-order boundary value problems (HOBVPs) for differential equations are essential for modelling a wide range of physical and chemical phenomena in all areas of natural science. In most cases, obtaining an exact solution to these boundary value problems is impossible. Therefore, there is growing interest in developing a new numerical method for finding a reliable approximate solution or understanding the exact solution's qualitative nature. This paper presents a new approximate method, parameterised differential transform, for solving HOBVPs. To show the applicability and effectiveness of PDTM, we will solve an illustrative fourth-order boundary value problem using this method.

Zhou firstly developed the classical differential transform method (DTM) in 1986 to solve some boundary value problems that arise when modelling electrical circuits [1]. In recent years, the application of classical DTM and its various generalisation to the solution of (HOBVPs) has attracted great interest. For example, Momami and Noor demonstrated different analytical techniques using the classical differential transform method, Adomian decomposition method (ADM) and homotopy perturbation method and gave a numerical comparison of these methods when solving a special fourth-order boundary value problem [2]. Hassan and Ertürk employed the DTM to solve HOBVPs [3]. Hussin and Kılıçman applied the DTM and ADM to solve linear and nonlinear HOBVPs [4]. Zahar used the DTM to obtain numerical solutions of singular perturbed fourth-order BVP's [5]. Ertürk and Momani used the DTM and ADM to get a numerical solution for fourth-

[1]merve.yucel@outlook.com.tr (Corresponding Author); [2]fahreddinmuhtarov@gmail.com; [3]omukhtarov@yahoo.com

[1]Department of Mathematics, Faculty of Arts and Sciences, Hitit University, Çorum, Türkiye

[2]Institute of Mathematics and Mechanics, Azerbaijan National Academy of Sciences, Baku, Azerbaijan

[3]Department of Mathematics, Faculty of Arts and Sciences, Tokat Gaziosmanpaşa University, Tokat, Türkiye

order BVP [6]. They also gave a numerical comparison between these methods. Wazwaz used a modified decomposition method to obtain the numerical solution of special type HOBVPs [7]. In some papers, the DTM is generalised so that it can be used to study approximate solutions and the spectral properties of various types of Sturm-Liouville problems (see [8-11]).

In [12], Boukary et al. use the ADM to solve the fourth-order parabolic type partial differential equations. Kwami et al. [13] introduced a new modification of ADM for solving fourth-order ODEs. This modification is based on transforming the considered fourth-order ODE into an equivalent integral equation of the Volterra type. Mukhtarov and Yücel [14] utilised the ADM to investigate the eigenvalues and eigenfunctions of two-interval SLPs that arise in modelling many phenomena in physics and engineering. Rysak and Gregorczyk [15] have shown the effectiveness of the DTM in solving problems arising in fractional dynamical systems.

Yücel and Mukhtarov [16] developed a new generalisation of the DTM for solving nonclassical boundary value problems, which differs from the classical boundary value problems in that, the boundary conditions contain some internal points at which given additional conditions. Al-Saif and Harfash compare the reduced DTM and perturbation-iteration method in [17] solving two-dimensional Navier-Stokes equations. Duan et al. [18] provided an overview of the DTM and its applications in solving fractional-order differential equations. The applicability of DTM to a system of differential equations was investigated by Ayaz [19].

2. Parameterized DTM

Let $s: [c, d] \rightarrow R$ be a real-valued analytic function and $\alpha \in [0,1]$ be any real parameter.

Definition 2.1. [10] We say the sequence $\big(S_\alpha(c,d)\big)_n(s)$ is the parameterised differential transform of the original function $s(t)$ if

$$\big(S_\alpha(c,d)\big)_n(s) := \alpha\big(S_c(s)\big)_n + (1-\alpha)\big(S_d(s)\big)_n$$

where

$$\big(S_c(s)\big)_n := \frac{d^n s(c)}{n!} \text{ and } \big(S_d(s)\big)_n := \frac{d^n s(d)}{n!}$$

Definition 2.2. [10] We say the function s(t) is the inverse differential transform if

$$s_\alpha(t) := \sum_{n=0}^{\infty} \big(S_\alpha(c,d)\big)_n(s)\big(t - (\alpha c + (1-\alpha)d)\big)^n \tag{1}$$

provided that the series is convergent. The inverse differential transforms, we will denote by $(S_\alpha^{-1}(c,d)_n)(s)$.

Definition 2.3. [10] The N-th partial sum of the series (1) is said to be an N-th parameterised approximation of the original function s(t) and is denoted by $s_{\alpha,N}(t)$, that is

$$s_{\alpha,N}(t) := \sum_{n=0}^{N} \big(S_\alpha(c,d)\big)_n(s)\big(t - (\alpha c + (1-\alpha)d)\big)^n \tag{2}$$

By Definition 2.1., we can show that the parameterised differential transform has the following properties:

 i. $\big(S_\alpha(c,d)\big)_n(\mu s) = \mu\big(S_\alpha(c,d)(s)\big)_n$

 ii. $\big(S_\alpha(c,d)\big)_n(f \pm s) = \big(S_\alpha(c,d)\big)_n(f) \pm \big(S_\alpha(c,d)\big)_n(s)$

 iii. $\big(S_\alpha(c,d)\big)_n\left(\frac{d^m s}{dt^m}\right) = \frac{(n+m)!}{n!}\big(S_\alpha(c,d)\big)_n(s)$

3. Numerical Results

Example 3.1. Consider the following HOBVP

$$y^{(4)}(t) = 4e^t + y(t), 0 < t < 1 \tag{3}$$

subject to the boundary conditions

$$y(0) = 1, y''(0) = 3, y(1) = 2e, \text{ and } y''(1) = 4e \tag{4}$$

The exact solution for the problem is $y(t) = (1 + t)e^t$. A graph of the exact solution to the problem is presented in Fig. 1 as follows:
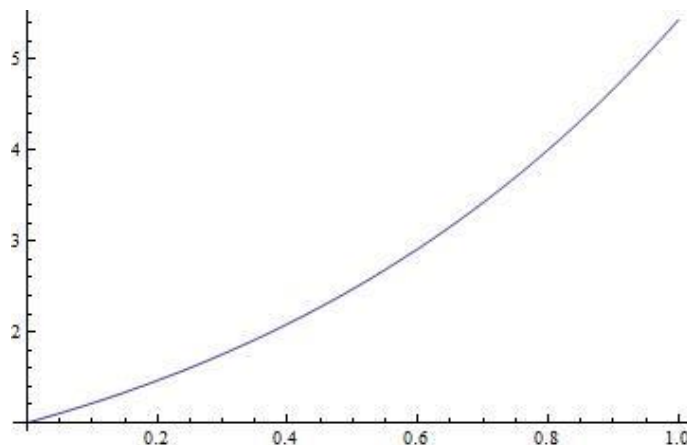

Fig. 1. Graph of the exact solution for the problem provided in (3)-(4)

If it is applied *PDT* to both sides of (3), then we obtain

$$\left(S_\alpha(0,1)\right)_{n+4}(y)(n+1)(n+2)(n+3)(n+4) = \left(\frac{4}{n!} + \left(S_\alpha(0,1)\right)_n(y)\right) \tag{5}$$

Therefore, from the definition of *PDT*,

$$y_\alpha(t) = \sum_{n=0}^{\infty} \left(S_\alpha(0,1)\right)_n(y)(t - t_\alpha)^n$$

and

$$y_\alpha''(t) = \sum_{n=0}^{\infty} \left(S_\alpha(0,1)\right)_n(y)n(n-1)(t - t_\alpha)^{n-2}$$

Moreover, for the boundary conditions $y(0) = 1, y''(0) = 3, y(1) = 2e, y''(1) = 4e$,

$$y_\alpha(0) = \sum_{n=0}^{N} \left(S_\alpha(0,1)\right)_n(y)(\alpha - 1)^n = 1$$

$$y_\alpha''(0) = \sum_{n=0}^{N} \left(S_\alpha(0,1)\right)_n(y)n(n-1)(\alpha - 1)^{n-2} = 3$$

$$y_\alpha(1) = \sum_{n=0}^{N} \left(S_\alpha(0,1)\right)_n(y)(\alpha)^n = 2e$$

$$y_\alpha''(1) = \sum_{n=0}^{N} \left(S_\alpha(0,1)\right)_n(y)n(n-1)(\alpha)^{n-2} = 4e$$

respectively. Here, let $(S_\alpha(0,1))_0(y) = \rho$, $(S_\alpha(0,1))_1(y) = \sigma$, $(S_\alpha(0,1))_2(y) = \tau$, and $(S_\alpha(0,1))_3(y) = \omega$, then substituting in the recursive relation (5), we can calculate the other terms of the *PDT* as

$$(S_\alpha(0,1))_4(y) = \frac{1}{3!} + \frac{\rho}{4!}, (S_\alpha(0,1))_5(y) = \frac{4}{5!} + \frac{\sigma}{5!}, (S_\alpha(0,1))_6(y) = \frac{4}{6!} + \frac{\tau}{6!}$$

$$(S_\alpha(0,1))_7(y) = \frac{4}{7!} + \frac{6\omega}{7!}, (S_\alpha(0,1))_8(y) = \frac{8}{8!} + \frac{\rho}{8!}, (S_\alpha(0,1))_9(y) = \frac{8}{9!} + \frac{\sigma}{9!}$$

$$(S_\alpha(0,1))_{10}(y) = \frac{8}{10!} + \frac{2\tau}{10!}, (S_\alpha(0,1))_{11}(y) = \frac{8}{11!} + \frac{6\omega}{11!}, (S_\alpha(0,1))_{12}(y) = \frac{12}{12!} + \frac{\rho}{12!}$$

$$(S_\alpha(0,1))_{13}(y) = \frac{12}{13!} + \frac{\sigma}{13!}, (S_\alpha(0,1))_{14}(y) = \frac{12}{14!} + \frac{2\tau}{14!}, (S_\alpha(0,1))_{15}(y) = \frac{12}{15!} + \frac{6\omega}{15!}, \dots$$

Hence, the parameterised series solution $y_\alpha(t)$ is evaluated up to $N = 15$:

$$y_\alpha(t) = \sum_{n=0}^{15} (S_\alpha(0,1))_n(y)(t - t_\alpha)^n$$

$$= \rho + \sigma(t - 1 + \alpha) + \tau(t - 1 + \alpha)^2 + \omega(t - 1 + \alpha)^3 + \left(\frac{1}{3!} + \frac{\rho}{4!}\right)(t - 1 + \alpha)^4$$

$$+ \left(\frac{4}{5!} + \frac{\sigma}{5!}\right)(t - 1 + \alpha)^5 + \left(\frac{4}{6!} + \frac{\tau}{6!}\right)(t - 1 + \alpha)^6 + \left(\frac{4}{7!} + \frac{6\omega}{7!}\right)(t - 1 + \alpha)^7$$

$$+ \left(\frac{8}{8!} + \frac{\rho}{8!}\right)(t - 1 + \alpha)^8 + \left(\frac{8}{9!} + \frac{\sigma}{9!}\right)(t - 1 + \alpha)^9 + \left(\frac{8}{10!} + \frac{2\tau}{10!}\right)(t - 1 + \alpha)^{10}$$

$$+ \left(\frac{8}{11!} + \frac{6\omega}{11!}\right)(t - 1 + \alpha)^{11} + \left(\frac{12}{12!} + \frac{\rho}{12!}\right)(t - 1 + \alpha)^{12} + \left(\frac{12}{13!} + \frac{\sigma}{13!}\right)(t - 1 + \alpha)^{13}$$

$$+ \left(\frac{12}{14!} + \frac{2\tau}{14!}\right)(t - 1 + \alpha)^{14} + \left(\frac{12}{15!} + \frac{6\omega}{15!}\right)(t - 1 + \alpha)^{15}$$

Furthermore, the numbers $\rho, \sigma, \tau, \omega$ are evaluated from the boundary conditions (4).

For $\alpha = \frac{1}{2}, \alpha = \frac{1}{5}, \alpha = \frac{999}{1000}$ the numerical *PDT* solutions are presented in Fig. 2-4 as follows:
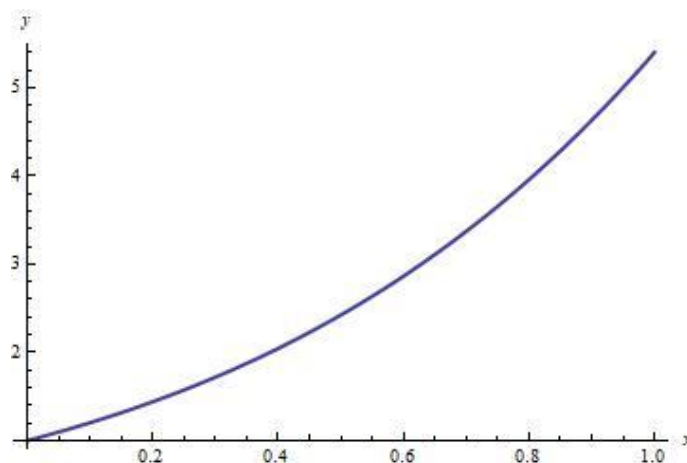

Fig. 2. Graph of the PDTM solution for the problem provided in (3)-(4) ($\alpha = \frac{1}{2}$)
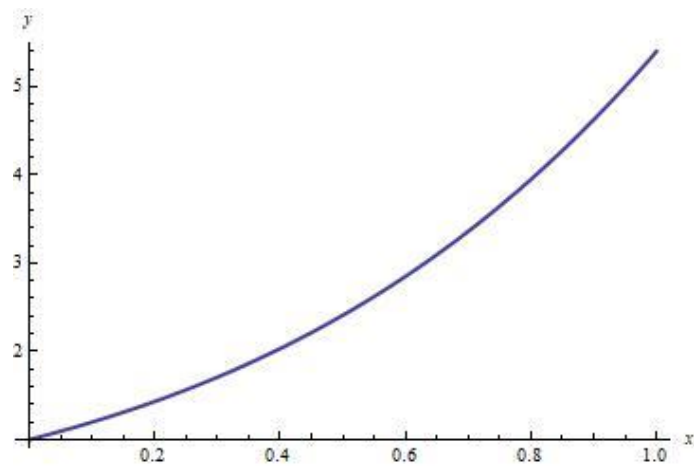
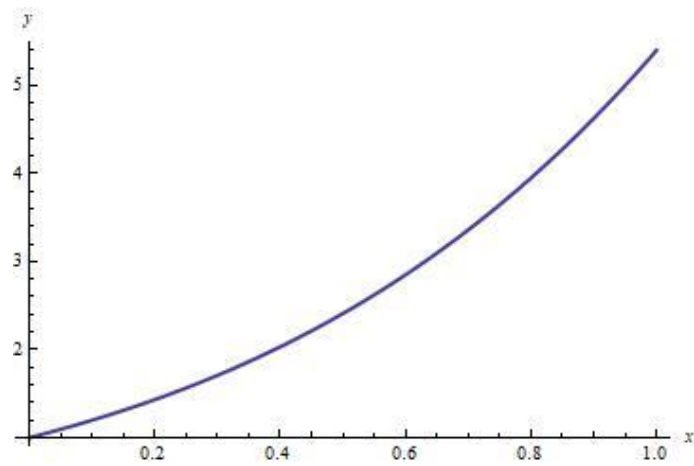**Fig. 3.** Graph of the PDTM solution ($\alpha = \frac{1}{5}$)

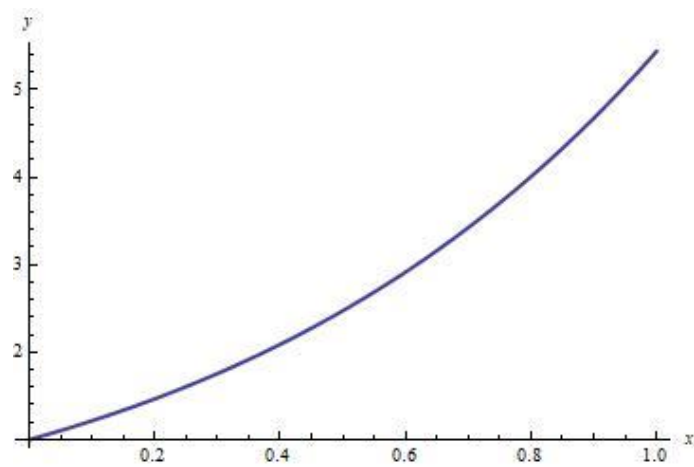**Fig. 4.** Graph of the PDTM solution $\left(\alpha = \frac{999}{1000} \right)$

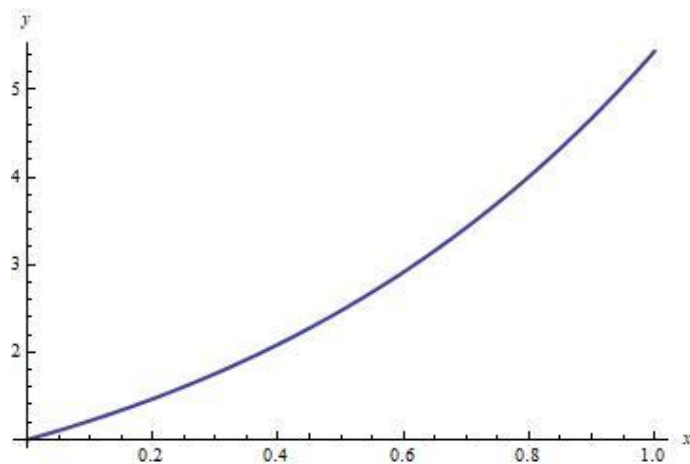**Fig. 5.** Graph of the ADM solution for the problem provided in (3)-(4) (See, [7])

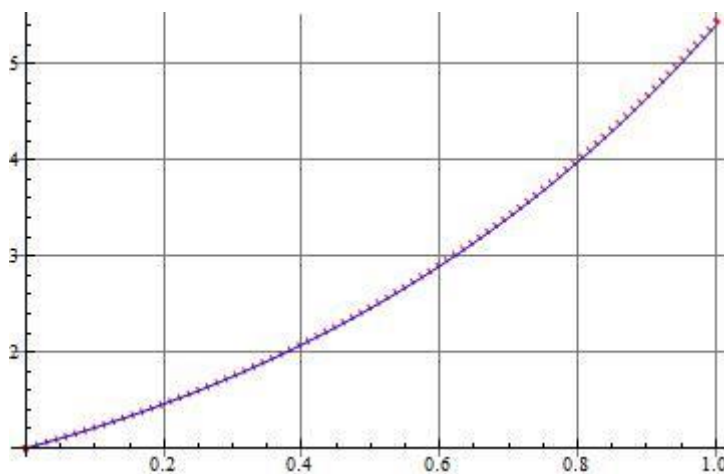**Fig. 6.** Graph of the DTM solution for the problem provided in (3)-(4) (See, [6])

Fig. 7. Comparison of exact solution (red line) and the approximate solution for problem provided in (3)-(4) obtained by using DTM [6] (blue line)
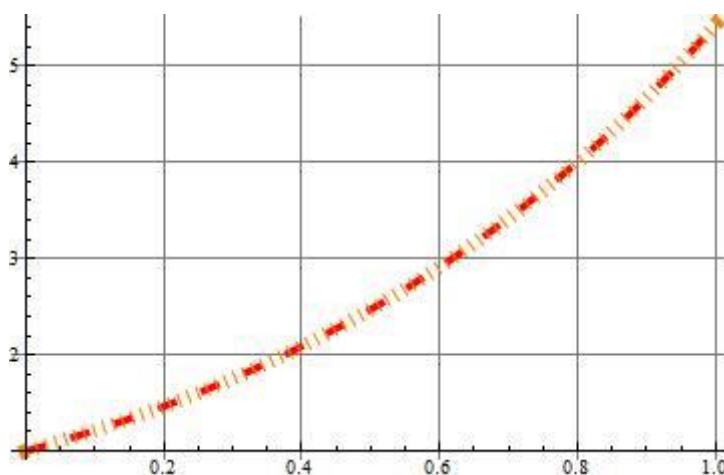

Fig. 8. Comparison of exact solution (red line) and the approximate solution for problem provided in (3)-(4) obtained by using PDTM (orange line)
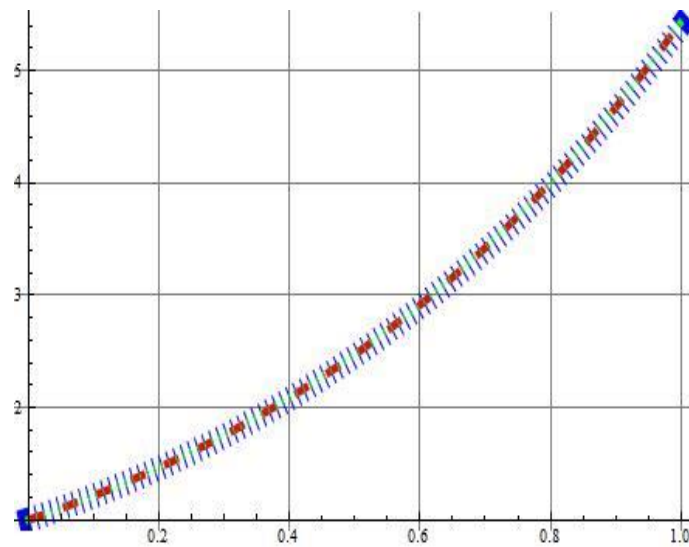
Fig. 9. Comparison of exact solution (red line) and the approximate solution for problem provided in (3)-(4) obtained by using ADM [7] (green line), PDTM (blue line)
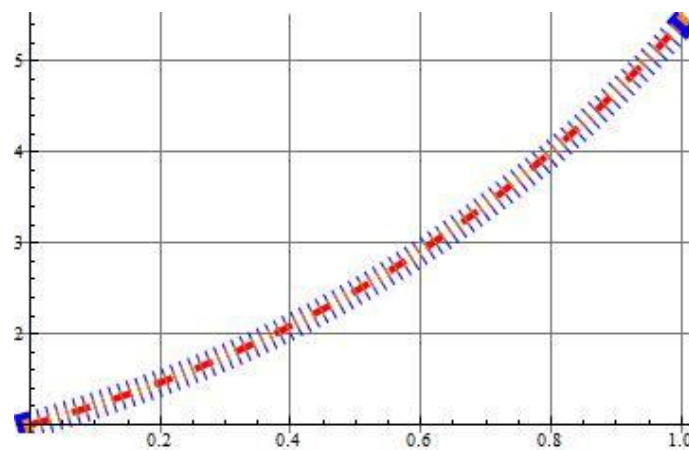

Fig. 10. Comparison of exact solution (red line) and the approximate solution for problem provided in (3)-(4) obtained by using DTM [6] (orange line), PDTM (blue line)

Example 3.2. Consider the boundary value problem

$$y^{(4)}(t) = y(t) + y''(t) + e^t(t-3) \tag{6}$$

subject to the boundary conditions

$$y(0) = 1, y'(0) = 0, y(1) = 0, y'(1) = -e \tag{7}$$

The exact solution to the problem is

$$y(t) = (1-t)e^t$$

If it is applied *PDT* to both sides of (6), then we obtain

$$\left(S_\alpha(0,1)\right)_{n+4}(y)(n+1)(n+2)(n+3)(n+4) = \left(S_\alpha(0,1)\right)_n(y) + \left(S_\alpha(0,1)\right)_{n+2}(y)(k+1)(k+2)$$

$$-\frac{3}{n!} + \sum_{n_1}^{n} \frac{\delta(n_1 - 1)}{(n - n_1)!} \tag{8}$$

Therefore, from the definition of PDT,

$$y_\alpha(t) = \sum_{n=0}^{\infty} \big(S_\alpha(0,1)\big)_n(y)(t - t_\alpha)^n$$

and

$$y'_\alpha(t) = \sum_{n=0}^{\infty} \big(S_\alpha(0,1)\big)_n(y)n(t - t_\alpha)^{n-1}.$$

Moreover, for the boundary conditions $y(0) = 1, y'(0) = 0, y(1) = 0, y'(1) = -e$,

$$y_\alpha(0) = \sum_{n=0}^{N} \big(S_\alpha(0,1)\big)_n(y)(\alpha - 1)^n = 1$$

$$y'_\alpha(0) = \sum_{n=0}^{N} \big(S_\alpha(0,1)\big)_n(y)n(\alpha - 1)^{n-1} = 0$$

$$y_\alpha(1) = \sum_{n=0}^{N} \big(S_\alpha(0,1)\big)_n(y)(\alpha)^n = 0$$

$$y'_\alpha(1) = \sum_{n=0}^{N} \big(S_\alpha(0,1)\big)_n(y)n(\alpha)^{n-1} = -e$$

respectively. Here, let $\big(S_\alpha(0,1)\big)_0(y) = \rho_1, \big(S_\alpha(0,1)\big)_1(y) = \rho_2, \big(S_\alpha(0,1)\big)_2(y) = \rho_3, \big(S_\alpha(0,1)\big)_3(y) = \rho_4$ and then substituting in the recursive relation (8), we can calculate the other terms of the PDT as

$$\big(S_\alpha(0,1)\big)_4(y) = \frac{1}{4!}(\rho_1 + 2\rho_3 - 3) \qquad \big(S_\alpha(0,1)\big)_5(y) = \frac{1}{120}(\rho_2 + 6\rho_4 - 2)$$

$$\big(S_\alpha(0,1)\big)_6(y) = \frac{1}{360}\left(\frac{\rho_1}{2} + 2\rho_3 - 2\right) \qquad \big(S_\alpha(0,1)\big)_7(y) = \frac{1}{840}\left(\frac{\rho_2 + 12\rho_4 - 2}{6}\right)$$

$$\big(S_\alpha(0,1)\big)_8(y) = \frac{1}{1680}\left(\frac{\rho_1}{12} + \frac{\rho_3}{4} - \frac{1}{4}\right) \qquad \big(S_\alpha(0,1)\big)_9(y) = \frac{1}{3024}\left(\frac{\rho_2}{60} + \frac{3\rho_4}{20} - \frac{1}{60}\right)$$

$$\big(S_\alpha(0,1)\big)_{10}(y) = \frac{1}{5040}\left(\frac{3\rho_1}{720} + \frac{5\rho_3}{360} - \frac{7}{720}\right)$$

Hence, the parameterised series solution $y_\alpha(t)$ is evaluated up to $N = 10$:

$$y_\alpha(t) = \sum_{n=0}^{10} \big(S_\alpha(0,1)\big)_n(y)(t - t_\alpha)^n$$

$$= \rho_1 + \rho_2(t - 1 + \alpha) + \rho_3(t - 1 + \alpha)^2 + \rho_4(t - 1 + \alpha)^3 + \frac{1}{4!}(\rho_1 + 2\rho_3 - 3)(t - 1 + \alpha)^4$$

$$+ \frac{1}{120}(\rho_2 + 6\rho_4 - 2)(t - 1 + \alpha)^5 + \frac{1}{360}\left(\frac{\rho_1}{2} + 2\rho_3 - 2\right)(t - 1 + \alpha)^6$$

$$+ \frac{1}{840}\left(\frac{\rho_2 + 12\rho_4 - 2}{6}\right)(t - 1 + \alpha)^7 + \frac{1}{1680}\left(\frac{\rho_1}{12} + \frac{\rho_3}{4} - \frac{1}{4}\right)(t - 1 + \alpha)^8$$

$$+ \frac{1}{3024}\left(\frac{\rho_2}{60} + \frac{3\rho_4}{20} - \frac{1}{60}\right)(t - 1 + \alpha)^9 + \frac{1}{5040}\left(\frac{3\rho_1}{720} + \frac{5\rho_3}{360} - \frac{7}{720}\right)(t - 1 + \alpha)^{10}$$

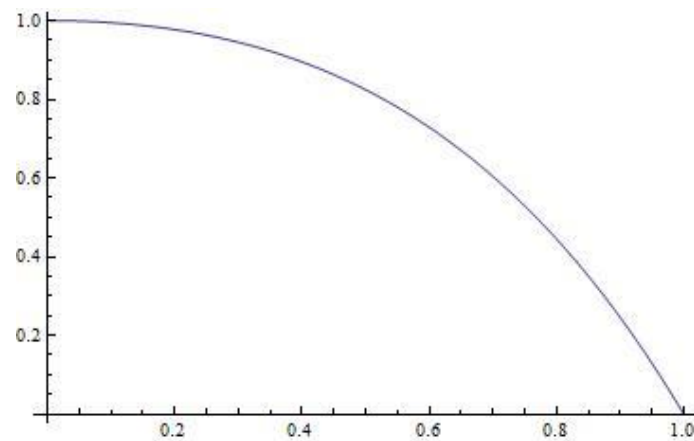A graph of the exact solution to the problem is presented in Fig. 11 as follows:

Fig. 11. Graph of the exact solution of the problem provided in (6)-(7)

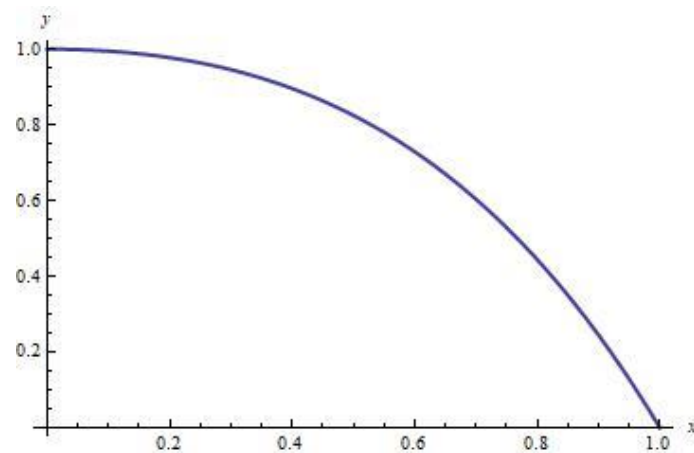For $\alpha = \frac{1}{2}$ the numerical *PDT* solution is presented in Fig. 12 as follows:

Fig. 12. Graph of the numerical PDT solution for $\alpha = \frac{1}{2}$ of the problem provided in (6)-(7)
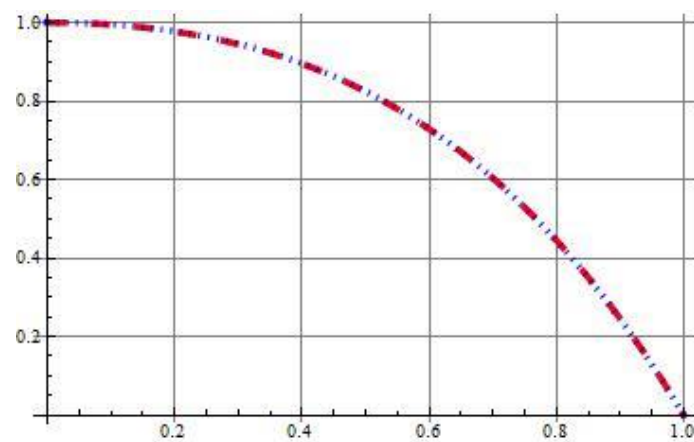

Fig. 13. Comparison of the exact solution (red dashing) with the PDT solution for $\alpha = \frac{1}{2}$ (blue line)

4. Conclusion

This paper provides a new semi-analytical method, the so-called parameterised differential transform method (P DTM), to find an exact solution in the series form or approximate various high-order boundary value problems. To show the reliability of our method, we solved an illustrative high-order boundary value problem. We compared the resulting solutions with the analytical solution and with the solutions obtained by the traditional DTM and ADM methods. Figures 5-10 and 13 show that the PDTM is the efficient method for solving high-order boundary value problems.

Author Contributions

All the authors contributed equally to this work. They all read and approved the last version of the manuscript.

Conflict of Interest

All the authors declare no conflict of interest.

References

[1] J. K. Zhou, Differential Transformation and Its Application for Electrical Circuits, Huazhong University Press, Wuhan, China, 1986.

[2] S. Momani, M. A. Noor, *Numerical Comparison of Methods for Solving a Special Fourth-Order Boundary Value Problem*, Applied Mathematics and Computation, 191 (1) (2007) 218–224.

[3] I. A. H. Hassan, V. S. Erturk, *Solutions of Different Types of the Linear and Nonlinear Higher-Order Boundary Value Problems by Differential Transformation Method*, European Journal of Pure and Applied Mathematics 2 (3) (2009) 426–447.

[4] C. H. Che Hussin, A. Kiliçman, *On the Solutions of Nonlinear Higher-Order Boundary Value Problems by Using Differential Transformation Method and Adomian Decomposition Method*, Mathematical problems in engineering (2011).

[5] E. R. El-Zahar, *Approximate Analytical Solutions of Singularly Perturbed Fourth Order Boundary Value Problems Using Differential Transform Method*, Journal of king Saud university-science 25 (3) (2013) 257–265.

[6] V. S. Ertürk, S. Momani, *Comparing Numerical Methods for Solving Fourth-Order Boundary Value Problems,* Applied Mathematics and Computation 188 (2) (2007) 1963–1968.

[7] A. M. Wazwaz, *The Numerical Solution of Special Fourth-Order Boundary Value Problems by the Modified Decomposition Method*, International journal of computer mathematics 79 (3) (2002) 345–356.

[8] D. Arslan, *Approximate Solutions of the Fourth-Order Eigenvalue Problem*, Journal of Advanced Research in Natural and Applied Sciences 8 (2) (2022) 214–221.

[9] O. Mukhtarov, M. Yücel, K. Aydemir, *A New Generalization of the Differential Transform Method for Solving Boundary Value Problems*, Journal of New Results in Science 10 (2) (2021) 49–58.

[10] O. Mukhtarov, M. Yücel, K. Aydemir, *Treatment a New Approximation Method and its Justification for Sturm–Liouville Problems*, Complexity Article ID 8019460 (2020) 8 Pages.

[11] O. Mukhtarov, S. Çavuşoğlu, H. Olğar, *Numerical Solution of One Boundary Value Problem Using Finite Difference Method*, Turkish Journal of Mathematics and Computer Science 11 (2019) 85–89.

[12] B. Boukary, J. Loufouilou-Mouyedo, J. Bonazebi-Yindoula, G. Bissanga, *Application of the Adomian Decomposition Method (ADM) for Solving the Singular Fourth-Order Parabolic Partial differential equation*, Journal of Applied Mathematics and Physics 6 (07) (2018) 14–76.

[13] A. Kwami, M. Salisu, J. Hussaini, M. Garba, *Modified Adomian Decomposition Method for the Solution of Fourth Order Ordinary Differential Equations*, GSJ 8(4) (2020).

[14] O. S. Mukhtarov, M. Yücel, *A Study of the Eigenfunctions of the Singular Sturm–Liouville Problem Using the Analytical Method and the Decomposition Technique*, Mathematics 8 (3) (2020) 415.

[15] A. Rysak, M. Gregorczyk, *Differential Transform Method as an Effective Tool for investigating fractional dynamical systems*, Applied Sciences 11 (15) (2021), 69–55.

[16] M. Yücel, O. S. Mukhtarov, *A New Treatment of the Decomposition Method for Nonclassical Boundary Value Problems*, Journal of Advanced Physics 7 (2) (2018), 161–166.

[17] A. S. J. Al-Saif, A. J. Harfash, *A Comparison Between the Reduced Differential Transform Method and Perturbation-Iteration Algorithm for Solving Two-Dimensional Unsteady Incompressible Navier-Stokes Equations*, Journal of Applied Mathematics and Physics 6 (12) (2018), 2518–2543.

[18] J. S. Duan, R. Rach, D. Baleanu, A. M. Wazwaz, *A Review of the Adomian Decomposition Method and its Applications to Fractional Differential Equations*, Communications in Fractional Calculus, 3 (2) (2012), 73–99.

[19] F. Ayaz, *Solutions of the System of Differential Equations by Differential Transform Method*, Applied Mathematics and Computation, 147 (2) (2004), 547–567.